School of Civil and Environmental Engineering

Addis Ababa Institute of Technology

Addis Ababa University

Dynamic Analysis of Middle Awash Multi-purpose Dam

A thesis submitted to the School of Civil and Environmental Engineering in partial fulfillment of the Degree of Masters of Science in Civil Engineering (Major in Hydraulic Engineering)

Advisor: *Dr. Asie Kemal*

By *Yared Mulat*

2015/16

School of Civil and Environmental Engineering

Addis Ababa Institute of Technology

Addis Ababa University

Dynamic Analysis of Middle Awash Multi-purpose Dam

By yared Mulat

Approval by Board of Examiners

----------	----------
Chairman (department of graduate committee)	Signature
Dr. Assie Kemal	----------
Advisor	*Signature*
Dr. Mebrate Tafese	----------
External Examiner	*Signature*
Dr. Yilma Sileshi	----------
Internal Examiner	*Signature*

DECLARATION

I, the undersigned, declare that this thesis is my work and that all sources of material used for the thesis have been duly acknowledged.

Name: Yared Mulat

Signature:_____

Place: Addis Ababa Institute of Technology, Addis Ababa University, Addis Ababa.

Date of Submission: May, 2016.

Acknowledgment

I would like to give the prior recognition to God, whom my life rests up on. Then my thanks go to my research advisor, Doctor Asie Kemal, who guides me well in the research I conducted.

I would like to thank Water Works Design and Supervision Enterprise for supplying me most of the necessary data I used in my research.

Last but not least, I want to thank my family and friends, for being with me in all my critical times.

Table of Contents

List of Figures

List of Tables

List of Symbols
MCE: Maximum credible earthquake
DBE: Design base earthquake
Ha: Hectare
UTM: Universal transverse Mercator
g: Gravity
FEM: Finite element method
LEM: Limit equilibrium method
m.a.s.l: Meters Above Sea Level
Km^2: Killo meter square
Km: Killo meter
N: Northing
E: Easting
MER: Main Ethiopian Rift
ICOLD: International Commission on Large Dams

ABSTRACT

In this dynamic analysis research, Middle Awash high dam which is located in Ethiopian rift valley seismic zone is analyzed for pre and post earthquake stability and permanent deformations due to earthquake loads.

The dynamic analysis is done adopting three elsewhere recorded earthquake time histories, which have different period and duration. Applying these seismic shocks and using the Newmark deformation method, it is found that the induced deformations do not require additional extension of dam or cumber height. The upstream and downstream slopes showed sufficient performance against sliding.

The upstream section steepening is found to be more economical, yet achieving the minimum required factors of safety for static and post earthquake sliding failure.

The thick alluvium foundation of the dam is found to liquefy immediately after the design base earthquake started.

The pseudo-static seismic analysis recommends uneconomical dam section modification.

The Finite Element and Limit Equilibrium Methods shown to be conservative in calculating sliding factor of safety for downstream and upstream slopes, respectively.

Key words: Maximum credible earthquake, Design base earthquake, Finite element method, Limit equilibrium method, Permanent deformation and Liquefaction.

1. Introduction

1.1 Background

The Awash basin is one the 12 river basins in Ethiopia which originates from the central high land and drains towards Djibouti, crossing the east African Rift Valley The river basin has a total drainage area of 112, 696 km^2. The source of the Awash starts at an altitude of around 2500 m.a.s.l in plateau to the west of Addis Ababa, near a place called Ginchi. The basin is characterized by heterogeneous topographic feature characterized by small hilly watersheds and flood plains.

There exist different water resource developments in the basin and more potential for development in future. Koka Dam, which came into operation in 1960 and later developments such as Awash II, Awash III can be mentioned. Recently Kesem-Kebena, Fantale, Walenchiti and Tendaho projects can be mentioned which are on the verge of completion mainly planned for irrigation development.

After starting its journey at Ginchi, in the reach between Koka and Awash Station, the Awash River is joined by small tributaries like Keleta, Wererso and Arba draining the highlands, which define the catchment boundaries to the east. Beyond Awash station, the Awash River basin expands into the eastern plains as the Rift valley widens. Although the eastern plains account for some 40% of the area of the basin, its drainage channels terminate before reaching the Awash and also receive low rainfall (less than 600 mm per year).Between the Awash Station and the Gedebessa swamp (Hertale Station) major tributaries, the Kesem and the Kebena, enter the Awash originating from western highlands after passing through deeply incise gorges. From the eastern side the Herdini River joins the Awash. From the Hertale Station to the Tendaho Station the Ataye, the Borkena, the Chelela and the Mille rivers originating from Wollo highlands joined the Awash River in this reach contributing about 900 Million Cubic Meter of water annually. The hydrology regime is complicated by major losses in the Gedebessa

swamp complex. Estimated losses vary from 400 Million Cubic Meter to 2900 Million Cubic Meter per year. (WWDSE, 2016)

The Awash Basin Authority in its Growth and Transformation Plan Program anticipates the development of flood control development project in Middle Awash area by constructing multi-purpose dam which can also be used for water supply and for the irrigation of existing command area in Amibara project, which is around 40,000 ha of land. (WWDSE, 2016)

The Middle Awash Multi-Purpose dam will be constructed in Afar and Oromia National Regional State, around Awash town, at about 200 km northeast of Addis Ababa. Specifically, the dam site selected is on main Awash River just upstream of the Addis Ababa-Djibouti road main bridge on Awash. The dam site is proposed to be located at a geographical location of UTM629786E, UTM990686N. The location map of project area is given in Figure 1 and Figure 2 below.

The project design of Middle Awash is given to Water Works Design and Supervision Enterprise. The design feasibility stage has been completed selecting the dam site and dam type with preliminary design. The dam type selection process has thoroughly analyzed the different options leading to confirm that the most suitable dam type options for the Middle Awash dam is rock/shell fill with central clay core.

The layout of the project consists of a 120m high dam with a crest length of 453m across Awash River with a side channel spillway on the left abutment and combined intake and diversion structure on the right abutment. The reservoir area is within the valley which a peculiar attention was given to exclude Awash fall within the inundation area. The reservoir is contained within the upper rolling hill catchment and in the valley of the Awash River.

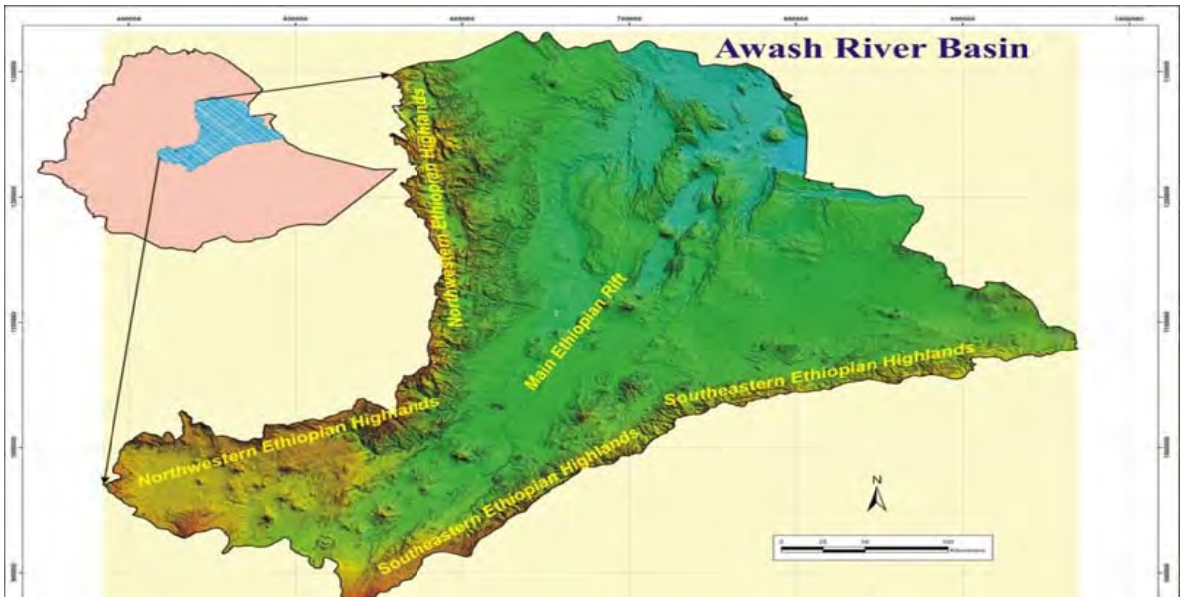

Figure 1: Location map of Middle Awash Dam (WWDSE, 2016)

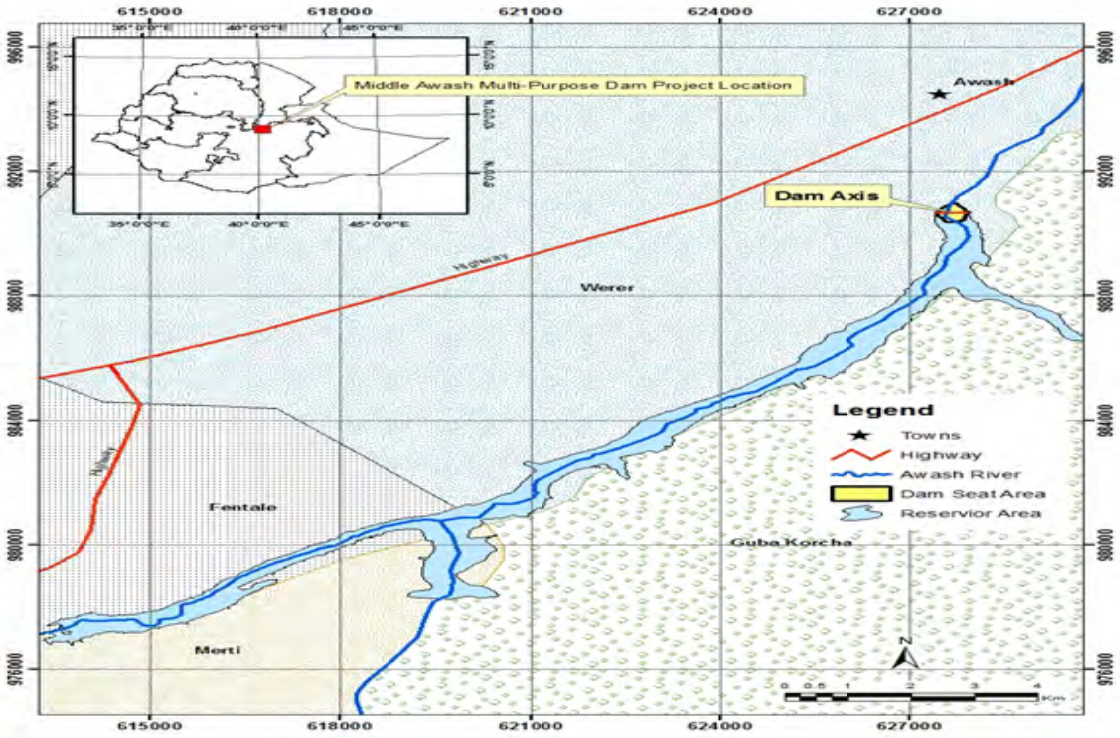

Figure 2: Location map of Middle Awash Dam (WWDSE, 2016)

The Middle Awash Multi-purpose Dam Project is located in the Main Ethiopian Rift (MER) of Afar Depression. (Figure 3) The rift is one of the well-developed continental rift segments in East Africa that marks the boundary between Nubia and Somalia plates. Rifting is evident from topographic expression, geology, volcanism and seismicity. The narrow rift valley topography of MER is primarily caused by subsidence of fault bounded sedimentary basins and uplifts of the adjacent rift flanks. (WWDSE, 2016)

The dam site is located at the rift axis, on top of the active rift floor. (UTM629786E, UTM990686N) Hypo-central depths of well-constrained events are 5–7 km from modeled earthquakes in the Main Ethiopian Rift, which is the approximate elastic plate thickness in Afar and the Main Ethiopian Rift. The shallowness of the depth estimates agree with the macro-seismic reports available from a wide area reported for Hosanna and Yirgalem earthquakes in South Ethiopia. (WWDSE, 2016)

Dams more than 45m high and which are in seismic zones, where an active fault is in 10km radius are located in hazardous region. (ICOLD, bulletin 072) Seismic analysis of dams started before a few decades. The previous most dominant analysis type of earthquake load was static or pseudo-static seismic analysis. Now days with the advancement of numeric based computer applications, dynamic analysis of a dam is becoming compulsory for high and seismic region dams. Deformations due to earthquakes and other characters of a dam during earthquakes which cannot be captured by pseudo-static analysis can be done using dynamic analysis with the help of computer tools.

Due to seismic load a few millimeters of deformation up to a total collapse of a project could happen. This is determined by the character of the earthquake, soil behavior of the site, dam material and dam geometry. Using developed models to relate interaction between these factors, a dynamic analysis of Middle Awash Multi-purpose dam is conducted on this research to evaluate the dam's performance of serviceability and safety during earthquake.

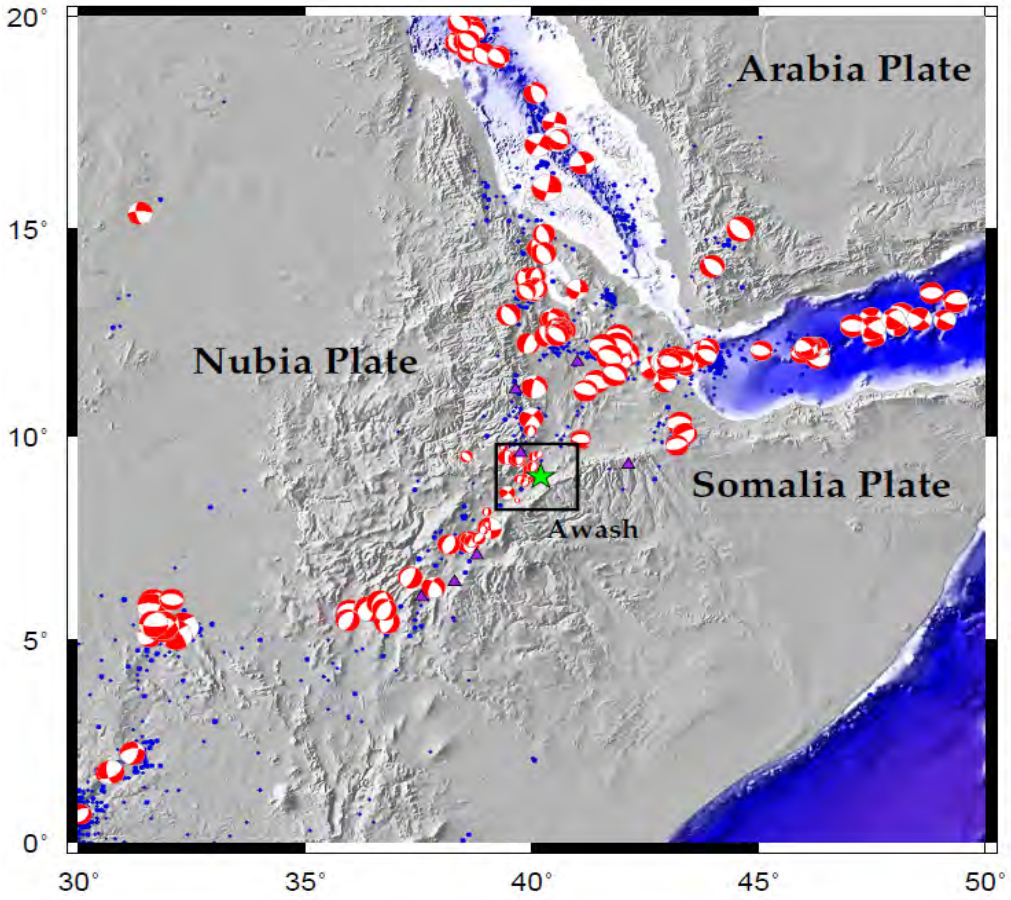

Figure 3: Seismicity data for the Horn of Africa (WWDSE, 2016);

In the above figure, blue circles represent earthquakes that occurred for the last 110 years in the region and size of the circles is proportional with magnitude. The green star shows the location of the Middle Awash Dam Project site.

1.2 Statement of the problem

The Middle Awash multi-purpose dam project is intended to irrigate a 40,000 ha of land in addition to water supply and flood control purpose. The dam site selected is at the rift axis, just on top of the active rift floor. The area is located on the highly seismically active zone, Eastern African Rift Valley, in which a sudden earthquake might happen and shake the lithosphere, the upper surface layer. The expected earthquakes hypo-central depth is very shallow ranging 5-7km. A comparison of rift structures and topographic relief in MER reveals that Tertiary volcanoes and flood basalts also contribute to the high amplitude and short wavelength aspects of the topography, particularly in the vicinity of the rift system. Earthquake is an erratic event, which is affected and determined by a complex relation of different factors. Dams in seismically active areas must be checked for their safety first and serviceability then.

In addition of the seismic activity, the Middle Awash dam is planned to rest on a foundation which is about 15 thick alluvium deposits. Alluvium deposits are suspected for liquefaction, which could lead to a large scale or total collapse of the project.

High dams which are located in an earthquake zone with expected amplitude of acceleration equal or greater than 0.25g are categorized under hazardous type. According to the geotechnical study report, the dam site has an expected maximum credible earthquake acceleration which is greater than 0.25g.

Unwell seismic analysis of high dams in earthquake zone could lead to a disastrous collapse and limited serviceability. In other end, if the analysis ended with amplified remedial measures which are not necessary, the project will end being uneconomical. Pseudo-static seismic analysis of a dam could not capture all events during the earthquake. In addition, the conservative results of it could lead to uneconomical conclusions. The dynamic analysis considers a set of materials character and the earthquake nature in different considered cases of condition.

The project's success is expected to bring dramatic changes in the community. It will highly improve the livelihood of the surrounding people. Flood risked woreda's from previous experiences, the Amibara, Gewane and Gelaelo will not face flood destruction anymore. In addition to crop production where pastoralist form of livelihood prevails previously, supply of potable water for the community cannot be undermined purpose of the project, especially for Gewane town where people travels 35 km to fetch water for household consumption. The projects failure due to earthquake as a result of its location in highly seismic zone will bring loss of the above benefits and leads to the priceless loss of life downstream of the project. (WWDSE, 2015)

1.3 Objective

1.3.1 General objective

The objective of this research is to determine the Middle Awash Multi-purpose project site seismic character and to evaluate and ensure the safety of project.

1.3.2 Specific objectives

- Evaluating seismic character of the project site.
- Determining and minimizing expected damage on the dam and its foundation related to liquefaction and deformation due to seismic load.
- Checking static and dynamic slope stability of upstream and downstream face of the dam.
- Evaluating the optimization level of the dam geometry.

2. Literature review

2.1 Theoretical review

2.1.1 Origin and classification of earthquake

An earthquake is mainly a result of a release of strain energy by a rupture of rock at plate boundaries. The strain energy storing process is a result of plate tectonics. Plate tectonics (plate movement) is a large scale motion of the earth's lithosphere. The most accepted explanation of the source of the plate movements is the requirement of thermo mechanical equilibrium of the earth's materials. There are two types of plate: continental plate and ocean plate as shown in figure 4. These two types of plate are different in their position, thickness, composition and density. When these plates move, one plate might slide underneath the other. In another case plates might rub sideways against each other or both the plates neither go easily underneath that they crumble together. During these processes strain energy will be stored in the boundaries of the plate, which will be release when it reaches its limit. But there are other factors which can induce an earthquake. Nuclear activity and reservoir fill are among them. A reservoir fill increases the pore water pressure of a strain developing region. This reduces shear strength which results a strain energy release.

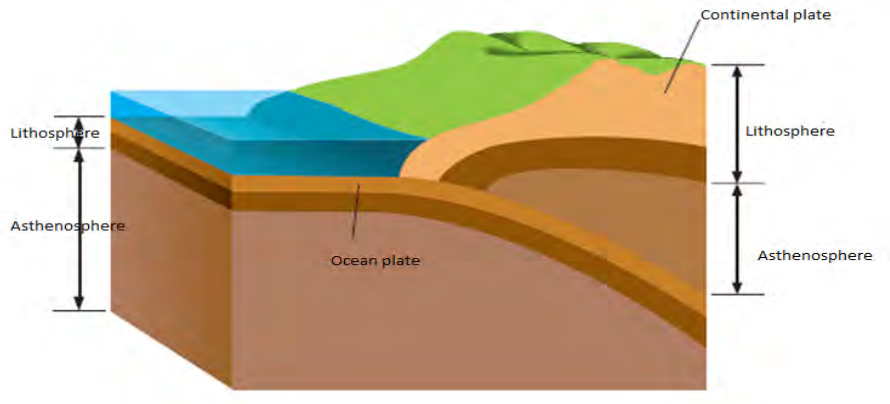

Figure 4: Earth stratum

Depending on their source, earthquakes can be categorized in to two: “Plate boundaries type” and “Inland type”. The “Plate boundaries type” occurs when continental plate is pulled by oceanic plate. As figure 5 presents, the “Inland type” occurs near field strain energy storage. Due to the energy of plate tectonics the faults created in a continental plate might be a source of another earthquake. Such faults near the earth surface are termed as “Active faults”.

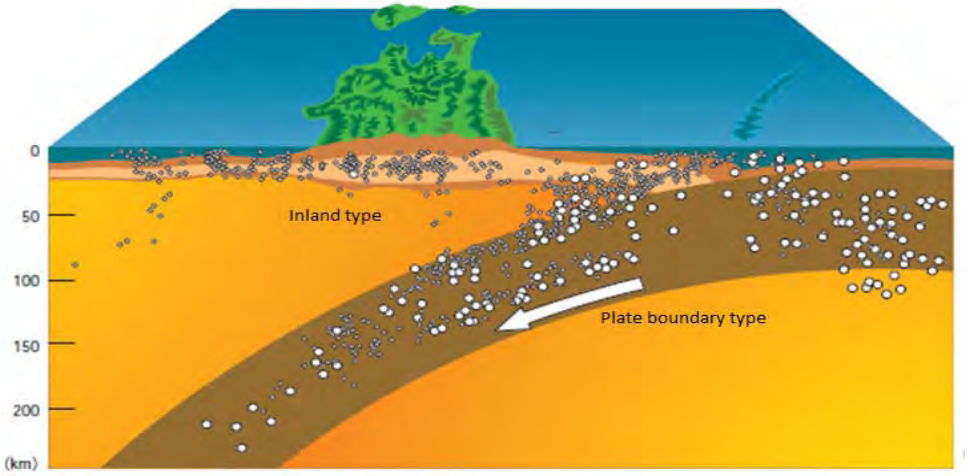

Figure 5: Earthquake originating earth stratum

A Focus or Hypocenter is the point of plate boundaries where strain energy is released. Epicenter is a point on the surface vertically above the focus point. Epicenter distance and Hypocenter distance are distance from the observation point to the epicenter and hypocenter, respectively.

During earthquake different type of seismic waves are released. Body waves and surface waves are the main category of these waves. Body waves are released from the hypocenter. Under body waves the two main waves are primary waves and secondary waves. Primary waves are fast and have a compression effect on the ground. Secondary waves are slower in speed as compared to the primary waves, and

have a shearing effect. Surface waves are waves emanating from the epicenter like a water wave emanating in a pond due to a thrown stone. They occur as a result of interaction between body waves and the surface and layers of the earth. Their effect is swaying and rolling the ground.

To conclude, Earthquake result when the stresses within the earth build up over a long period of time until they exceed the strength of the rock, which then fails and displacement along a fault results. Once ruptured, the fault is a weakness which can result an earthquake again in the future.

2.1.2 Size of earthquake

Size of an earthquake can be defined by its intensity, magnitude and energy. Earthquake intensity is an observational evaluation of earthquake from its damage result and intensity to be felt. Earthquake magnitude is related to the motion resulted from earthquake. The most known magnitude definition comes from Charles Richter in 1935. He defines magnitude as the logarithm of the maximum trace amplitude recorded on a Wood-Anderson seismometer, located at 100 km from the epicenter of the earthquake. Earthquake energy is the total energy released during its occurrence. In most equations developed, it is related with the earthquake moment magnitude.

When come to the motion on the ground created by the earthquake, the three characters which defines earthquake motion are

- Amplitude
- Frequency
- Duration of motion

The amplitude is the main character of definition. It is a measure of acceleration, velocity or displacement of the ground as a result of the shake. If one of these parameters is recorded in the form of time history data the others can be computed. From the accelerogram of the component, the largest values of horizontal acceleration are obtained for pseudo-static analysis. But vertical forces and acceleration are ignored mostly because the static safety design is sufficient to react against dynamic instability in this direction. The frequency describes how the amplitude of the ground motion is distributed in different frequency. Since loads are cyclic in earthquake, the inverse of the time taken to accomplish one cycle, can provide the frequency of the motion. The duration of the motion is the time or period of the earthquake. In loose saturated sand pore water pressure development until liquefaction occurrence is not only a function of the amplitude of the cyclic load, but also the duration of the cyclic load. Strong amplitude earthquake might not result damage if its duration is short. As the area and length of fault rupture increases the duration of the motion increases.

The shaking strength of an earthquake depends up on

- Size of the earthquake
- Location of the earthquake
- Size character of the earthquake.

2.1.3 Engineering consideration of waves

During earthquake the ground motion involves three components of translational and rotational motions. But in practice, the translational motions are measured in orthogonal directions.

2.1.4 Susceptibility of seismic instability

A strain energy, which is a source of earthquake, is created at plate boundaries where plate tectonics is governing. There are 13 continental plates in which they are moving one on the other, one rubbing the other and both crumbling together as the mountains of Himalaya. Considering this geology and earthquake records, Kramer (1996) presented the below two maps showing earthquake susceptibility.

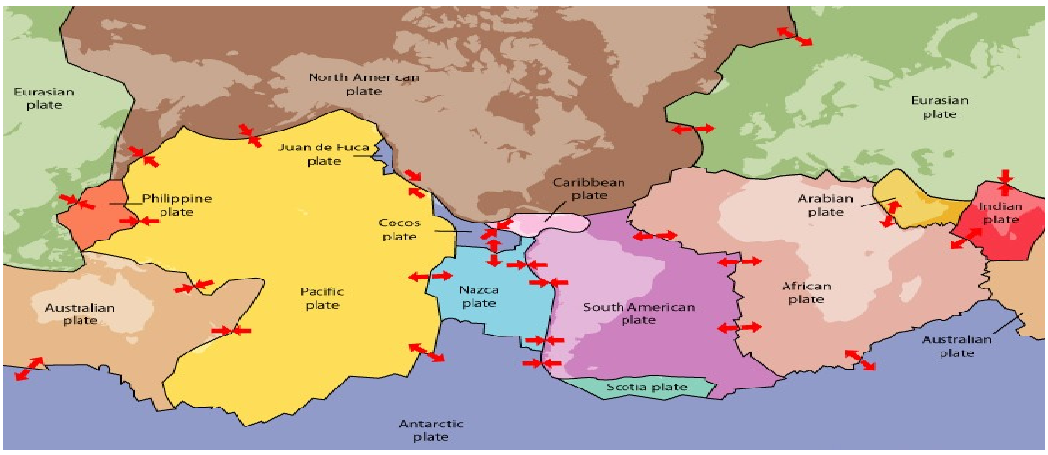

Figure 6: Major tectonic plates

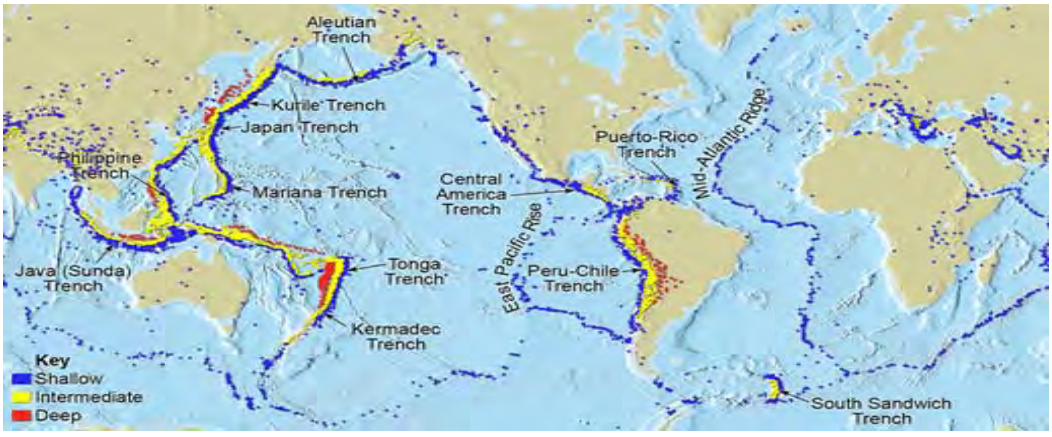

Figure 7: Global seismic activity

2.1.5 Dams and earthquake load

If any fault crosses a dam axis beneath, designer should take in to account a motion and load of earthquake for the dam design. The loading and dam characteristics that make seismic potential failure modes to occur more likely are listed below. (ICOLD, 2001)

- Peak Horizontal Acceleration > 20% acceleration of gravity
- Capable fault beneath the embankment (Active fault which have received movement in the last 10,000 years)
- Hydraulic fill embankment
- Sand embankment
- Loose saturated alluvial foundation
- Fine-grained soils susceptible of cyclic failure
- Thin impervious cores
- Thin filter zones
- Conduit embedded in embankment
- History of seismic damage
- Earth embankment-concrete section interface

In evaluation of seismic stability in concrete dams, the focuses are analysis on its ability to resist induced lateral forces and movements and excessive crack due to overstress on the concrete. On embankment dams the focuses are pore water pressure development, excessive deformation, slumping settlement, cracking and planar or rotational failure of embankment. Embankment dams have a vibration range between 0.5-1.5 seconds. (ICOLD, 1989)

During earthquake, the previous loading and stress condition of the embankment material will be changed. The new load mode will be dynamic which changes stress state that might result shear or tensile failure of material. (USBR, 2012)

The main broad issues that need to be resolved in assessing the seismic performance of earth dams under earthquakes are:

a) Stability: - This deals with the capability or the strength of the dam against collapse.

b) Deformation: - This deals with its serviceability performance after accommodating some damage. (Visible or invisible)

The first failure of a dam due to earthquake reported in the literature is Augusta Dam, during 1886 Charleston earthquake. (Dr. Gopi Siddappa, 2000) After 1950 percentage of dam failure due to earthquake becomes 3.4.

In dealing with earth structures during earthquake the major categories of issues to be considered are

(a) The motion, movement and inertial forces that occur during the shaking,

(b) The generation of excess pore-water pressures, the potential reduction of the soil shears strength,

(c) The effect on stability created by the inertial forces, excess pore-water pressures and possible shear strength loses, and

(d) The redistribution of excess pore-water pressures and possible strain softening of the soil after the shaking has stopped.

To make it more clear and practical, the four main issues to consider in earthquake are:

- The general design of the dam particularly the provision of filters , to prevent or control internal erosion of the dam and foundation, and provision of zones with good drainage capacity.(e.g. free draining rock fill)
- The stability of embankment during and immediately after the earthquake.
- Deformations induced by the earthquake (settlement, cracking) and dam free board.
- The potential for liquefaction of saturated sandy and silty soils and some gravel with a sand and silt matrix in the foundation, and possibly in the embankment, and how this affects stability and deformations during and immediately after the earthquake.

2.1.6 Dynamic and static loading

In static loading after assessing the strength of the structure by comparing it with external destabilizing force, the major concern is to evaluate the factor of safety against failure. Failure in soil occurs at a few percent of strain level. So, a static problem deals with a few percent of strain level, which can occur due to compression or consolidation. The strain level is in order of 10^{-3} or greater. In dynamic problems the soil is in motion and the large impact of inertial force due to velocity change is considered. As the duration of time for deformations become shorter the role of inertia becomes larger and larger. In such a cyclic motion even if the strain level is so small, the inertial force will increase in proportion to the square of the cyclic frequency. Due to this fact, up to a strain level of 10^{-6} such consideration must be given for dynamic loading.

The other issue differentiating dynamic problem with that of static is the rapidity of load. Problem where the load is applied for more than tens of seconds is cited as static. If the load application time is less than this, the problem is of dynamic type. In addition of the time of application, the other factor differentiating dynamic and static problem is the

loading repetition in dynamic loading. The period of impulse in earthquake is from 0.1-3 seconds.

In static loading since we deal with a strain level of 10^{-3} or greater which is a failure state, the deformation characteristic is not dependent on shear strains. But in dynamic loading, the deformation characteristic is dependent on shear strain. The below table show the relation between strain level and mechanical properties, with expected phenomena to occur.

Table 1: Variation of soil properties with strain

10^{-6} 10^{-5} 10^{-4} 10^{-3} 10^{-2} 10^{-1} (strain)		
Wave propagation, vibration	Cracks, differential settlement	Slide, compaction, liquefaction
Elasticity	Elasto-plasticity	Rupture/Fracture

2.1.7 Seismic hazard and dynamic analysis for a dam

Earthquake can be designed for maximum credible earthquake (MCE) and Operating Basis Earthquake (OBE). Maximum credible earthquake is the largest or maximum expected conceivable earthquake that appears along a recognized fault. In considering MCE, extensive damages of the dam due to the earthquake are tolerated as long as no catastrophic flooding occurs. Time history data is needed to define the earthquake character. The other design option is design for Operating Basis Earthquake (DBE), which only minor damages are acceptable. It is lower than the MCE. (ICOLD, 1989) To elaborate this in other words, Operating Basis Earthquake is expected to occur within the service life of the project, that is, with a 50% probability of exceedance during the

service life. But Maximum Design Earthquake is a minimum of 10% chance of being exceeded in a 100 year period, or a 1000 year return period.

Dams with more than 45 meter height and with a reservoir capacity of 120 hecto-meter cubes need dynamic analysis. The rate of seismic hazard is related with site conditions in the below table. (ICOLD, 1989)

Table 2: Rate of seismic hazard

Rate of seismic hazard	
Condition	Hazard
PGA<0.1gravity	Low
0.1gravity<=PGA<=0.25gravity	Medium
PGA>0.25gravity(but no active fault in 10km radius)	High
PGA>0.25gravity(with active fault in 10km radius)	Extreme

Dynamic analysis of a dam can follow the below steps.

Step 1: Determine pre-earthquake static stress using a static numerical model of the embankment for initial effective normal stress and shear stress along the potential failure surface. The numerical models are usually based on finite element or finite difference approximations

Step 2: Evaluate the dynamic soil behavior from in-situ and cyclic laboratory tests for input soil properties required in the dynamic analyses.

Step 3: For the numerical model developed in Step 1, determine the dynamic response of the dam or embankment and foundation using a basket of plausible base rock motions. The base rock motions should include appropriate accelerograms representing earthquakes of magnitude and peak acceleration similar to those of the design earthquake from earthquakes recorded in a similar geologic environment. The response of the embankment is determined by dynamic finite element or finite difference modeling, using either equivalent linear or nonlinear procedures.

Step 4: The stress-strain models used in the dynamic analysis should reasonably represent the following aspects of material behavior: (a) material non-linearity, (b) stress and strain dependence, (c) stress-path dependence, (d) inherent anisotropy, and (e) strain rate dependence. Calibration of the stress-strain model should ideally be based on testing of undisturbed samples.

Step 5: Evaluate embankment deformations on the basis of strain potential for the individual elements, which corresponds to the strain that would be experienced if the element were not constrained by surrounding soil.

Step 6: Calculate total embankment deformation on the basis of gravity loads and softened material properties to determine whether they are within the acceptable limits.

2.1.8 Seismic activity in Ethiopia

From 1900 to 2013 earthquakes in Ethiopia have caused a total of 93 deaths, 165 injuries, 420 homeless and 11,000 people affected. And the estimated economic loss is around 7 million US dollars. (Siân Herbert, 2013) In east Africa, there are three main seismic weaknesses. These weaknesses are the East African rift system, the Gulf of Aden and the Red sea. The Afar Triangle is made up from these weaknesses. But in Ethiopia 90 % of the seismic activity are related to the East African rift system. The rift system is 50-60km wide and 3000km long extending up to Zambezi. The below figure is a seismic hazard map of Ethiopia done by World Health Organization in 2010.

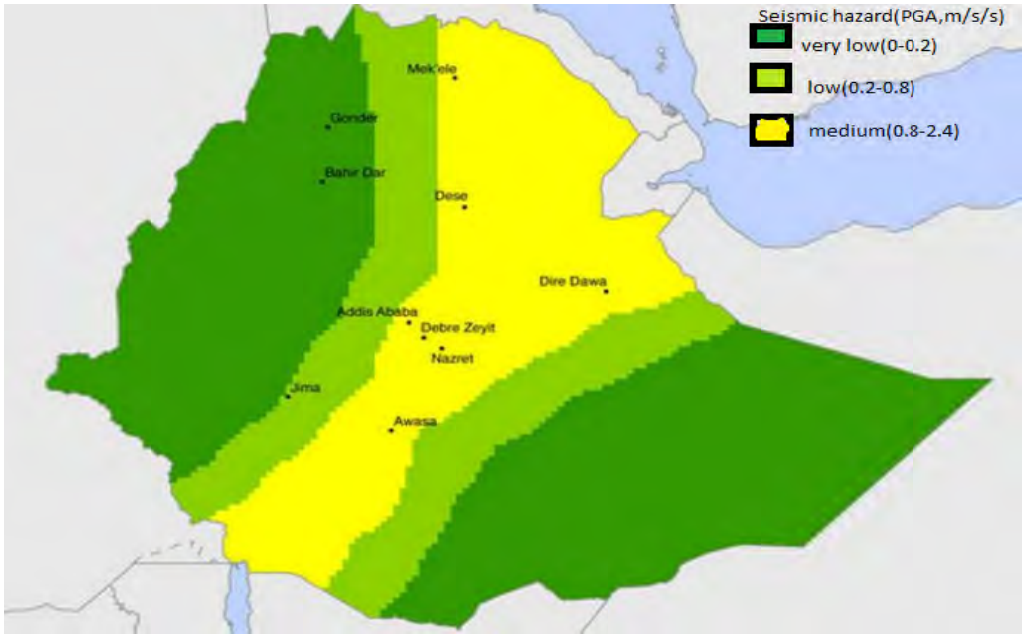

Figure 8: Seismic hazard map of Ethiopia

The Ethiopian building code standard subdivides the country in to seismic zones depending on the local hazard in 1995. The hazard is described in terms of effective peak ground acceleration in rock or firm soil. The code recommends a simple and reduced seismic design procedure for certain types or categories of structure if they are to be constructed in zones with peak ground acceleration less than 0.05g. The below figure show the seismic zones and their respective peak ground acceleration for a return period of 100 years provided by the code.

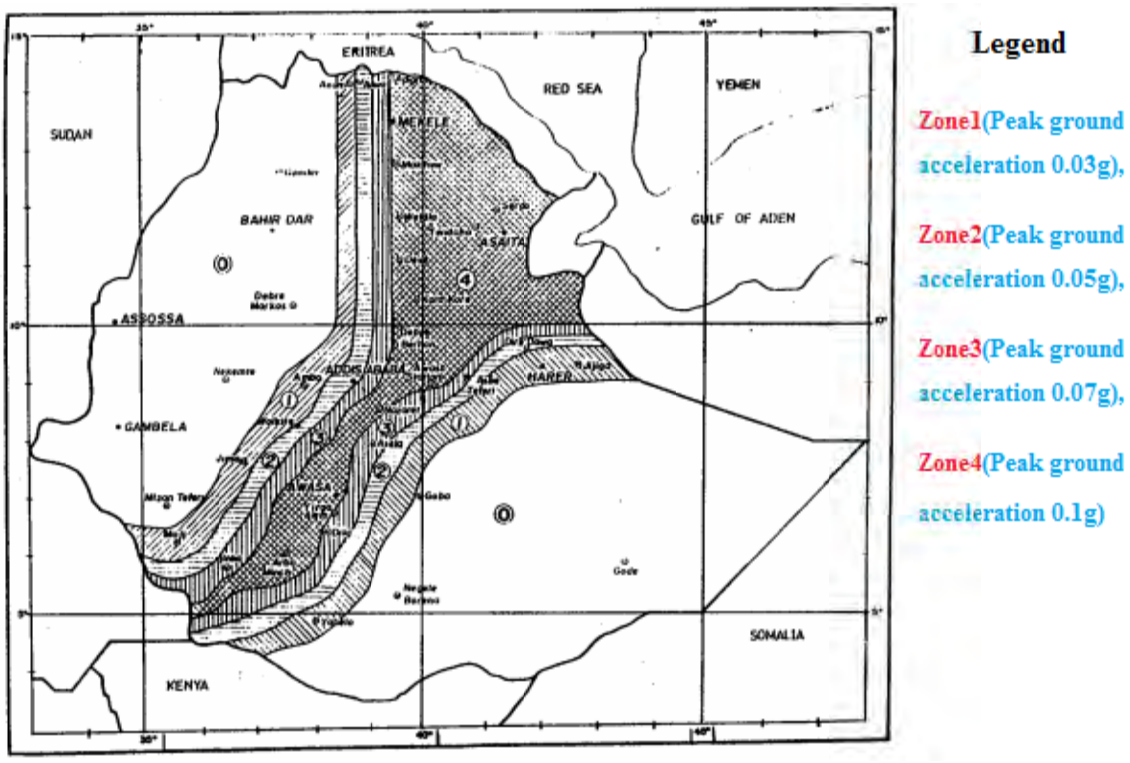

Figure 9: Seismic zone map of Ethiopia (EBCS, 1995)

2.1.9 Cyclic loading and material behavior during earthquake

The major ground motion cause is body wave during earthquake. Less consideration is given to surface waves for their effect. As discussed earlier, body waves have compression (primary/longitudinal) wave and shear (secondary) waves. The compression wave has a vertical and horizontal component on the ground. But in a leveled ground the soil element is not allowed to deform horizontally. In this case vertical normal stress is related to horizontal stress by a Poisson ratio as described below.

$\sigma_{dh}/\ \sigma_{dv} = \upsilon/1-\ \upsilon$…..Equation 1: normal and horizontal stress relation

Where, σ= stress, υ= Poisson ratio

Vertical and horizontal normal stresses are considered equal nearly for soft soils, where initial shear modulus is less than 50mpa. Because of this the deviator stress will be zero, nearly. As a result, the effective stress will not be changed. Thus, compressional waves are ignored for this reason. Horizontal shear stress is the main consideration in one dimensional stability analysis.

When come to the effect of cycles number on the dynamic behavior of soils, experiments made on sands have showed that shear modulus and damping ratio at 2^{nd} and 10^{th} cycle differs by 10% at most. After the 10^{th} cycle, the effect disappeared.

In evaluating soil materials under earthquake load, determination of dynamic properties of soil is a fundamental part of the solution. When the strain level is less than 10^{-6}, it indicates elastic properties represented by wave propagation. For the sake of simplicity in applying mathematical theory of elasticity, soil is generally considered as a linear mass and with such assumptions, the dynamic soil properties can be theoretically handled easily. Up to a strain level of 10^{-6}, beyond which the non-linear behavior becomes prominent, an approximate analysis is carried out using the so called 'equivalent linearization method', which takes into consider the changes in deformation coefficient and damping ratio. Recently, soil has been represented by an elasto-plastic model to enable the realistic analysis of failure phenomenon.

The soil properties that influence wave propagation and other low strain phenomena include stiffness, damping, poison ratio and density, in which the first two are the most influential. The main mechanical characters of an earth material under dynamic load are dynamic stress-strain relationship and dynamic shear strength. These mechanical characters are highly dependent on initial relative density or degree of compaction, degree of saturation, and rate of loading. (P Bertacchi, 1981)

This mechanical character of the materials needs special focus because of the below two reasons that happens during earthquake loading. (M.Nose and Dr Eng K.BABA, 1981)

- Permanent shear strains occur after each cycle of stress application and that
- Permanent volume contraction(densification) occurs after each cycle of loading (except for extremely dense material)

During earthquake the two broad categories of dynamic properties are soil stiffness and generation of excessive pore-pressure. (Quake/W, 2007)

Damping is a resistance of vibration. It is the energy absorbing capacity of a soil. Damping ratio is influenced by many factors. Damping ratio of high plastic soil is lower than those of low plasticity soil. Damping ratio is also influenced by effective confining pressure particularly for soils of low plasticity. Damping ratio decreases with confining pressure, void ratio, and geologic age. Damping ratio increases with cyclic shear strain. Damping is mostly rate-independent and of hysteretic in nature. In general, for sands, damping ratio increase with increasing shear strain to a value of 25% of the initial damping when the shear strain increases by 0.5%.

Shear modulus is a ratio of shear stress by shear strain. Modulus ratio (G/G_o) is a ratio of shear modulus at a time and the initial shear stress. The initial shear stress slope is always greater than or equal to any shear stress at a time. Shear modulus ratio is a dynamic soil property. It increases with confining pressure, void ratio, plasticity index and geologic age. It decreases with cyclic strain and number of loading cycles. In general, for sands, the shear modulus decreases with increasing strain down to about one tenth of the initial value, if the strain increases to a level of 0.5%.

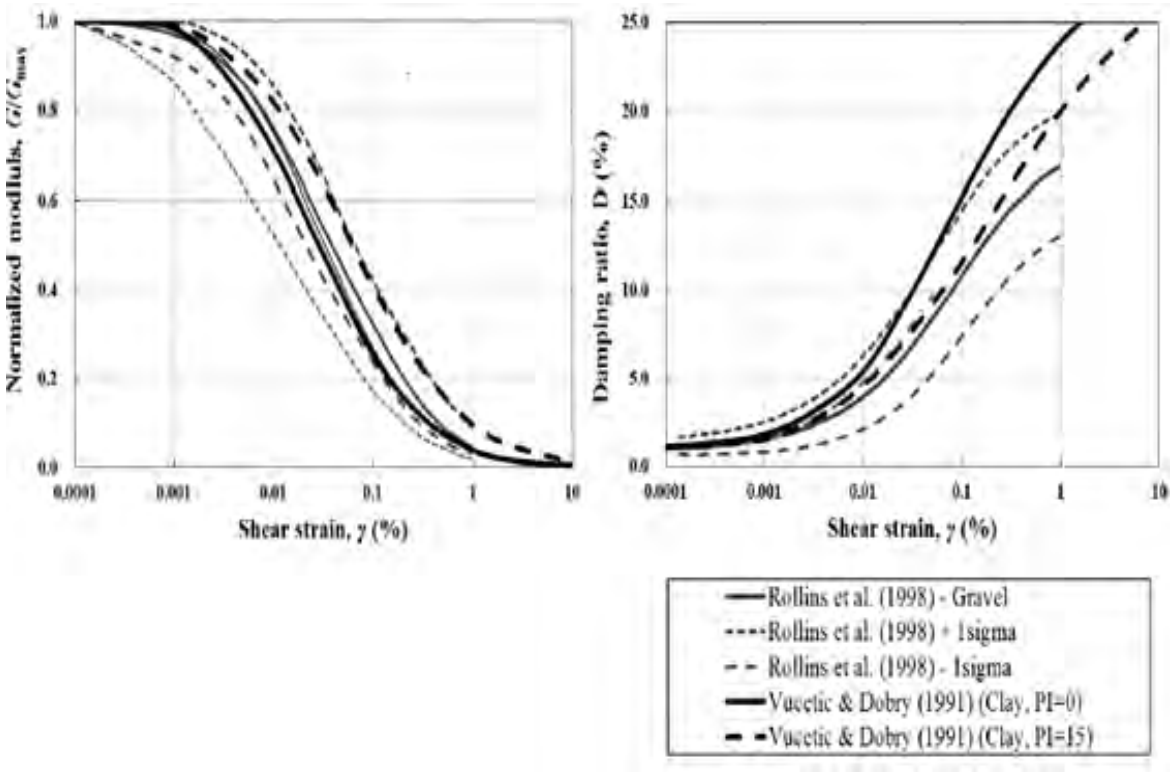

Figure 10: G/G_{max} and damping ratio curves dependent on shear strain by different researchers.

2.1.10 Rock-fill and asphalt material behavior during earthquake

Rock-fill dams have better performance than earthen fill dams due to two reasons considering earthquake load. The first reason is the flexibility of steepening slopes, making it economical by achieving stability conditions setting other factors the same. In impervious saturated soils earthquake stresses are applied under un-drained condition. This is achieved with no drainage or dissipation of excessive pore water pressure. But in highly pervious materials like gravel and rock fill, there is a dissipation of pore water pressure even if the duration of the shaking is for short time. This eliminates the susceptibility of such sections and parts of the dam for liquefaction potential. (P Bertacchi, 1981)

Coming to asphalt material, it is more seismic resistant because of its self healing and adjusting behavior of strain occurred. The study on Meyjaran asphalt core dam, recently constructed in Northern Iran, with 60m height and 180 crest length shows that, the induced shear strains in the asphalt core are less than 1% during an earthquake with peak ground acceleration of 0.25g and the asphalt core remains watertight. In addition the induced deformations in the asphalt core under an impact load with a large acceleration of 7.6 m/s^2 were very small. (Sh. Salemi,M. H. Baziar,C. M. Merrifield and T. Heidari,2008)

2.1.11 Liquefaction

When a loose, cohesionless and saturated soil is subjected to dynamic loading due to earthquake, shear stress develops. At this time soil particles try to rearrange their position due to this stress. The contraction created by the rearrangement, develops pore water pressure because the water in pores is almost incompressible. Then the result will be a decrease in effective stress. If the effective stress is lowered down to zero, liquefaction will happen. At this phase the material will tend to act like a liquid even though its previous category was solid. Liquid tend to move continuously in response to shear load. (USBR, 2012) Liquefaction occurs only in a saturated soil. The change of state occurs most readily in loose to moderately dense granular soils with poor drainage, such as silty sands or sands and gravels capped by or containing seams of impermeable sediment. (Raymond B. Seed, 2011) Liquefaction can be subdivided in to two: flow liquefaction and cyclic mobility.

Flow liquefaction is the major cause of flow failures. This occurs when the shear stress required for static equilibrium of a soil is greater than the liquefied shear strength of a soil. The main character of this liquefaction is that it’s driven by the static shear stresses. Here the cyclic stress may bring instability at which the soil strength drops sufficiently to allow static stress to result flow failure. This type of liquefaction is characterized by its sudden action and the large distance of movement.

Cyclic mobility occurs when the shear stress required for static equilibrium of a soil is greater than the liquefied shear strength of the liquefied soil. The deformation occurs incrementally while shaking, and its driven by both cyclic and static shear stresses. This type of deformation is termed as lateral spreading and occurs in a gentle slope of water near soil materials.

2.1.12 Failure due to earthquake

Dynamic loading from an earthquake changes the stress states within an embankment, causing permanent damage if the stress changes cause shear or tensile strength to be exceeded. In loose saturated and cohesionless soil the initial shearing can contract as the soil particles are rearranged due to the dynamic loading. Water is considered almost incompressible, so the shear stress transferred to the pore water will increase, decreasing the shear strength of the soil material. Large amount of strength reduction beneath an embankment slope triggers a flow slide. In dense saturated cohesionless soils, the temporary occurrence of excess pore water ratio with strain results a lateral spreading of slopes.

In saturated, cohesionless soils, large shear displacements may not occur. Instead, the temporary occurrence of excess pore water ratios of 100 percent (or initial liquefaction) is accompanied by the development of limited strains, resulting in progressive and incremental lateral spreading of slopes.

Whether or not the soil of an embankment or its foundation liquefies completely, pore pressure increases can still result in a decrease in shearing resistance. If enough reduction occurs, over a sufficient extent, large deformations can result. A translational failure can occur if the entire foundation beneath an embankment liquefies and the reservoir pushes the embankment downstream, catastrophically. Overtopping erosion failure can occur if crest deformations exceed the freeboard. If the deformations do not result in an immediate release of the reservoir, the

embankment can be cracked or disrupted to the point where internal erosion can occur through the damaged remnant. This failure mechanism can occur with or without liquefaction. There are many ways in which cracking can occur due to seismic shaking, such as differential settlement upon shaking, general disruption of the embankment crest, offset of a foundation fault, or separation at spillway walls.

Possible ways in which an earthquake may cause the failure of embankment dams are given below.

- Disruption of the dam by major fault movements in the foundation
- Loss of freeboard due to differential tectonic ground movements
- Slope failures induced by ground motions
- Loss of freeboard due to slope failures or soil compaction
- Sliding of the dam on weak foundation materials
- Piping failure through cracks induced by ground motions
- Overtopping of the dam due to water waves in the reservoir
- Overtopping of the dam due to earth or rock slides in the reservoir
- Failure of spillway or outlet structures

2.1.13 Modeling

In modeling material response to stress and strain, the most populous material property models are linear elastic model, equivalent linear model and Non-linear model. The linear-elastic model is the simplest constitutive model in which stress is directly related to strain by a Young's modulus. The relationship is simply linear and doesn't consider the strength of the material. Such a model is limited to represent the actual condition because soil stress-strain relationship is non-linear. (Quake/W, 2007)

The other model type is equivalent linear. Though this model is very similar to the linear-elastic, the soil stiffness is modified in response to computed strain in each step. This model starts the dynamic analysis with a specified stiffness of the soil. Then stiffness is modified by the computed strain for the next analysis. In such a way one specified stiffness stays for current iteration and gets changed when passed to the next.

Non- Linear model is the unusually applied model. The generation of excess pore pressure affects the dynamic response of a particular site dramatically. In this model after calculating the pore water pressure the material property changed considering the effect of the pore pressure. In this way the model will be non linear to relate stress and strain.

The two most popular simulations of real physical processes are numerical modeling and physical modeling. Numerical modeling is a mathematical simulation of physical process. Seep/W simulates the real physical process by the mathematical approach of Darcy's law. But when we come to the physical modeling the real situation is modeled by a scaled physical modeling in laboratory or field. Software's like Geo-studio are typical examples of numerical modeling. (Seep/W, 2007)

2.1.14 Pseudo-static earthquake analysis

This analysis consider a seismic coefficient of acceleration for both horizontal and vertical force computation and add more two external forces due to earthquake other than the static force. At the ground motion the seismic coefficients will be taken which creates an inertial movement, then changed to a force multiplying by the mass of the material of slices. This approach is a limit equilibrium approach.

Dynamic analysis ensures safety of the dam from deformation and the pseudo-static analysis indicates unsafe conditions. This implies that the dynamic response analysis shows an earthquake analysis, which cannot be observed by the pseudo-static one. So,

pseudo-static analysis leads to conservative design, which will be uneconomical. (Fantahun Getachew, unknown)

2.1.15 Time- History Data

For dynamic analysis a time history data of the amplitude of the earthquake is a fundamental input. Time history data of earthquake amplitude is the value of the velocity, acceleration or displacement in a constant time interval between records for some period of the earthquake shaking. Time history data describes the set of the three earthquake motion characters in one graph: amplitude, frequency and duration.

The cyclic shear stress in a dynamic analysis is calculated as an inertial force in every time step. To calculate this inertial force oscillating in fraction of seconds during earthquake shaking, the time history data of acceleration usually in every 0.02 seconds must be provided for the computation. But in most places including Ethiopia, it is hard to find a recorded time history data of earthquake. If it was available even in far places from where the dam in dynamic analysis is available, a deconvolution technique (i.e. changing the recorded surface ground motion to the source bed rock motion) can be done and applied to the bed rock under the dam in analysis. But the recently recorded time history data amplitude in Addis Ababa is so small that it undermines the probable earthquake to happen. To overcome this problem a selection criteria to choose between elsewhere recorded data must incorporate the below factors. (US Army Corps of Engineers, 2003)

- Tectonic environment
- Earthquake magnitude and type of faulting
- Earthquake source to site distance
- Subsurface condition
- Response spectrum characteristics of time history data

- Duration of strong motion

2.2 Empirical review

In the journal titled "*Seismic evaluation of existing earth-cored rock fill dams based on the finite element and Newmark type analysis*", about 21 dams were evaluated for pseudo-static and finite element Newmark dynamic analysis in Korea. In the Korean seismic dam design code updated in 2011, Newmark type approach was specified as a major dynamic analysis for seismic evaluation of dams. Permanent deformation occurs when the slope mass acceleration exceeds the static yield acceleration. Yield acceleration is determined by computing seismic coefficient that yield factor of safety one. The constitutive model applied for pseudo-static analysis is Mohr-Coulomb model and for the dynamic analysis is equivalent- linear model. In the analysis reservoir water level was set up to normal high water level. The pseudo-static Factor of safety at 1.2 is over conservative. And the result of the dynamic analysis was governed by

- Friction angle of shell
- The location of critical slip
- Dynamic soil properties
- Input motions
- Mesh size
- Two way sliding (upstream and downstream)

An upstream slope is dynamically vulnerable to instability due to the full saturation by the water stored in the upstream. The paper concludes that Pseudo-static analysis might not be appropriate for seismic safety evaluation. Dynamic analysis with deformation prediction must be done.

Dams which experience earthquake during different times in different parts of the world are listed below with description of their performance.

La Villita Dam

The dam is located in the southwestern coast of Mexico. It is constructed in the Balsas River. The multi-purpose dam is of 60 meter height and 430 crest width. It has a central impervious clay core, well graded filter and transition zones and compacted rock fill shells. The dam is founded on 76 meter thick, well graded alluvial deposit.

In September 19, 1985 an earthquake with a Richter scale of 8.1 occurred at the dam site emanating from 25 km away epicenter. The strong motion continues up to 60 seconds of shaking.

The damage occurred in the dam was in the form of cracking, settlement and spreading. But the serviceability of the dam was not threatened. The central part of the dam settled from 20-32 cm.

Masiway Dam

Masiway dam is located in Philippines Island. The 25 meter high zoned earth fill dam with central clay core has a crest length of 427 meter and a crest width of 10 meter. The shell material consists of alluvial materials and conglomerate. The upstream and downstream slopes were 2.3:1 and 2:1 (H: V), respectively.

In july16, 1990 an earthquake with a Richter scale of 7.7 hit the dam location with an estimated peak ground acceleration of 0.65g. A probable liquefaction resulting an upstream shell slump up to 2 meters horizontally and 1m vertically occurred. An overall

settlement ranging between 13 cm-1m occurred with extensive cracks up to 1.7 meter depth.

Sheffield Dam

The Sheffield dam was located in north of the city of Santa Barbara, California. The dam was built in 1917. The 219 meter long dam had a maximum height of 7.6 meter. The body of the dam was composed of silty sand and sandy silt. The upstream face was covered by a 1.2 meter clay blanket, which was extended to 3 meter into the foundation to serve as a cutoff. The foundation of the dam was alluvium deposit with a 1.2-3 meter thickness lying on sandstone bedrock.

In June 29, 1925 an earthquake with a Richter scale of 6.3 which the epicenter located about 7 miles from the dam hits the dam site. At the time of the earthquake the reservoir level was filled 4.6-5.5 meters. After inspecting the damage, O'Shaughnessy reported that "a great mass of center, about 90 meters in length, slid downstream perhaps 30m". The city manager, Herbert Nunn wrote: "After examination by several prominent engineers, the conclusion has been reached that the base of the dam had become saturated, and that the shock of the earthquake….had opened vertical fissures from base to top: the water rushing through these fissures simply floated the dam out in sections". The accounts suggest that sliding occurred as a result of reduction of shear strength of the soil due to the pore water pressure enhancement by the earthquake shaking.

San Fernando Dam

The lower Fernando dam located in southern California was hit by a 6.6 Richter scale earthquake in 1971. The major failure mode occurred on the dam was upstream liquefaction. The dam was a hydraulic fill with a clay core overlying on a 5m alluvium deposit.

Figure 11: Liquefied lower Fernando dam upstream face

In 2006 in Canada, on Canadian Geotechnical Conference, the GEO-SLOPE International Ltd presented the evaluated case of the dam failure by modeling it using Geo-Studio software. The model showed similar result as the real phenomena occurred presented by Figure11. (Liquefaction of upstream face)

And the report concluded that analysis of a dam Using QUAKE/W in conjunction with SEEP/W, SIGMA/W and SLOPE/W provides a much clearer picture than using QUAKE/W in isolation.

3. Methodology

3.1 Data collection

One of a major challenge in dynamic analysis is availability of data. Geometrical, material property and earthquake data inputs are the major categories of the necessary data inputs. These data are collected from project office & reviewed literature. The dam zone and material data is collected from the project office. The feasibility study final submitted document before proceeding to the detail design is assessed for the dynamic stability. Cross-sections at different chainages compared and the most vulnerable section for dynamic instability has been taken. This is done by considering the alluvium deposit thickness of foundation and the section size.

3.2 Methods of analysis

3.2.1 Steady state seepage

To compute the seepage discharge and the phearatic line which will be used for both the initial stress and dynamic analysis of the dam, the steady state seepage analysis when the reservoir water level is at normal level was first computed by the Seep/W component of the Geo-Studio 2007 software developed by the GEO-SLOPE International Ltd, in 2007. Seep/W uses darcy's law. The steady state analysis of Seep/W assumes that the water inflow is equal to the water outflow. During the analysis of rapid drawdown stability, transient seepage, in which the inflow is not equal to outflow, is used.

The material model used in the seep/W component is saturated/unsaturated for all the materials.

In unsaturated soil, the difference between the air and the water pressure, the matric suction varies the volume of water stored in the soil. To account for this the sample function in the software are used by inserting the saturated water content for the materials. Saturated water content is almost equal to the porosity of the soil. Hydraulic conductivity of materials is also defined with respect to the matric suction. Having the boundary condition of the static water pressure up to the normal water level in the upstream side, zero pressure water is expected at the rock toe of the dam.

3.2.2 Liquefaction Potential

At the time of loading, particles will try to rearrange their distribution to retain equilibrium. During this time a load will be transferred to pore water, creating an increase in pore water pressure. This minimizes the effective stress on the soil solid particle which in turn decreases the stress and internal friction angle component of shear strength. When it decreases to zero liquefaction will occur. Cohesionless soil of loose sand and saturated sand will not have any remaining shear strength at this condition due to their zero cohesion shear strength.

Assessment of liquefaction potential of the dam and foundation was conducted classifying the dam and the foundation material in to two broadly.

- Granular material assessment: - During earthquake load, liquefaction may occur in parts of the dam. Assessment of liquefaction potential of the mixes was conducted using the particle size distribution based Tsuchida graph. (Sitaharam,unknown) The graph is shown in Figure 12. This criterion considers uniformity, grading and particle size of the material for determining liquefaction potential. In the graph there is a region of boundary for most liquefiable soil, which is narrow showing more uniformity of particle size. But mostly the outer boundary for potentially liquefiable soil is a region of evaluation as in our case.

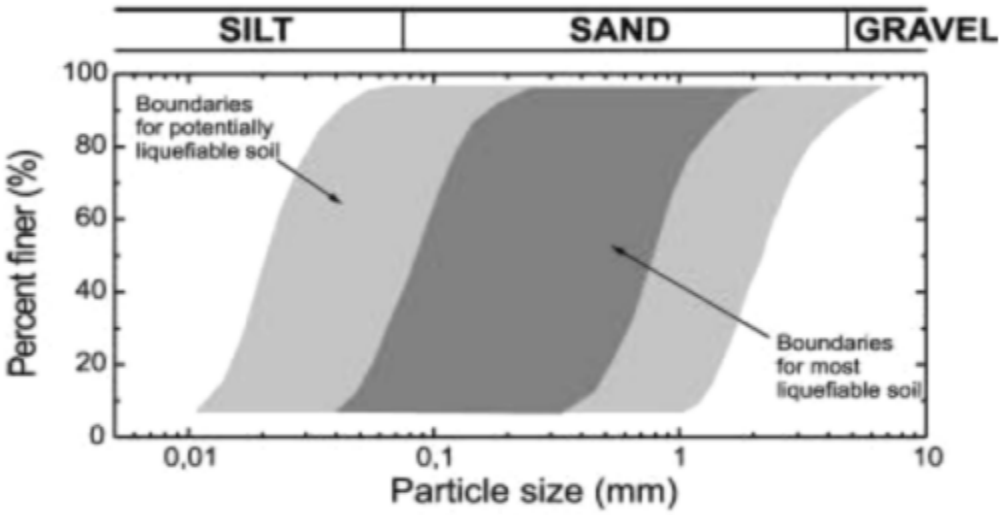

Figure 12: Tsuchida curve (Sitaharam,unknown)

The particle size distribution of material under liquefaction assessment must be drawn on the graph to determine the percentage of the soils having a tendency of liquefaction.

- Fine particles assessment: - This was done by using the model developed by Seed and Idriss (1982) which indicates that clayey soils could liquefy if all the three of the below requirements are met.
  - Clay content<=15% by weight (particles smaller than0.005)
  - The liquid limit is <=35%
  - The natural moisture content is >=0.9 times the liquid limit

3.2.3 Earthquake time history data, period and peak ground acceleration modification

In earthquake dynamic analysis time history data is fundamental but it is also the mostly unavailable data input. Recorded time history data is not available for Middle Awash dam site. So, following the approach of the Army Corps of Engineers recommendation

for selecting time history data, elsewhere recorded time history data compared considering this points of resemblance with the site which is on analysis.

- Tectonic environment
- Earthquake magnitude and type of faulting
- Earthquake source to site distance

After selection of the time history data, modifying its amplitude to the design base and maximum credible earthquake amplitude of the dam area is done to make it fit to the site condition.

For embankment dams, the frequency range is 0.5-5 hertz. Which means the period is from 0.2-2 second. Taking the 0.2 sec period ground acceleration will make the analysis conservative.

For Maximum Design Earthquake take ground motion which has a 10 percent chance of being exceeded in a 100-year period. (1000 years of return period) For Design Base Earthquake, ground motion which has 144 years of return period for the 100 year of project service life is taken. (Army Corps of Engineers, 2003)

The Ambrasey's equation for determination of period of a structure is adopted to determine the dam's period.

$T=2.61H/V_s$ ..... Equation 2: Ambrasey equation of dam's period

Where, T= period in second, H= the dam height and = V_s the shear wave velocity, which is a function of maximum shear modulus and density.

3.2.4 Initial static stress

The initial static stress is done before the dynamic analysis. The dynamic analysis gives the shear stresses due to the self weight, pore water pressure, hydrostatic pressure and the cyclic shear stress. In order to determine the specific dynamic shear stress, which is responsible for deformations and slope instability, the stress determined by the initial static stress is subtracted from the dynamic analysis stress. The constitutive material model selected for the analysis is elastic-plastic. In the analysis a pore water pressure contributes for the strength of the soil by altering the matric suction.

The Sigma /W analysis have a boundary condition constrained in both left and right borders by zero horizontal displacements. And the lower border of the analysis is also constrained by both zero vertical and horizontal displacements.

3.2.5 Slope stability analysis before the earthquake shaking

This section of the analysis is used to compare the instability occurred on the slope due to the earthquake after shaking. To do this the SLOPE/W component of the GEO-STUDIO software has been used.

The SLOPE/W component of the software uses the limit equilibrium analysis technique in the numeric. Limit equilibrium technique of numerical analysis tries to satisfy the equilibrium of statics.

For both the upstream and downstream face of the dam at steady state seepage, the slope stability factor of safety is determined before the earthquake. It can easily be guessed that the factor of safety for the upstream is more than for the downstream, because of the additional hydrostatic normal force of the impounded water in the upstream face.

The analysis used in this slope stability determination is the Spencer type. The Spencer type slope stability analysis tries to satisfy both the horizontal and moment equilibrium of statistics. The pore water pressure found in the Seep/W component is a parent for this analysis, to know the saturated part of the dam and foundation. The constitutive model for the materials is Mohr-Coulumb.

3.2.6 Material property and constitutive model for dynamic analysis

In an Equivalent- Linear model, soil stiffness is modified in response to computed strain in this model. This model starts the dynamic analysis with a specified stiffness of the soil. Then stiffness was modified by the computed strain for the next analysis. In such a way one specified stiffness stays for a specific iteration and gets changed when passed to the next.

The model requires the following parameters.

- Unit weight
- Poisson's ratio
- Effective cohesion
- Effective Internal friction angle
- Shear modulus reduction function
- Pore-water pressure function
- Cyclic number function
- Damping ratio
- Maximum shear modulus
- Correction coefficient for overburden
- Correction function for shear stress

Shear modulus reduction function is a function which the reduction in shear modulus is expressed in terms of the strain occurred. These functions for different soils and materials of the dam are obtained from the Shake (2000) software sample functions published by Seed and Idriss (1990) and Gazetas-Soil dynamics and Earthquake Eng. (1992).

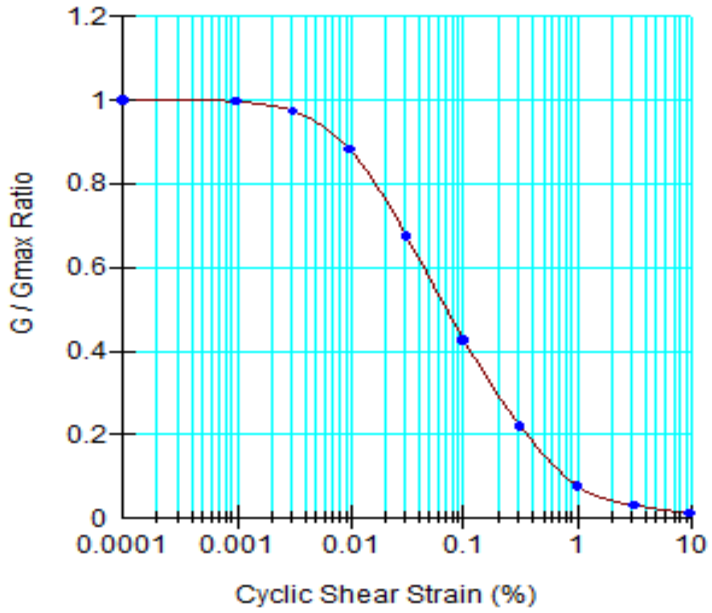

Figure 13: Typical Shear modulus reduction function for clay with plasticity index between 20-30, developed by Seed and Idriss

The damping ratio function is a function which explains the increasing response of the soil to dissipate energy as the strain gets higher. These functions for different soils and materials of the dam are obtained from the Shake (2000) software sample functions published by Seed and Idriss (1990), Gazetas-Soil dynamics and Earthquake Eng. (1992)

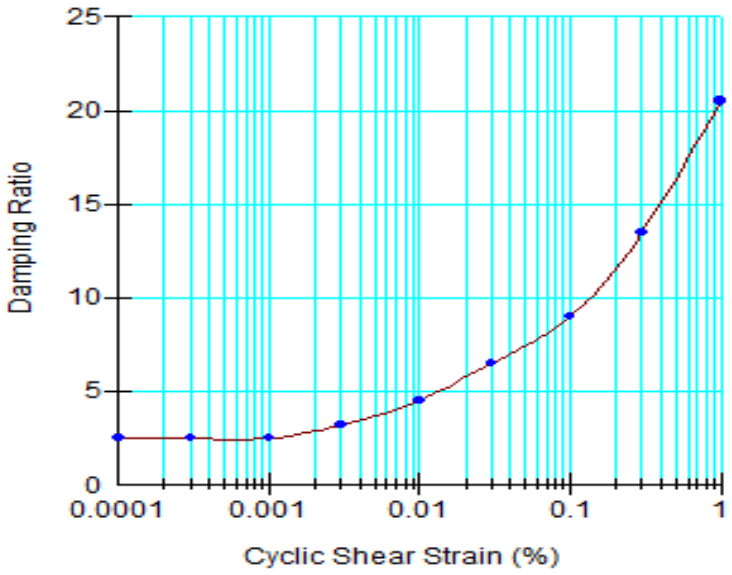

Figure 14: Average damping ratio for clays

This is the equation used by the Sigma/W to determine the pore water pressure, U.

$$r_u = \frac{1}{2} + \frac{1}{\pi}\sin^{-1}\left[2\left(\frac{N}{N_L}\right)^{1/\alpha} - 1\right]$$

.....Equation 3: Pore water pressure function

Where r_u = pore water pressure ratio, α= material constant and N/N_L= Stress ratio

If N, equivalent number of uniform cycles, which is a function of the earthquake magnitude and the N_L, the number of cycles , which will cause liquefaction for a particular soil under a particular set of stress condition and α, material constant are known, then r_u will be determined and pore-water pressure can easily be determined by the below function.

$u = r_u + \sigma'_{3(static)}$..... Equation 4: Pore water pressure

Where, $\sigma'_{3(static)}$ = confining pressure

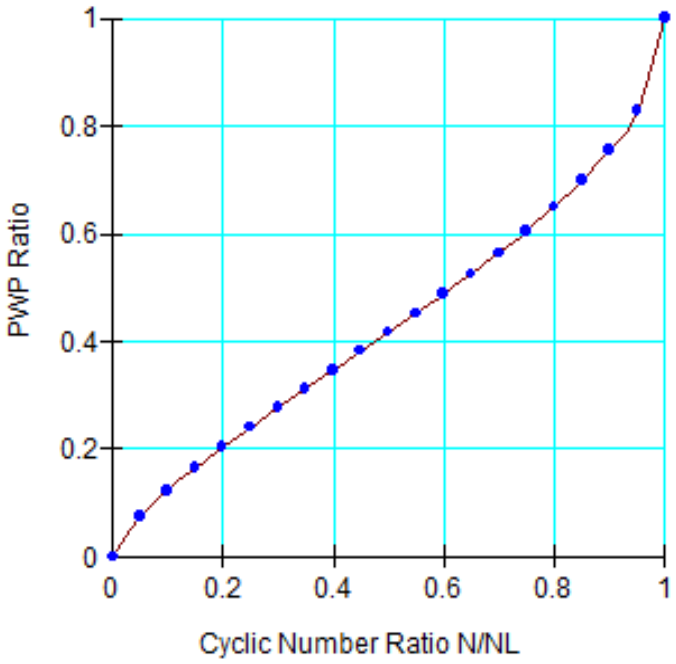

Figure 15: Typical pore water pressure ratio of alluvium deposit

3.2.7 Correction functions

As the confining stress increases the cyclic shear stress required to trigger liquefaction will increase also. The K_s correction function is attached to the cyclic number function to account for this effect. The variation of correction factor with effective overburden pressure for different soils reported by Marcuson et al. (1990) is used.

Depending on the density of the soil, the initial static stress also influences the cyclic stress required to trigger liquefaction. Depending up on the relative density for different soils, the report by Seed and Harder (1990) is used to determine shears stress correction.

3.2.8 Maximum shear modulus (G_{max})

The maximum shear modulus is a function of overburden stress. Soil which is under a thick soil layer, exhibits a greater shear modulus as compared to the same soil, but overburdened by a thin layer of soil.

For the granular soils including the rock-fill, the maximum shear modulus is determined by the below equation.

$G = K (\sigma m ') 0.5$ **.....**Equation 5: Maximum shear modulus function

Where G is the shear modulus, K_G is a soil modulus, σ m ' is the mean effective stress.

$\sigma m' = \sigma v + K o\sigma v + K o\sigma v/3$**.....**Equation 6: Mean effective stress function

Where σ_v= overburden stress, K_o=Coefficient of earth pressure at rest

3.2.9 Cyclic number function

To define the pore pressure, a cyclic number function must be developed. If the shear stress ratio is high, a few cycles might be required to cause liquefaction on the shell material. If otherwise, much number of cycles might be required to cause liquefaction. Quake/W has sample functions developed from literatures for loose, medium and dense sands. We use medium dense sand cyclic number function.

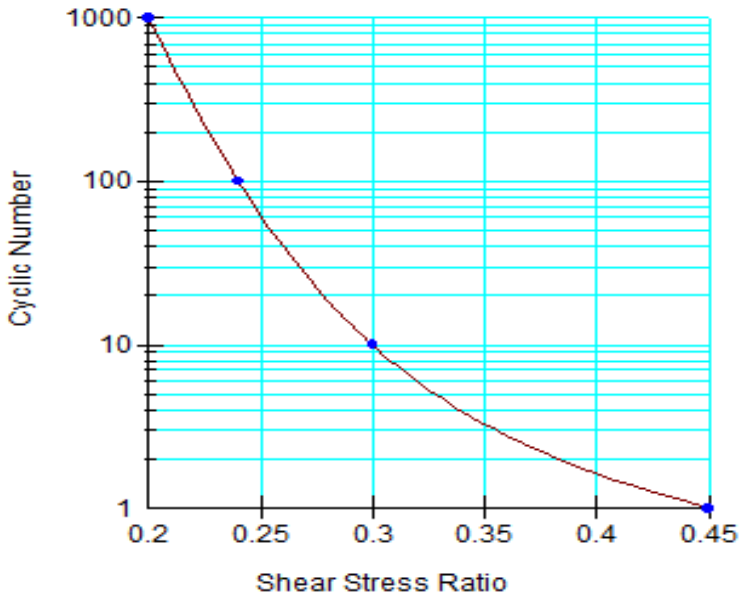

Figure 16: Typical cyclic number function for shell material

3.2.10 The slope stability after earthquake

Using the same method with that of slope stability before earthquake, the slope stability during earthquake is calculated by slice method. In the simple limit equilibrium and finite element method, which uses the stresses calculated by the Quake/W for all those fraction of seconds the slope stability is assessed for all potential slip surfaces and the critical one is considered. Additional inertial loads and dynamic shear stresses decreases the factor of safety from the static condition results.

3.2.11 Permanent deformation

For dams where pore water pressure development is not the main issue, i.e. for rock-fill and impervious homogeneous dams the permanent deformation is done by the Newmark Permanent Deformation model developed in 1965. After knowing all the dynamic shear stress along a slip surface, the average acceleration of the sliding mass will determined. Then all the average accelerations in the time of earthquake will be

plotted against time and factor of safety. The acceleration which lowers the static factor of safety to 1 is said to be yield acceleration. All the accelerations above the yield acceleration results a factor of safety below 1. During this time there is an expectation of a sliding movement along the slip surface. The movement is parallel to the slip surface. So the movement is rotational and translational. The area above the yield acceleration will be integrated to give velocity that results deformation. This velocity can be integrated to give displacement, which is summed up to give permanent deformation. This method ignores the upslope movement in reverse shear stresses.

3.2.12 Response spectrum

The material characters, dam height, dam slope and input ground accelerations altered the amplitude mainly, of the earthquake generated at the bed rock. So, the response spectrum at the crest and the base of the dam and foundation is checked to asses this.

4. Result and Discussion

4.1 Dam zones and materials

From the final feasibility design of the Middle Awash Multipurpose Dam project the selected dam type for the detail design is the Rock and shell fill with central clay core. It would have been better if all the structural material can be rock fill because of the steep slope flexibility of this type of dam. But lessons from other dams like Megech shows that after some level, production of rock for the fill will be hard, even if the quarry site have huge amount of parent rock. The shell material is mixed with rock fill due to this reason. The dam has different 5 section geometry and for this dynamic analysis of the dam, cross-section between chainage 0+235-0+240 is selected considering the thick alluvium deposit under the dam foundation and large cross-section. Recommendations for this section of the dam for the dynamic analysis of the long steady state case are conservative enough to apply for the other sections.

Below the dam features and characters are listed in words and tabular form with the dam section drawings.

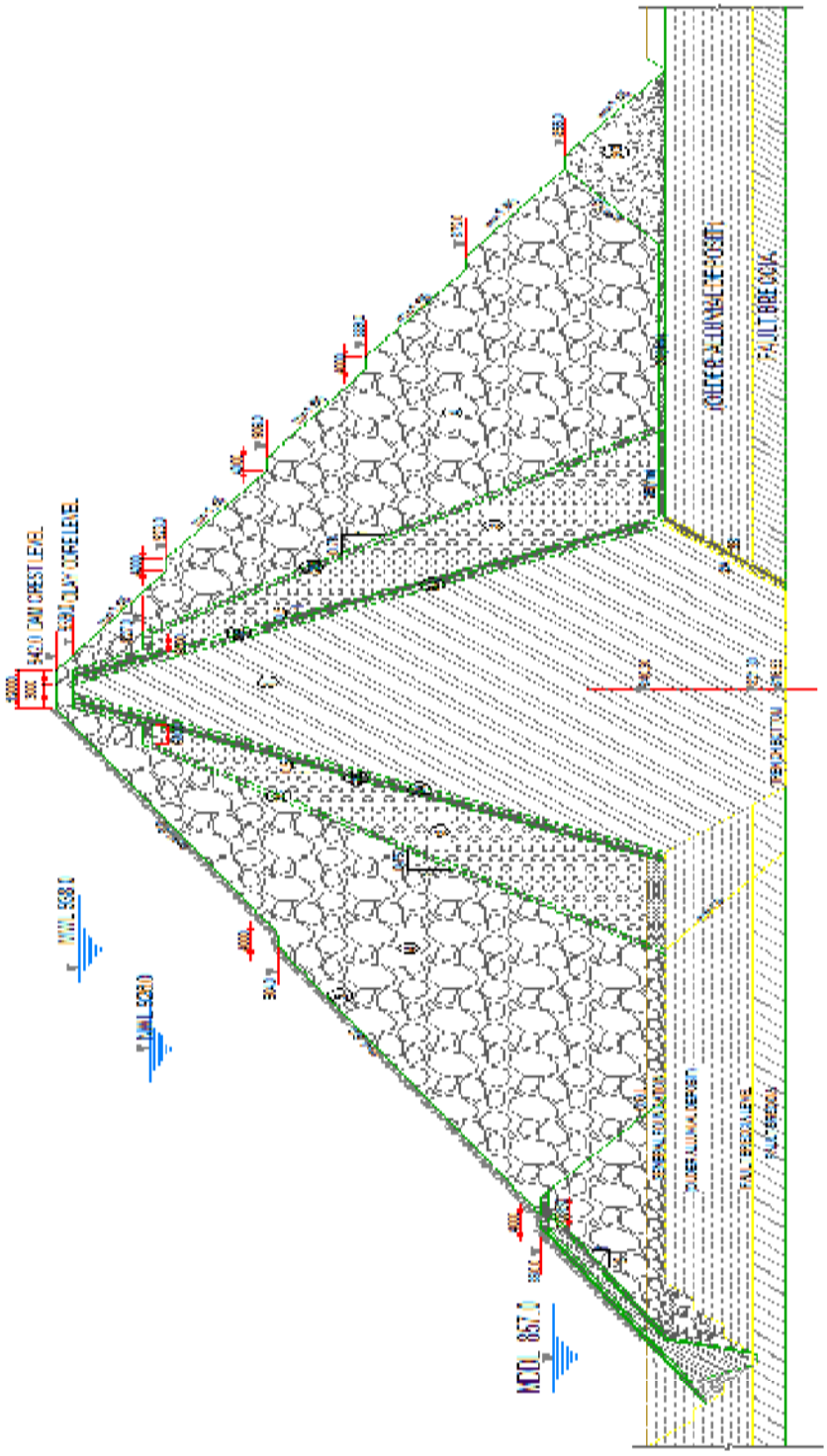

Figure 17: Geological profile at the dam axis (WWDSE, 2016)

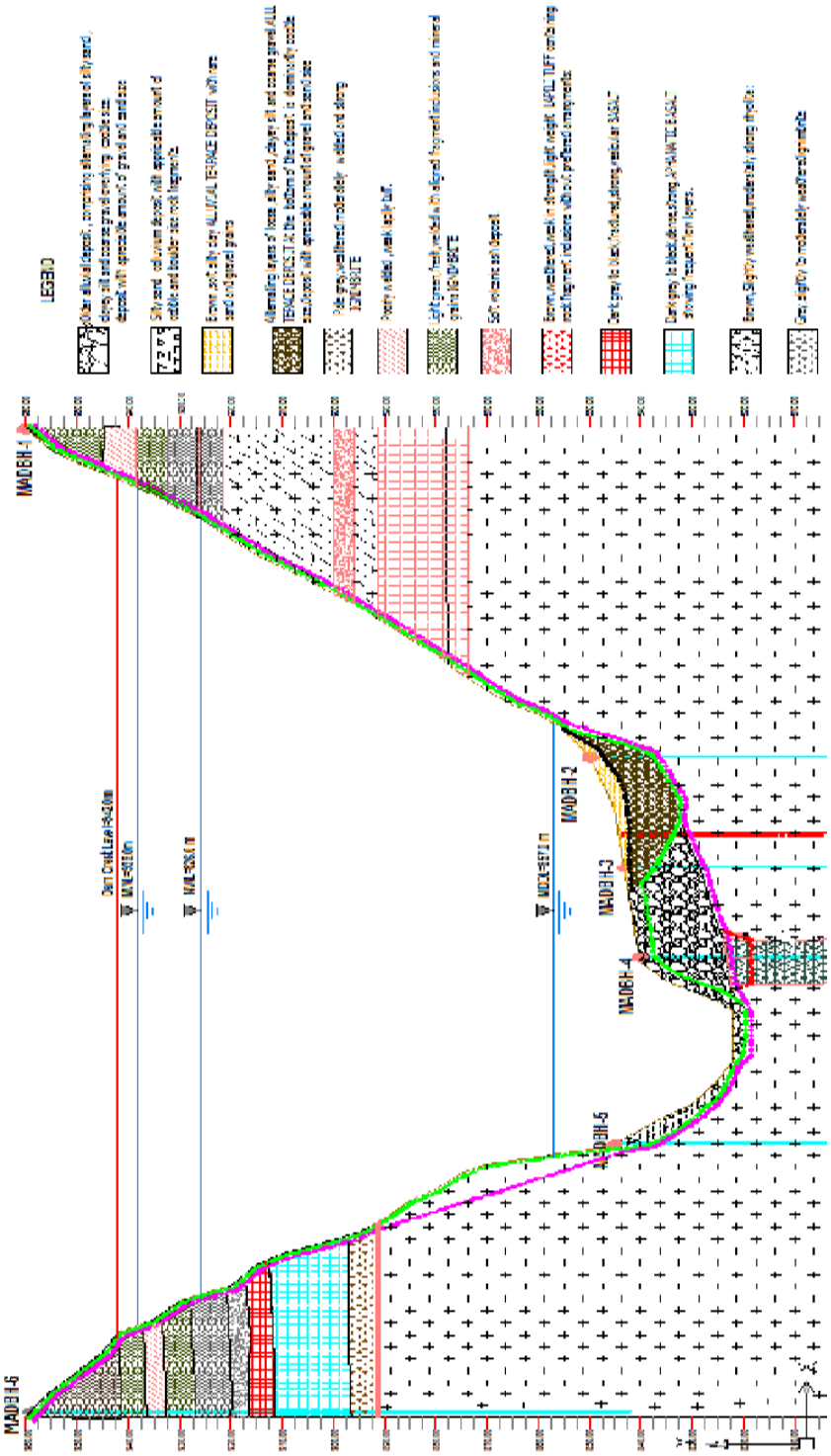

Figure 18: Geological profile at the dam axis (WWDSE, 2016)

Table 3: Zones and material properties (WWDSE, 2016)

Zone	Function	Unit Weight (KN/m^3)	Permeability (m/s)	C'(Kpa)	$\phi'^{(o)}$
1	Core	16.0	$4.76x10^{-8}$	20	23
2A	Fine filter	18.0	0.001	0.0	32
2B	Coarse filter	18.0	0.0019	0.0	34
2C	Transition	18.0	0.005	0.0	34
3	Granular shell	18.0	0.0017	10.0	34
4	Rock fill	22.0	0.01	0.0	42
5	Riprap	22.0	0.01	0.0	42
6	Rock toe	18.0	0.005	0.0	38
7	Old Alluvial	18.0	$1x10^{-5}$	10.0	34.0

Dam features

- Dam height above river bed: 124.75 meter
- Dam height above deepest foundation: 101 meter
- Crest level: 942 m.a.s.l
- Normal water level: 926 m.a.s.l
- Maximum water level: 938 m.a.s.l
- Minimum drawdown level: 857 m.a.s.l
- Crest width: 12 meter
- Crest length: 453 meter
- Upstream berms: 2 with a width of 4 meter
- Upstream slope: 1.9
- Downstream berms: 5 with a width of 4 meter
- Downstream slope: 1.65
- Fill volume: 7849169.18 m^3
- Alluvium deposit thickness below the dam: 15 meter

The Geo-studio dam zone and material is modeled as shown in figure 18.

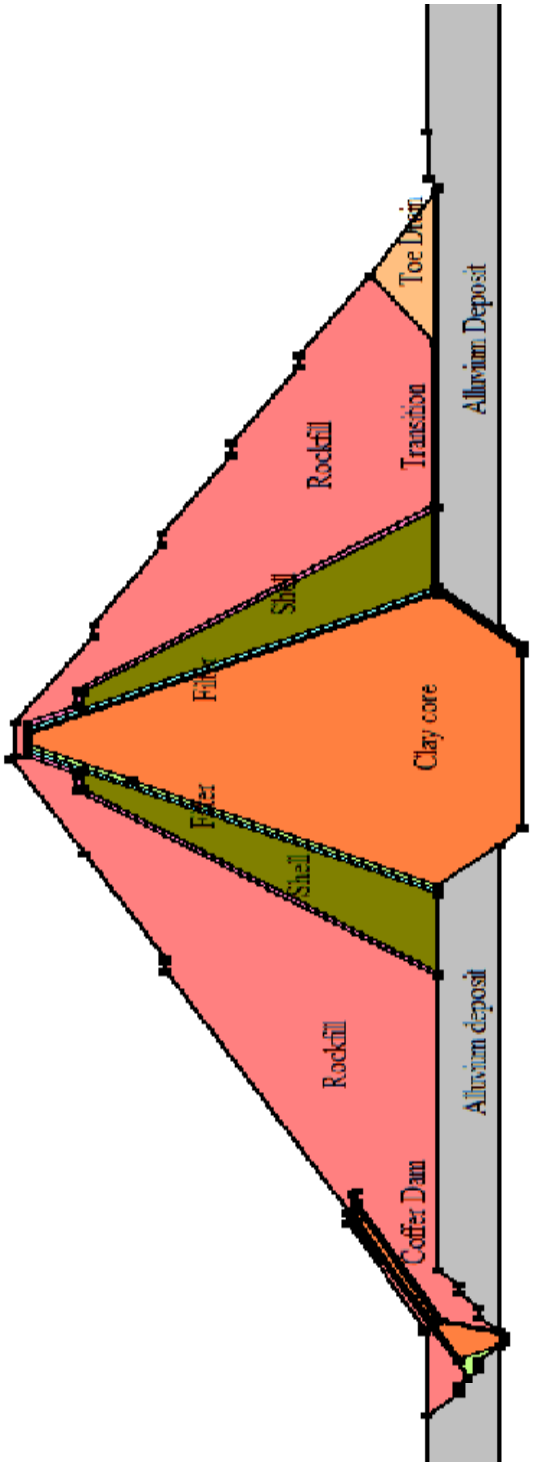

Figure 19: Geo-studio dam zone and material representation

4.2 Steady state seepage

To compute the seepage discharge and the phearatic line which will be used for both the initial stress and dynamic analysis of the dam, the steady state seepage analysis when the reservoir water is at normal level, is first computed by the Seep/W. The result of the analysis displayed that the seepage through the dam core is $3.2272*10^{-6}$ m^3/s, in meter width of the dam. The pore water pressure estimated is as below in figure 19.

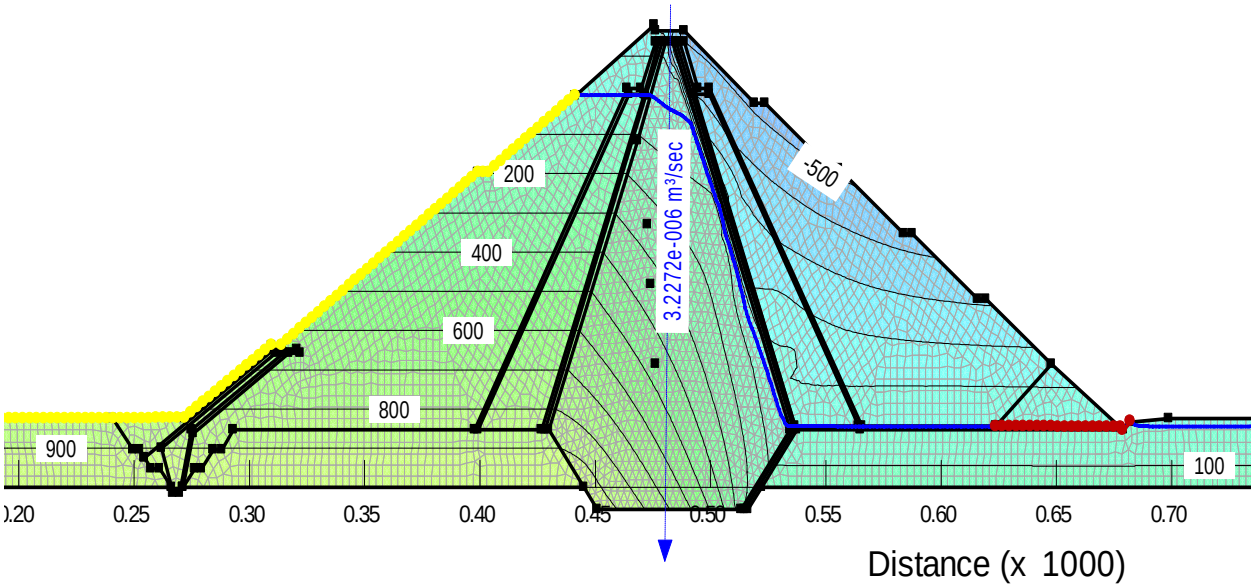

Figure 20: Steady state seepage result

4.3 Liquefaction potential assessment

Liquefaction potential assessment is done for different sections of the dam prior to determination of liquefied region.

❖ Main dam body which comprises

- The rock fill: - rock fill are neglected for liquefaction potential assessment because pore water pressure development is almost nonexistence due to much pore space between rocks.
- The clay core: - Seed and Idriss (1982), suggests that clayey soils could liquefy if all the three of the below requirements are met.
    - Clay content<=15% by weight (particles smaller than0.002)
    - The liquid limit is <=35%
    - The natural moisture content is >=0.9 times the liquid limit

During the geologic and material investigation, two borrow area for the clay core was identified: Borrow Area1 and Ettissa and Kurkura area.

Cases where clay content are fewer than 15% and liquid limit which are less than or equal to 35%, are very few, and both do criteria's do not meet simultaneously. This lead to the conclusion, that the clay core of the embankment dam is not potentially liquefiable.

- The shell material: - liquefaction potential of a soil material is highly influenced by relative density and particle size distribution of the soil. The shell material sample selected for dam at different pits shows that the gravel content is between 37-98%. This lies outside of the potential region.

❖ Foundation

Alluvium deposit of the slope (shell and rock fill) foundation comprises thick older terrace alluvial deposit consisting of dense granular terrace alluvial deposit predominantly coarse gravel and cobble sizes with minor fine proportions. Its thickness ranges from 13-17 meters. As figure 21 below indicates, 70% of the material and 53 % of the material are in potentially liquefiable and most liquefiable region in the chart,

respectively. The predominant cobble size and coarse gravel material volume of the foundation indicates that the thick older alluvium deposit decreases the liquefying potential significantly. But evaluation for liquefaction must be done considering worst case.

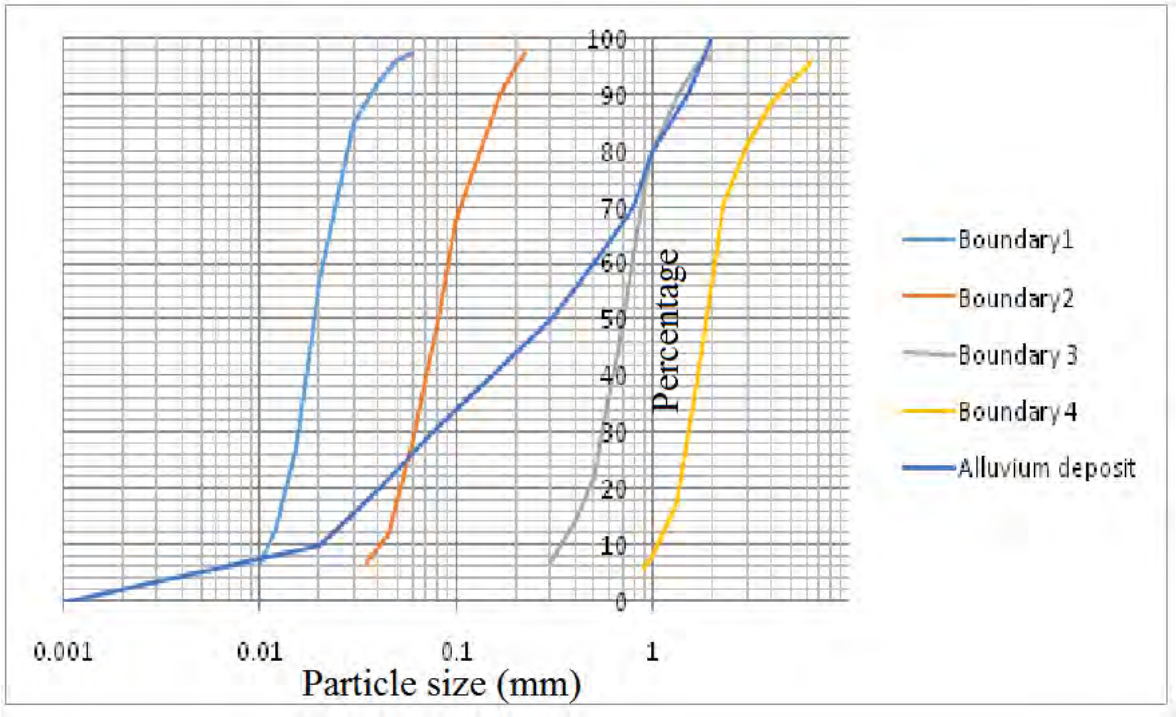

Figure 21: Alluvium deposit liquefaction assessment graph

In the above figure boundary 2 and boundary 3 are boundaries of most liquefiable soils. Boundary 1 and boundary 4 are boundaries of potentially liquefiable soils.

4.4 Earthquake time history data and peak ground acceleration modification

The Ambrasey's equation for determination of period of a structure is adopted to determine the dam's period. The dam period is found to be 0.33 sec considering the highest shell material shear modulus. Then the 0.2 sec period amplitude is selected being sufficiently conservative.

The below site specific hazard assessment report table presented the ground motion amplitude in percentage of gravity (%g) for rock and soil sites at different periods of motion and for different return periods at the Middle Awash multi-purpose dam project site.

Table 4: site specific acceleration of ground during shaking (WWDSE,2016)

Return periods in years	Ground Motion Amplitude in % of g for Boore-Joyner-Fumal (1993,1997)					
	Period =0.2sc		Period =1.0sc		Period =2.0sc	
	Rock	Soil	Rock	Soil	Rock	Soil
50	11.24	11.93	3.84	4.34	2.62	2.87
100	15.46	16.44	4.99	5.68	3.3	3.65
200	21.2	22.51	6.48	7.42	4.15	4.64
500	31.52	33.47	9.17	10.58	5.64	6.38
1,000	41.07	42.66	11.91	13.83	7.1	8.12
10,000	69.85	74.35	27.22	31.65	15.31	18.08

For Maximum Design Earthquake take ground motion which has a 10 percent chance of being exceeded in a 100-year period. (1000 years of return period) The selected peak ground acceleration corresponding to the Maximum Credible Earthquake for this design is 0.4107g. The material is chosen to be rock because the time history data is deconvolved.

For Design Base Earthquake, ground motion which has 144 years of return period for the 100 year of project service life is taken. (Army Corps of Engineers, 2003) The selected peak ground acceleration corresponding to this design is 0.212g. The material is chosen to be rock because the time history data is deconvolved.

Figure22 presents the site specific hazard assessment report presented a time history data for an earthquake happened in Hossana, and which was recorded in Addis Ababa. But the amplitude of this seismic data is very undermining the probable earthquake, which will likely occur.

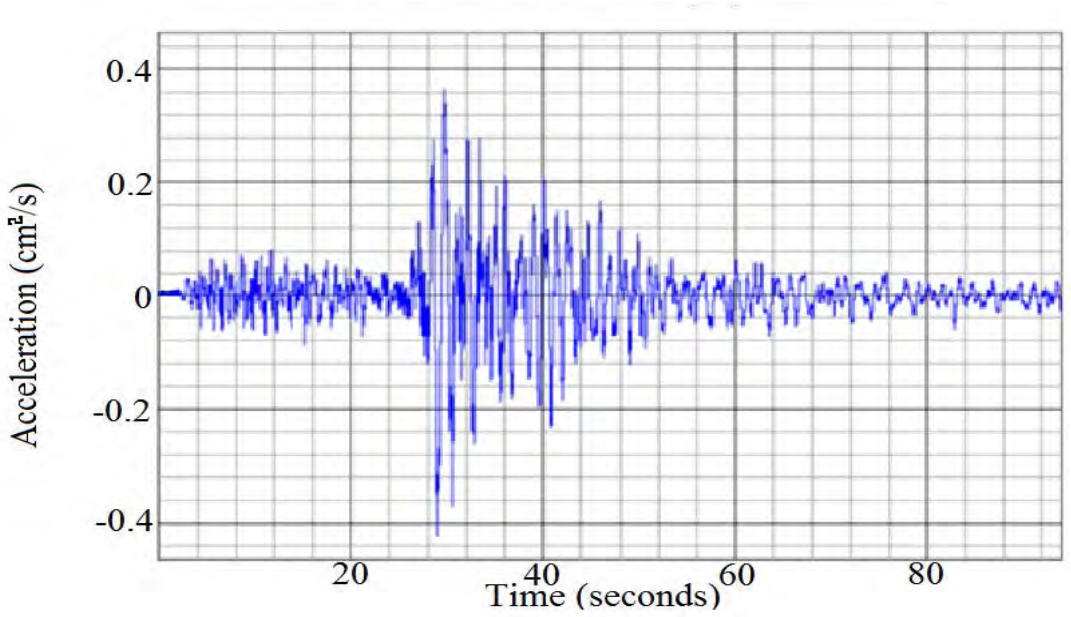

Figure 22: Time history data of earthquake that happened in Hossana on December 19, 2010, and which was recorded in Addis Ababa (WWDSE, 2016)

Because of the lack of time history data that fit the site, a deconvolved time history data, which eliminates site and path effects from other recorded earthquakes, will be used for the dynamic analysis. (Messele, 2006)But scaling or modification to the site peak ground acceleration need to be done. The selection of the time history data is based on

the earthquake magnitude and hypo central distance. The site specific hazard assessment report indicates that the earthquakes in Ethiopian rift valley are less than 15km in depth. In addition the sites near recorded Kara Kore earthquakes have a magnitude of 3.5-6.5 in Richter scale. Based on these two facts three recorded data elsewhere are selected. In addition as the below consecutive figures presents, the range difference of frequency and duration of the selected earthquakes widens the evaluation conditions.

- The 1940 Elcentro Record, USA (M=6.7, H=11km, R=11.5km)
- The 1995 Kobe JMA Record, Japan (M=7.2, H=14.3km, R=19km)
- The 1968 Hachinohe Record, Japan (M=7.9, H=0km, R=200km)

The vertical ground acceleration is taken to be half of the horizontal. (Messele, 2006) Scaling to the site peak ground acceleration and modification is done after selection. The below figures are the sample modified time history data of the dam site for Elcentro earthquakes.

i. The 1940 Elcentro Record, USA (M=6.7, H=11km, R=11.5km)

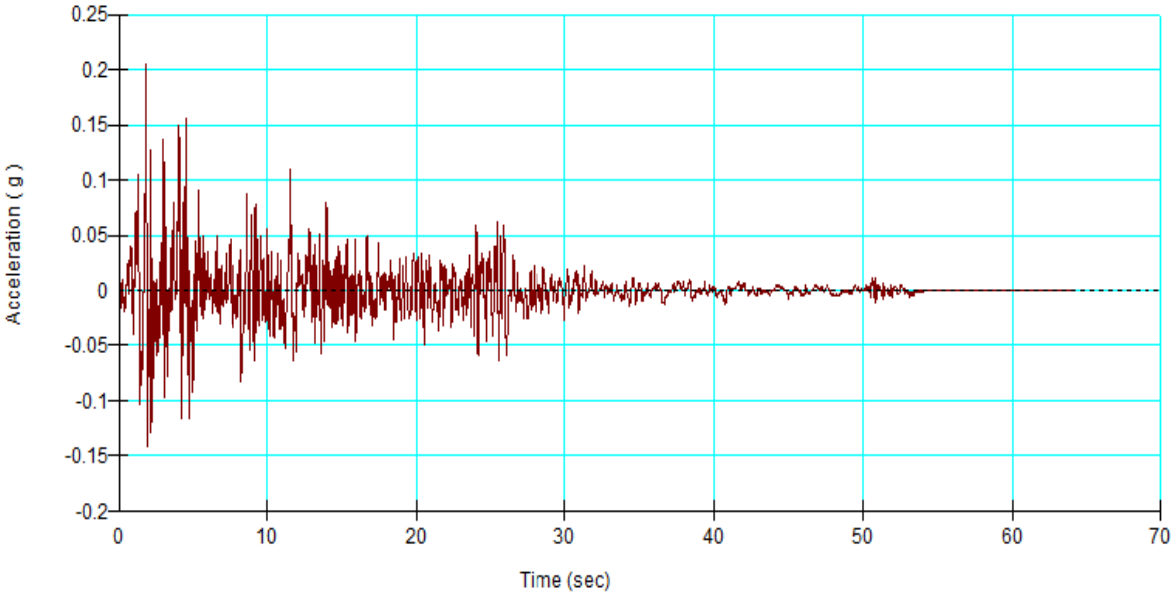

Figure 23: Maximum Credible Earthquake: Horizontal

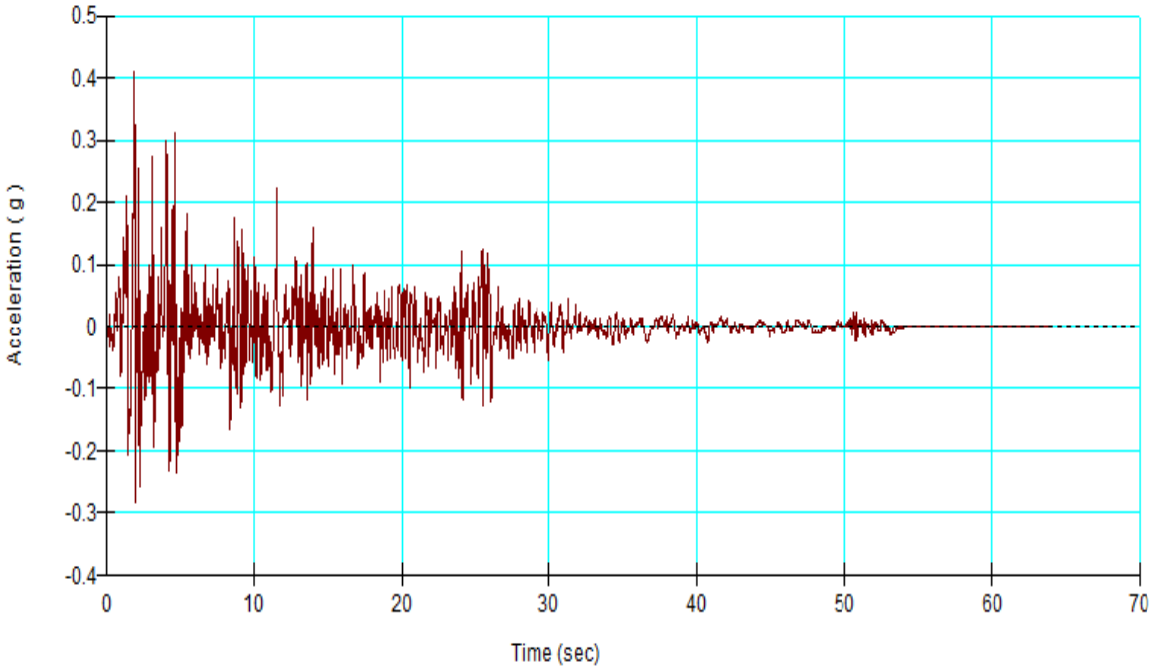

Figure 24: Maximum Credible Earthquake: Vertical

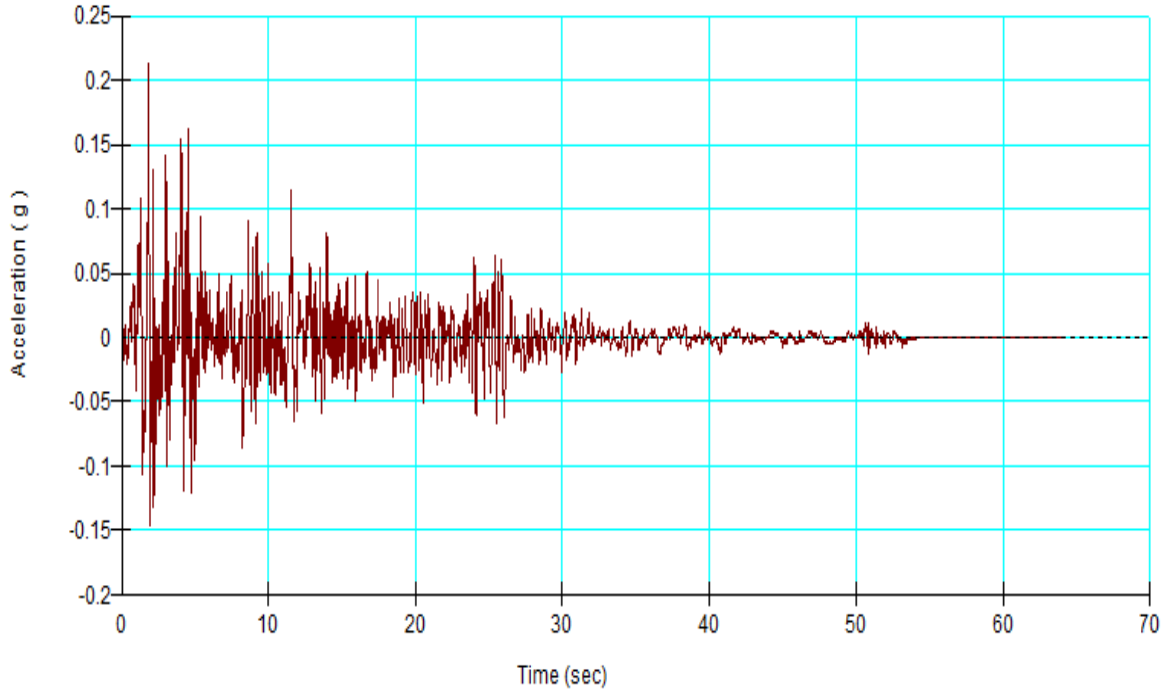

Figure 25: Design Base Earthquake: Horizontal

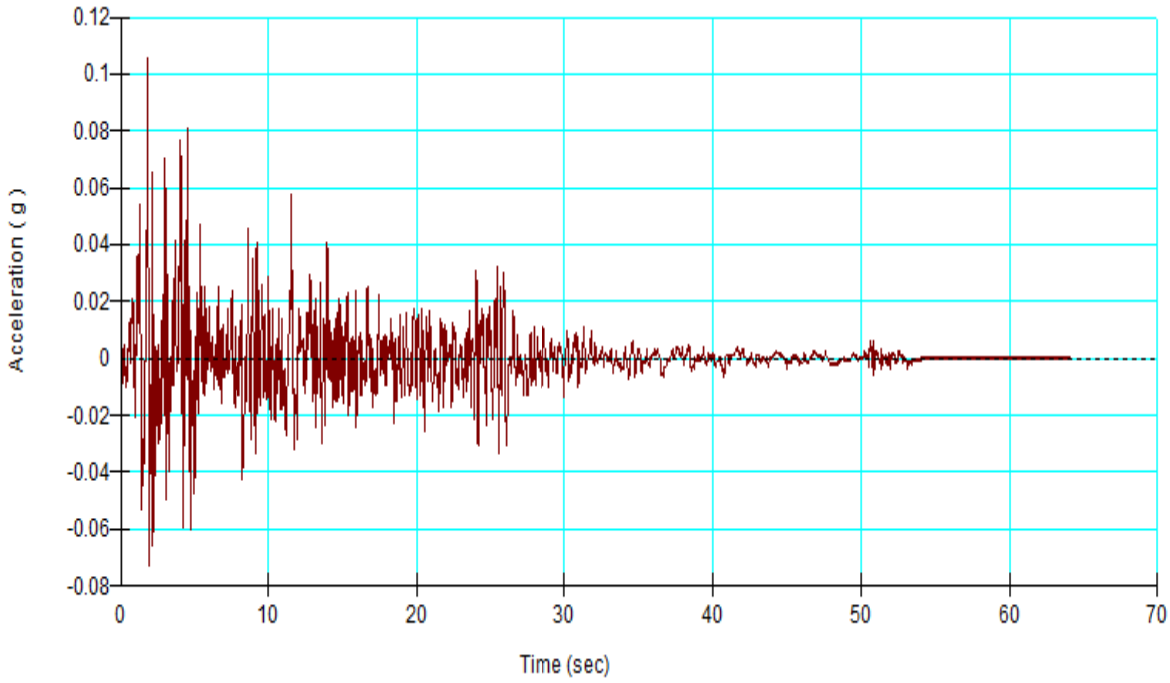

Figure 26: Design Base Earthquake: Vertical

4.5 Initial Static Stress

The constitutive material model selected for the analysis is elastic- plastic. In the analysis a pore water pressure which contribute for the strength of the soil, described by the matric suction are used. The material properties displayed in the below table are collected from the feasibility design document.

Table 5: Zone material properties (WWDSE)

Material	Unit Weight, γ (kN/m^3)	Poisson's Ratio, v	Damping Ratio	Modulus of Elasticity, E (kPa)	Maximum Shear Modulus, G_{max} (kPa)
Zone 1 (Core)	16	0.35	0.1	20,000	7,407
Zone 2a,2b (Filter)	18	0.30	0.12	50,000	19,231

Zone 3 (Shell)	18	0.3	0.1	100,000	38,461.5
Zone 4 (Rockfill)	22	0.15	0.1	50,000	21,739
Rhyolite Light Grey	24	0.18	0.1	2,000,000	847,458
Old Alluvial	18	0.2	0.1	100,000	41,6667

The Sigma /W analysis have a boundary condition constrained in both left and right borders by zero horizontal displacements. And the lower border of the analysis is also constrained by both zero vertical and horizontal displacements. The result of effective stress in the region of the embankment is displayed below with a labeled contour.

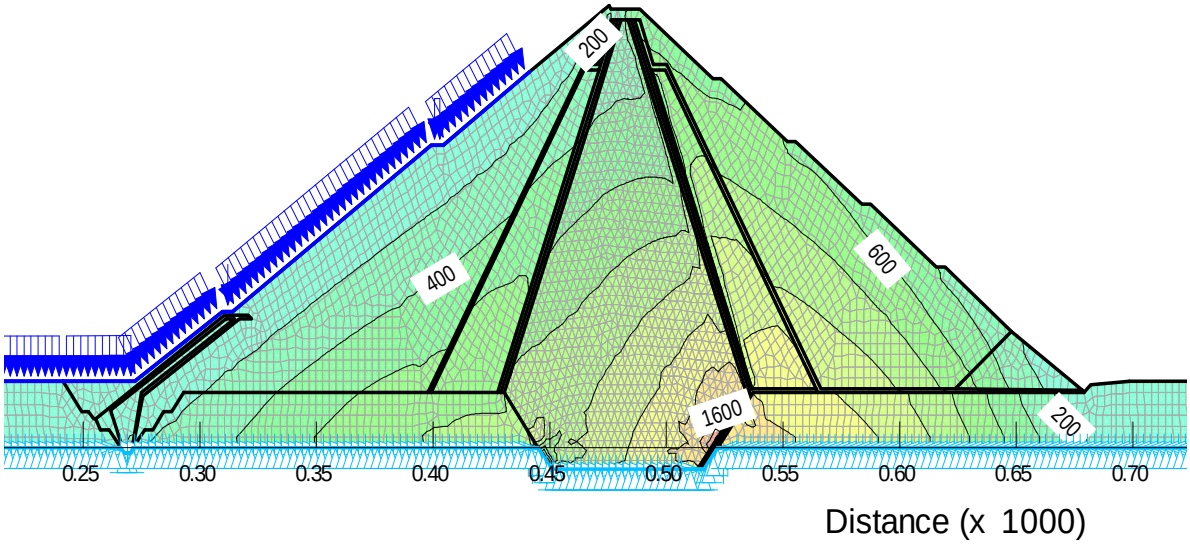

Figure 27: Effective stress distribution on the dam body and foundation

As the graphic result presents, maximum effective stress is recorded at the downstream toe of the clay core. (1600kpa) Effective stress is computed by minimizing pore water pressure from total stress. Due to the above stored water pore pressure, the upstream toe is a region where minimum effective stress is recorded.

4.6 Slope stability analysis before the earthquake shaking

The limit equilibrium and the finite element analysis method result for both upstream and downstream slope stability analysis before earthquake is done for comparison and for the assurance of static stability. For the upstream slope the calculated factor of safety in FEM and LEM method are 1.639 and 1.772, respectively against slope instability. For the downstream slope the calculated factor of safety in FEM and LEM method are 1.484 and 1.660, respectively against slope instability. Sliding masses and slip surfaces are presented by the consecutive below figures of the analysis result.

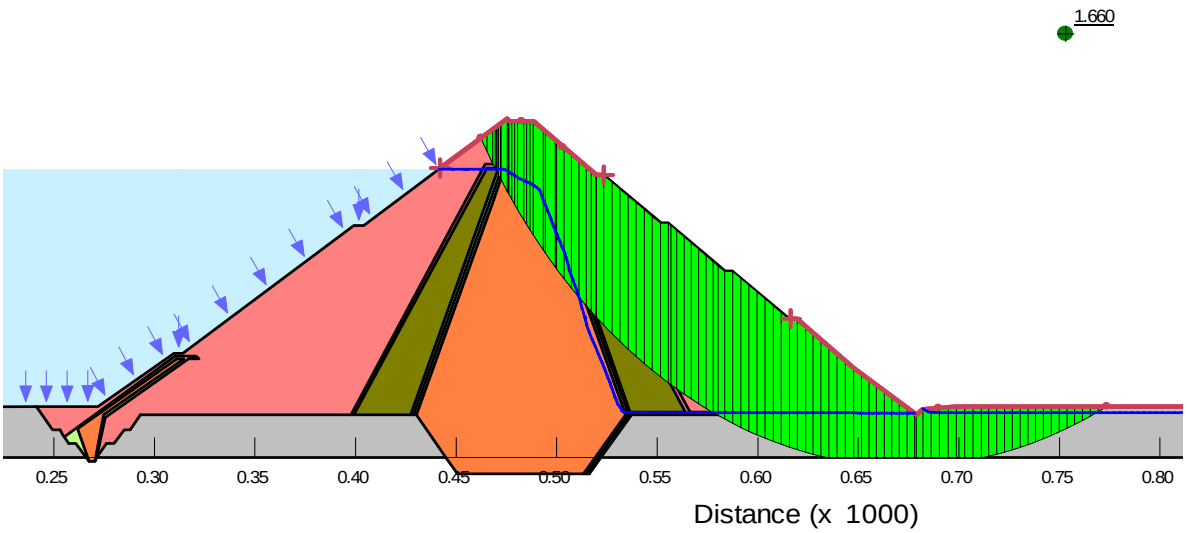

Figure 28: Downstream LEM

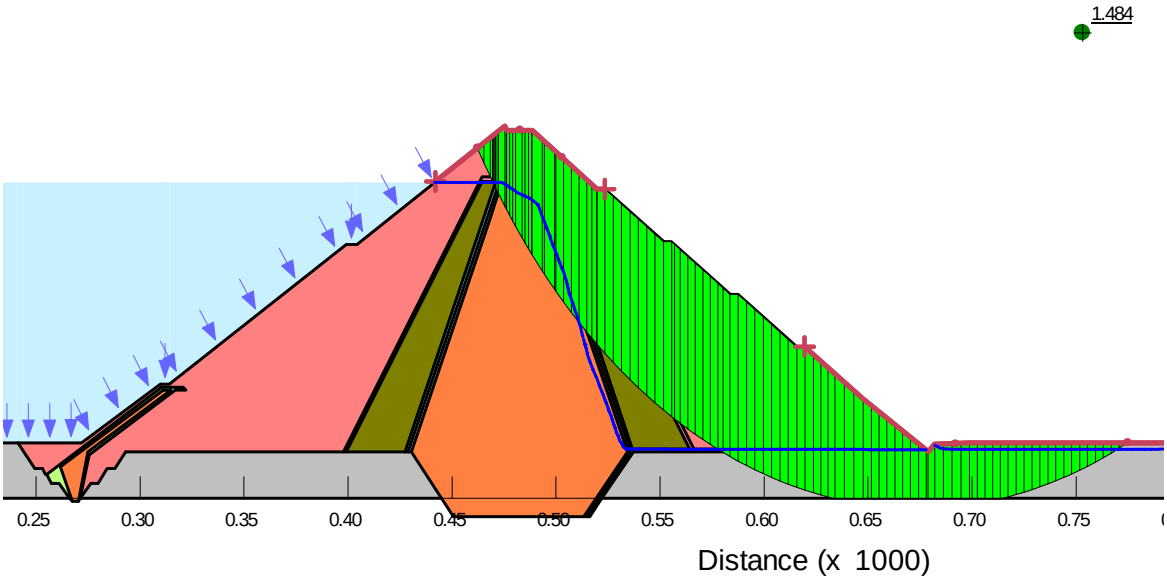

Figure 29: Downstream FEM

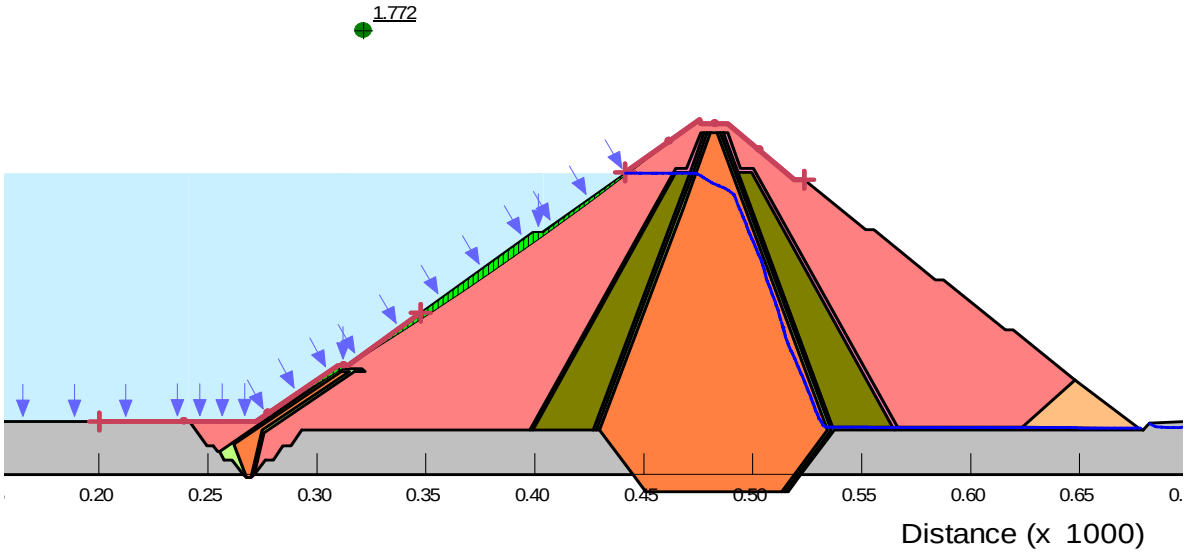

Figure 30: Upstream LEM

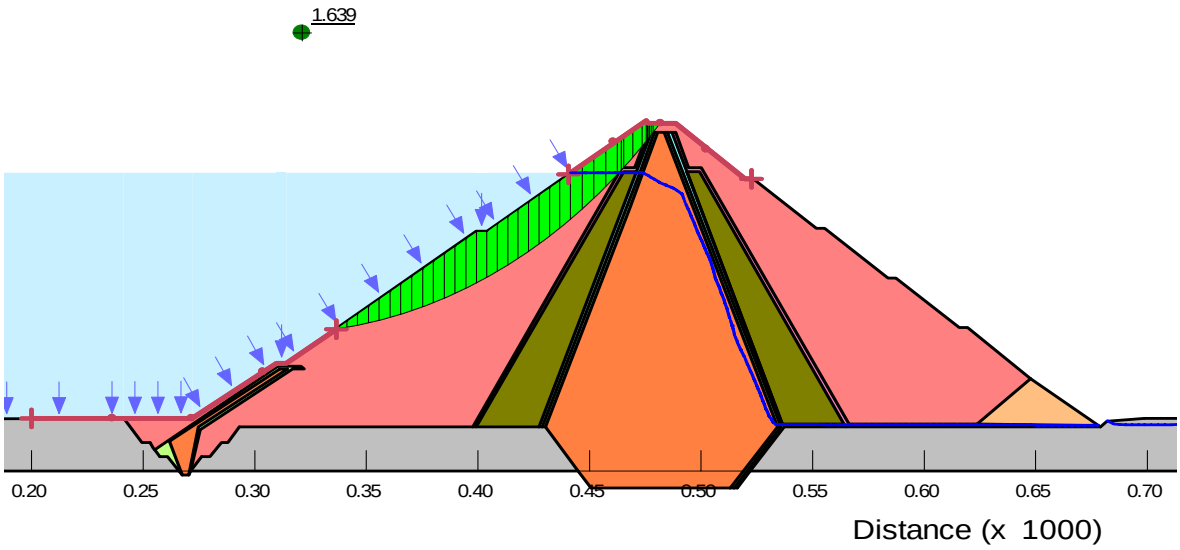

Figure 31: Upstream FEM

The factor of safety for a static condition at steady state seepage where the shear parameters are effective, the minimum required factor of safety is 1.5. (USBR, 2011/US Army Corps of Engineers, 2003) In our case, all computed factors of safety are greater than the minimum required 1.5, except the FEM calculated downstream slope stability factor of safety, which is very near. The slip surface chosen by FEM and LEM method in the downstream cases are similar. But, in upstream case the FEM slip surface is deep as compared to that of the LEM.

4.7 Dynamic analysis

The material property used in the dynamic analysis, which are collected from the feasibility design document are presented in the below table.

Table 6: Material properties of the dam and foundation (WWDSE, 2016)

Material	Unit Weight, γ (kN/m^3)	Poisson's Ratio, ν

Zone 1 (Core)	16	0.35
Zone 2a,2b (Filter)	18	0.3
Zone 3 (Shell)	18	0.3
Zone 4 (Rockfill)	22	0.15
Fault Breccia	17	0.25
Old Alluvial	18	0.2

4.7.1 Finite Element Modeling

The finite element model is done with both structured and unstructured mesh, depending on the geometry. The model consists of 4960 nodes in which equations are checked, and 5702 elements, where material properties are extracted. The Geo-Studio manual recommends elements not more than 1000 to shorten time of analysis and to avoid results which might be complex for interpretation. But, since Middle Awash dam is very large with a height above 100m, refined result with a realistic graphical representation must be considered including verification of the results by manual calculation at check points. The quads and triangular element geometry is selected for their compatibility in unstructured mesh.

The analysis tree followed for each type of earthquake (Elcentro, Kobe, Hachinhoe) in considered earthquake amplitude (DBE and MCE) is presented in the below figure.

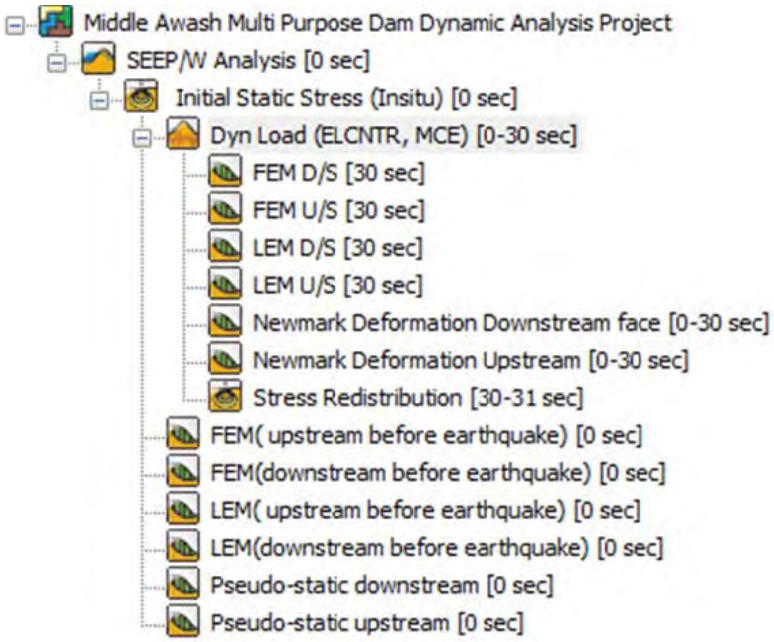

Figure 32: Analysis tree followed in Geo-studio

4.7.2 Amplification of acceleration in the dam body

Amplification of the bedrock acceleration amplitude is dependent on many factors including dam height, downstream and upstream slope, material properties and the input motion. The higher is the dam, the smaller the amplification in the crest level. On the other hand, the amplification distribution along a clay core earth-fill dam depicts that amplification in the upper part of the dam (approximately 80% of the dam height) is larger than the amplification at crest level. (Pelin Özener1 and Burak Kayhan Beşli,2014)

The above fact is revealed in the dynamic analysis result of Middle Awash multipurpose dam. The highest amplification of motion occurred at the 88m height of the dam above the river bed level. (0.84height of the dam) The analyzed amplification of motion shows that the 0.4107g horizontal peak input motion is amplified to 0.88g (at 2.78 sec), 0.71g

(at 8.56 sec) and 1.24g (at 12 sec) for Elcentro, Kobe and Hachinhoe type of earthquake in maximum credible earthquake. The amplification of motion for DBE shows that the 0.212g horizontal peak input motion is amplified to 0. 5g (at 3 sec), 0.4g (at 11 sec) and 0.375g (at 7.5 sec) for Elcentro, Kobe and Hachinhoe type of earthquake.(Figure 33) The recorded acceleration time history at this point shows that the input accelerations are amplified from 1.76-3.01 times.

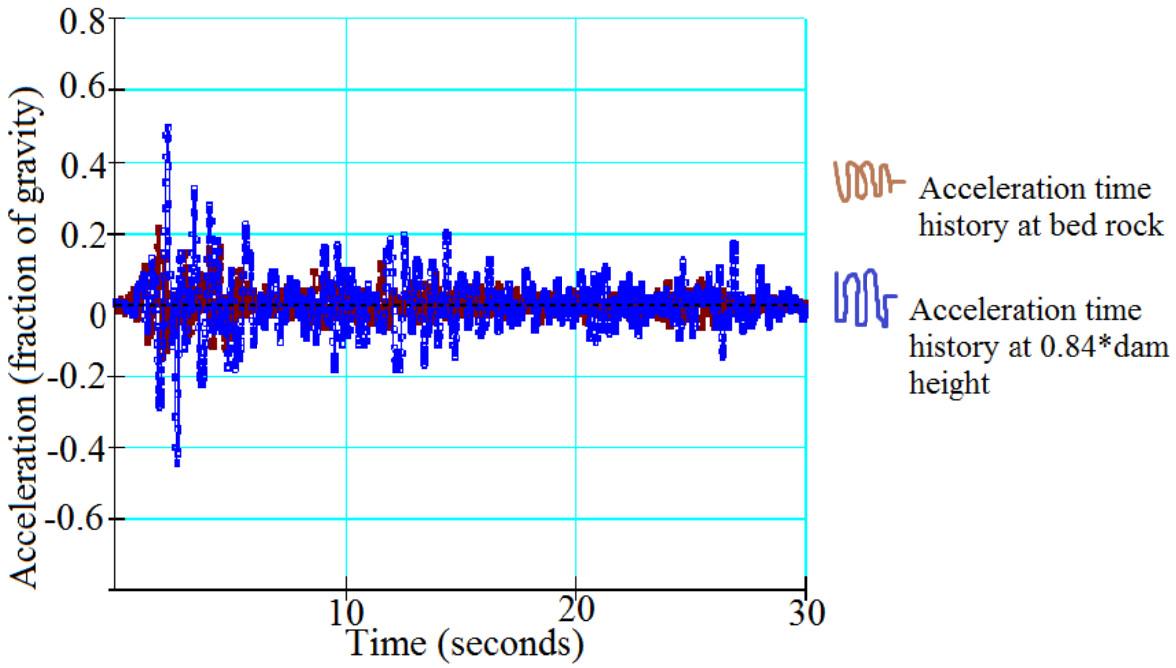

Figure 33: Amplification of the input motion for Elcentro in DBE (at peak point)

4.8 Slope stability analysis after earthquake shaking (post earthquake)

The limit equilibrium and the finite element analysis method do the slope stability in the same way as the static (before earthquake) analysis. The difference is that the analysis is done in every earthquake motion time steps. (0.02 sec) In the Limit equilibrium method the earthquake acceleration is changed to inertial force for every slice. For the Finite equilibrium analysis the additional dynamic shear stress in each element at the

base of the slice is averaged and added to the static finite element slope stability analysis for each time step. But since the dynamic shear stress is cyclic, the slope stability result is complex to interpret. For the upstream slope the calculated factor of safety in FEM method during both MCE and DBE ranges from 1.215-1.718. When the analysis method is changed to limit equilibrium the calculated factor safety ranges from 1.335-1.745. For the downstream slope the calculated factor of safety in FEM method during MCE and DBE ranges from 0.976-1.421. But, according to LEM for the downstream slope the calculated factor of safety in ranges from 1.028-1.125. See the summarized below table.

Table 7: Slope stability factor of safety (during earthquake)

SLOPE STABILITY AFTER EARTHQUAKE					
		FEM		LEM	
Earthquake type	Earthquake considered	Upstream	downstream	Upstream	Downstream
DBE	Elcentro	1.615	1.373	1.745	1.523
	Hachinhoe	1.215	0.976	1.336	1.033
	Kobe	1.609	1.421	1.745	1.523
MCE	Elcentro	1.718	1.331	1.745	1.523
	Hachinhoe	1.273	0.925	1.335	1.028
	Kobe	1.605	1.414	1.745	1.523

The below consecutive figures presents the slip surfaces with minimum factor of safety for Hachinhoe in design base earthquake conditions.

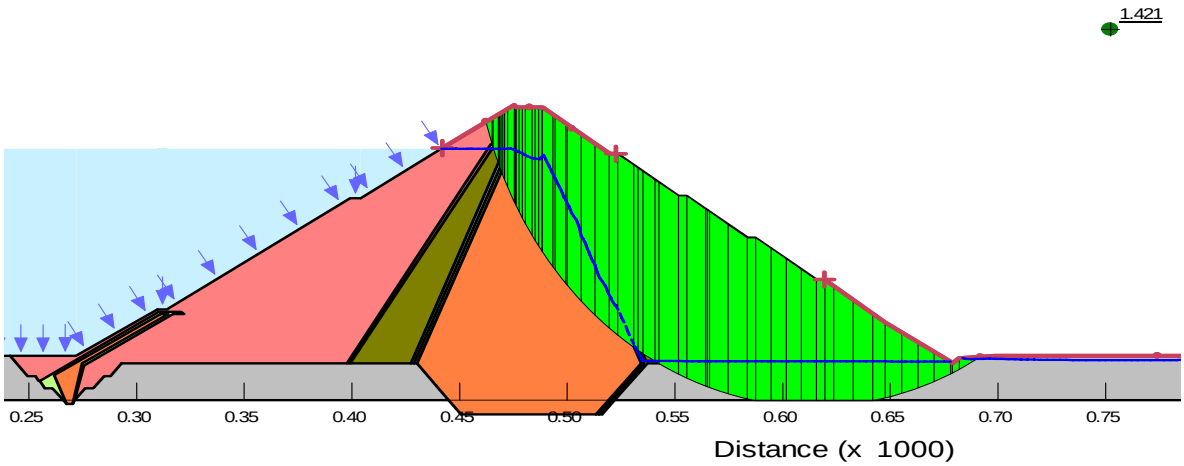

Figure 34: FEM D/S (HACHINHOE, DBE)

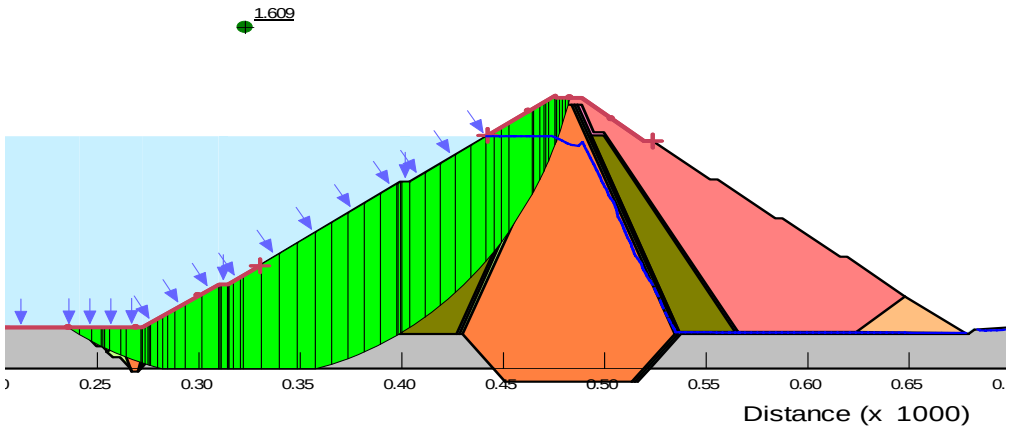

Figure 35: FEM U/S (HACHINOE, DBE)

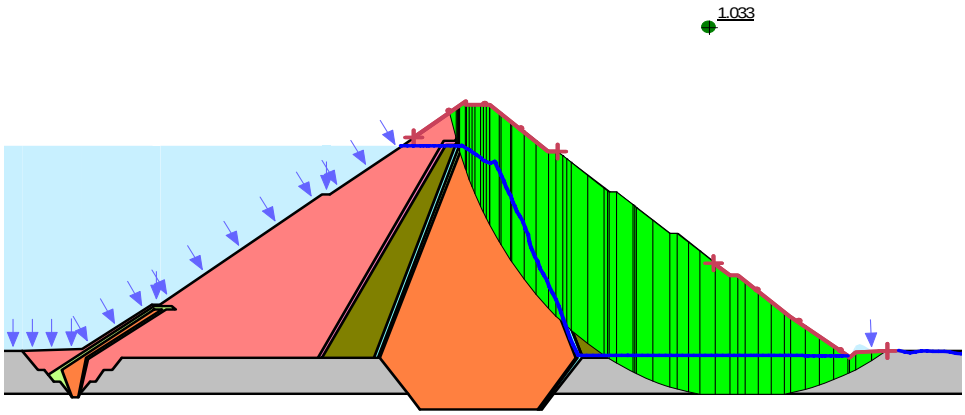

Figure 36: LEM D/S (HACHINHOE, DBE)

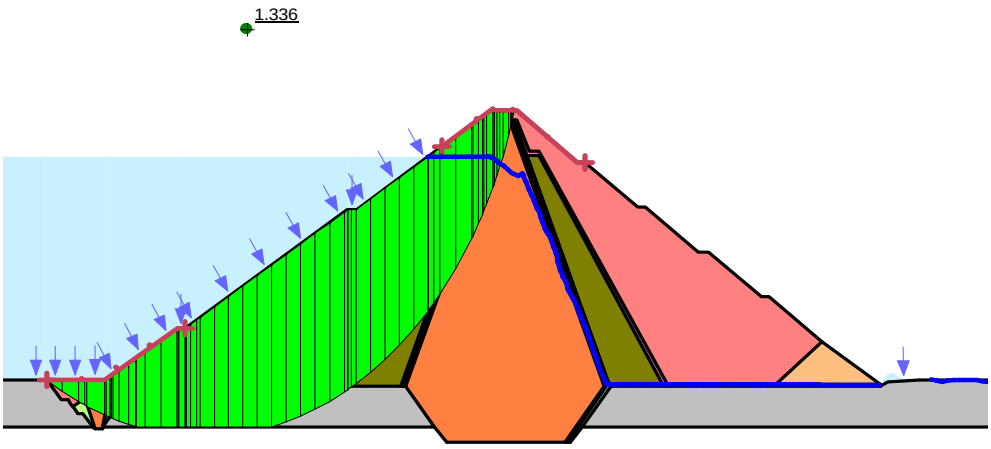

Figure 37: LEM U/S (HACHINHOE, DBE)

The calculated factors of safety with earthquakes are all greater than one in LEM, the minimum expected to be fulfilled. But, in FEM the downstream face factor of safety lowers to 0.925 in MCE and 0.976 in DBE. The minimum factor of safety for downstream face occurred during Hachinhoe type of earthquake. The typical character of this earthquake is longer duration, where amplitudes are near the peak in most of the cycles. The same is true for upstream face also. Comparing Kobe and Elcentro, the factor of safeties determined for the event when these earthquakes occurred are more or less similar in FEM. Their factor of safety calculated using the LEM is exactly the

same for both upstream and downstream slopes. Minimum factor of safety was expected in the Hachinhoe earthquake as determined.

A significant factor of safety difference was not determined for DBE and MCE. In FEM, the Elcentro and Hachinhoe post earthquake factor of safety in MCE are a little higher than DBE. But, in all other cases, the factors of safety in MCE are a little lower than DBE. Thus, the duration and the cycle's peak amplitude are more strong factors than peak amplitude acceleration in stability analysis.

4.9 Newmark Deformation

After knowing all the dynamic shear stress along a slip surface, the average acceleration of the sliding mass determined. Then all the average accelerations in the time of earthquake plotted against time and factor of safety. The acceleration which lowers the static factor of safety to 1 is said to be yield acceleration. All the accelerations above the yield acceleration results a factor of safety below 1. During this time there is an expectation of a sliding movement along the slip surface. The movement is parallel to the slip surface. So the movement is rotational and translational. The area above the yield acceleration integrated to give velocity that results deformation. This velocity can be integrated to give displacement, which is summed up to give permanent deformation.

The Newmark deformation analysis for Kobe and Elcentro earthquake showed no deformation at all. But for Hachinhoe, the below deformations have occurred for MCE and DBE cases.

Case1: Newmark Deformation of Hachinhoe for MCE

For different slip surfaces, different factor of safety and permanent deformation recorded for MCE.The below figures presented calculated safety factor for sample slip surfaces and their respective deformation in the upstream face of the dam.

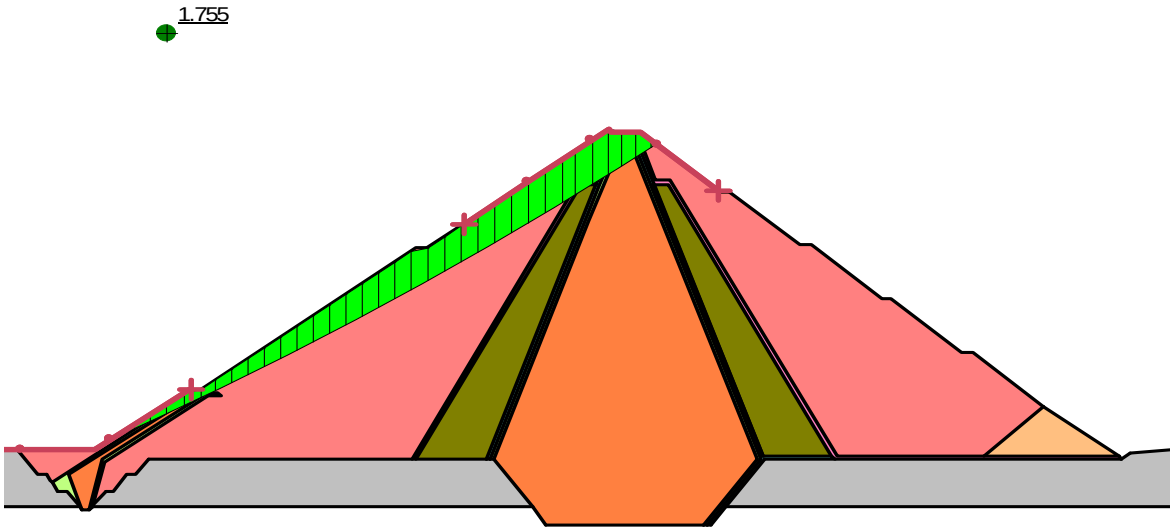

Figure 38 : Slip surface 1 factor of safety (Resulting deformation)

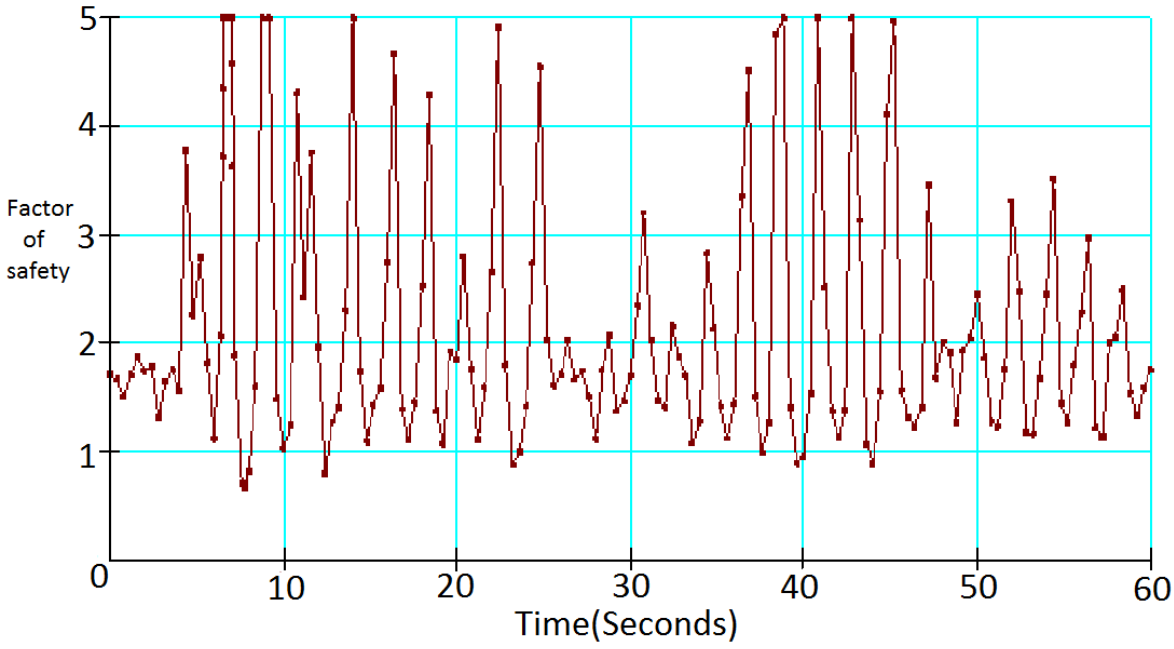

Figure 39: Factor of safety versus time for slip surface 1

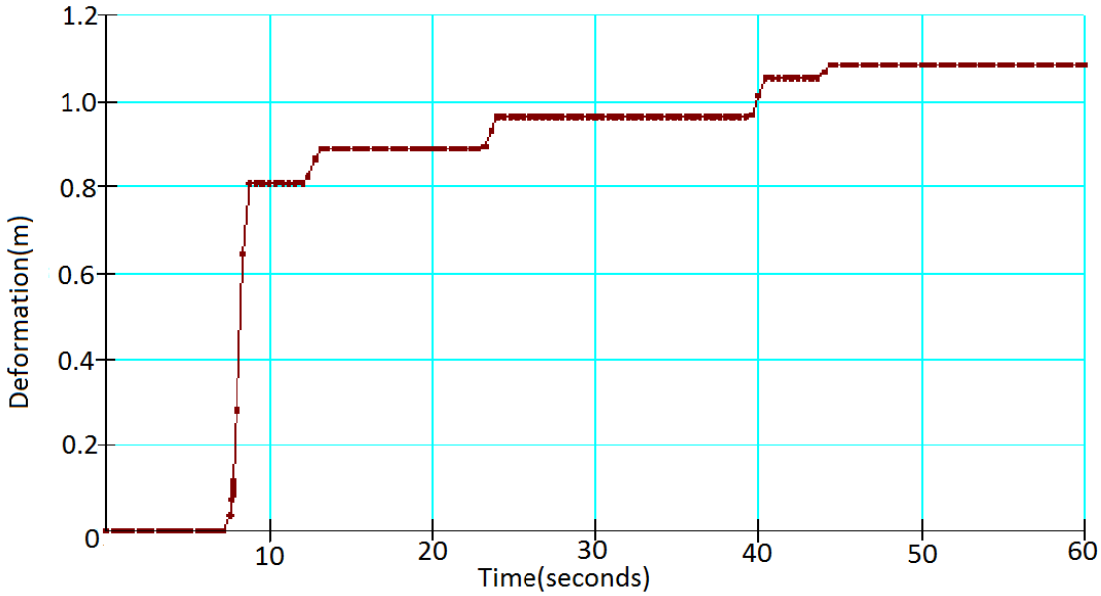

Figure 40: Deformation versus time for slip surface 1

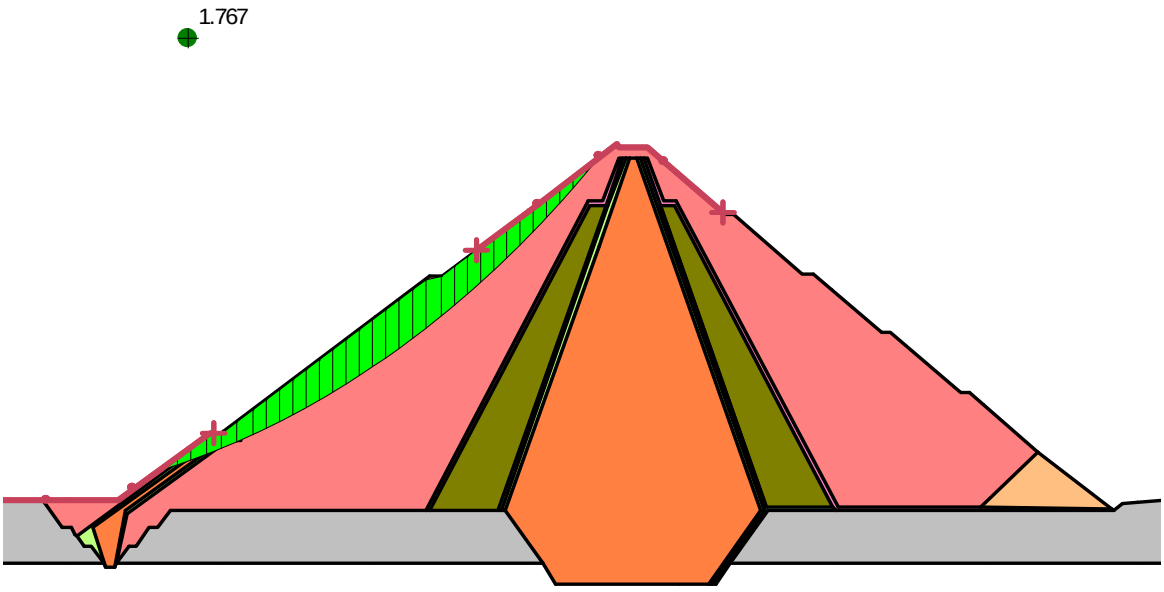

Figure 41: Slip surface 2 factor of safety (Resulting deformation)

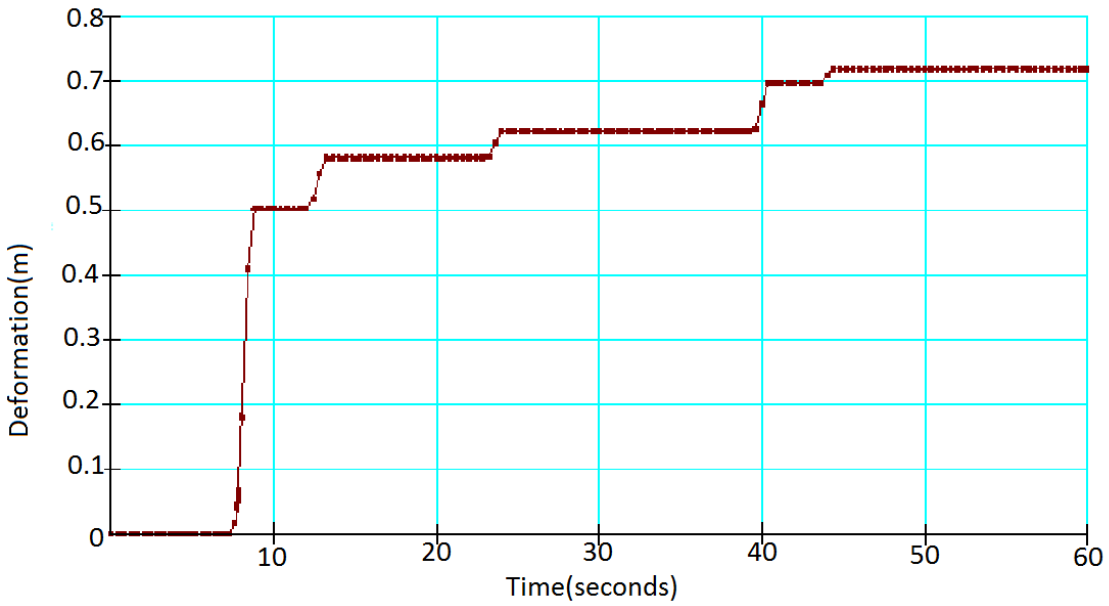

Figure 42: Deformation versus time for slip surface 1

The permanent deformation in this analysis is for the entire sliding block. Here, our main focus is to determine reduction in free board. Decomposition of horizontal and vertical displacement must be done. The direction of the deformation (resultant) is assumed to be in the direction of chord of the slip surface.(Messele, 2006) In such a way slip surface, crest involvement and decomposed free board reduction are tabulated below.

Table 8: Permanent vertical and horizontal displacement for MCE

Permanent deformation decomposition(m)					
No	Permanent	Chord	Crest	Vertical	Horizontal
1	1.0842	24°	100	0.44094414m	0.99041m
2	0.72001	26.5°	0	0.32126126m	0.644336m

3	0.42061	26.4°	100	0.18773927m	0.376740m
4	0.37076	23.8°	100	0.1496016m	0.339226m
5	0.28715	23.6°	100	0.11496021m	0.263132m
6	0.25818	23.75°	100	0.10397941m	0.236314m
7	0.11246	23.85°	100	0.0454720m	0.102856m
8	0.24871	21.25°	100	0.0901399m	0.231799m
9	0.41154	20.1°	100	0.1414257m	0.386474m

Deformation occurred only during a time of Hachinhoe earthquake. Thus, duration of earthquake reaching uniform peak acceleration in most of the cycles is the strong factor that result deformation in dams. During maximum credible earthquake, the maximum deformation occurred, which involves the crest 100% displace the upstream sliding mass 0.44m vertically downward and 0.99m horizontally to the left. This reduces the dam height by 0.44m after the earthquake. The maximum deformation occurred which do not involve the crest displace the sliding mass of the upstream 0.644m horizontally downward and 0.321m vertically to the left. This deformation does not reduce the dam height. As figure 41 displays, the deformation is shallow and recoverable. Downstream slope of the dam show no deformation during MCE. This is due to the effect of pore-water pressure on the upstream face, which lowers the effective stress, acting against sliding instability.

Case2: Newmark Deformation of Hachinhoe for DBE

For different slip surfaces, different factor of safety and permanent deformation recorded for DBE. The below figures display calculated safety factor for sample slip surfaces and their respective deformation in the upstream face of the dam.

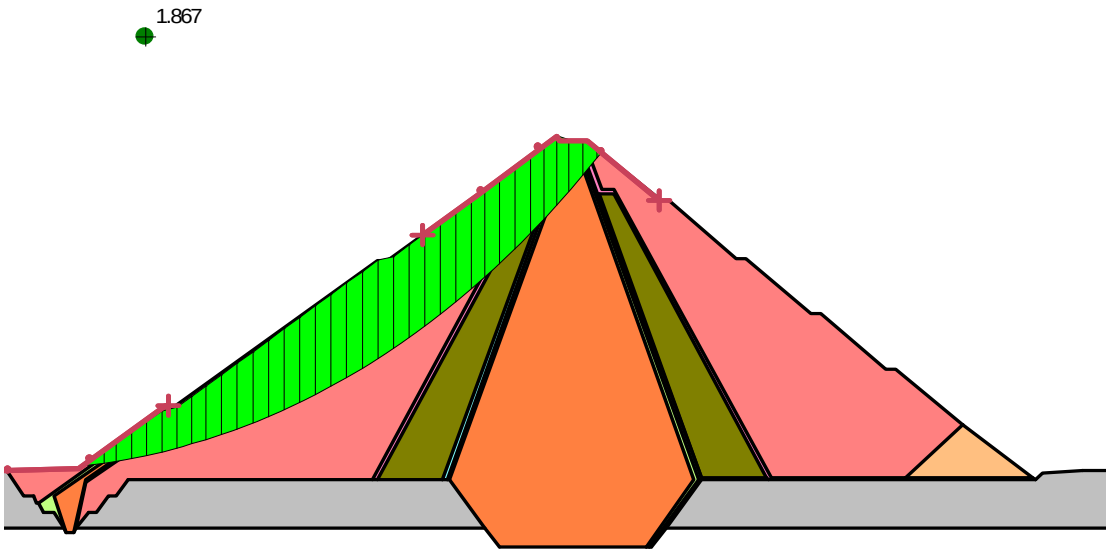

Figure 43: Slip surface 1 factor of safety (resulting deformation)

Table 9: Slip surface 1 deformation

Resultant displacement	0.0077365m
Slope angle of chord	23.8°
Yeild acceleration	0.18946m/s^2
Vertical displacement	0.00345m
Horizontal displacement	0.00693m

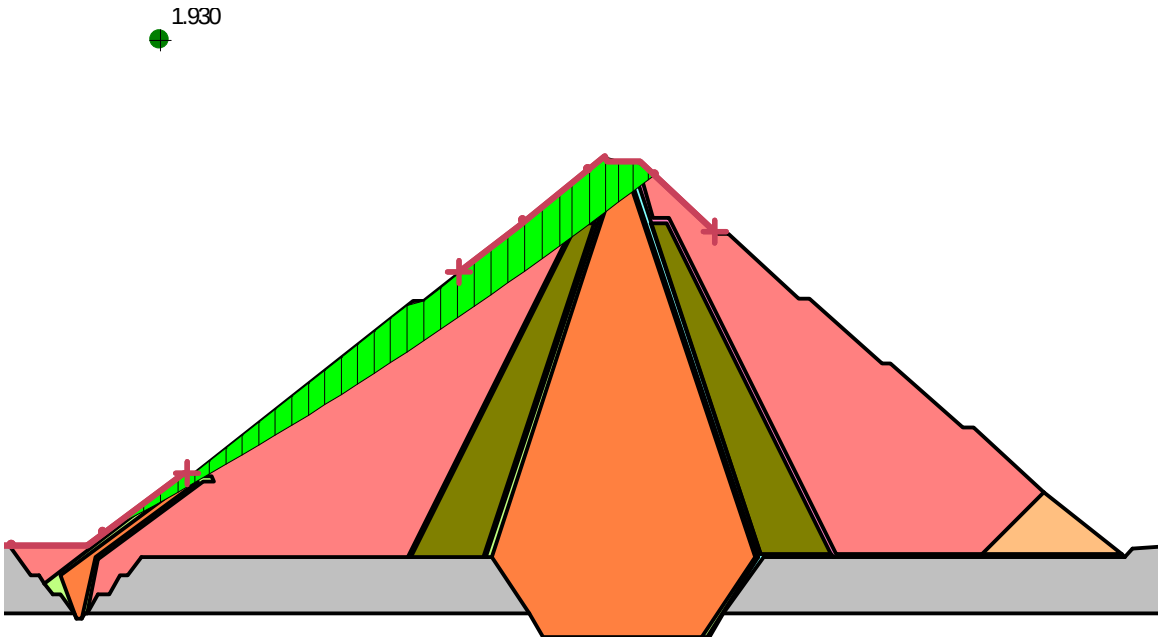

Figure 44: Slip surface 2 factor of safety (resulting deformation)

Table 10: Slip surface 2 deformation

Resultant displacement	0.021149
Slope angle of chord	23.6°
Yield acceleration	0.2076 m/s^2
Vertical displacement	0.00853m
Horizontal displacement	0.01935m

During design base earthquake occurrence, a maximum deformation of 19.35mm in horizontal direction and 8.53mm of vertical displacement are determined with a sliding mass, which involves 100% of the crest. This deformation reduces the dam height by less than 1cm. The maximum deformations which do not include the crest displace the

upstream face sliding mass 14.15mm horizontally and 6.18mm vertically. This deformation is very small and inconsiderable for repair. Downstream face of the dam doesn't show deformation in all cases as that of MCE.

The slip surfaces that result deformation in MCE and DBE cases have a shallow depth except those which their slip surface includes the crest. For DBE, the deformation that results the maximum vertical displacement of 8.53mm sliding mass has a depth of 15m, which involves the crest fully. The deepest slice depth in DBE case is 40m for a slide which results a vertical and horizontal displacement of 3.18mm and 7.23mm, respectively.

In MCE case, the deepest slice depths are 35m for a vertical and horizontal displacement of 0.18m and 0.37m, respectively. At the maximum deformation during MCE, where the vertical and horizontal displacements are 0.44m and 0.99m, the slip surface depth is 12m.

In DBE, all permanent deformation which involves the crest decreases the dam height by less than 1cm. This dam height reduction is very small.

In the feasibility document, a camber allowed for settlement is 1.25m. The maximum vertical displacement during DBE, which is 8.53mm is insignificant compared to the allowance. Even the MCE maximum vertical displacement which involves the crest is 0.44m. This dam height reduction can be entertained by the allowed cumber.

4.10 Liquefaction result

In the previous section we have determined the potential for liquefaction for the alluvium deposit foundation under the dam. Using Lade (1993) chart which relates relative density and instability collapse inclination angle is determined to be 18.5 degree. Sladen

et al. (1985b) view that the un-drained steady-state strengths at the Nerlerk Berm failures in the Beaufort Sea were less than about 2 kPa. So, the steady state strength of the alluvium deposit is set to 2kpa, since it is expected to show equal or more steady state strength than the Beaufort Sea sand.

While loading, the effective stress path follows a curved path with rising deviator stress until the maximum deviator stress (collapse point) is reached. At that point there is a sudden tendency for volumetric compression (collapse) which is offset by a rapid and large increase in the pore water pressures. The rapid rise in pore pressures leads to a decrease in mean effective stress (p') and deviator stress (q), resulting liquefaction. The strength path eventually intersects the critical state line, at which point the mean effective stress, deviator stress, and void ratio remain constant with further shearing.

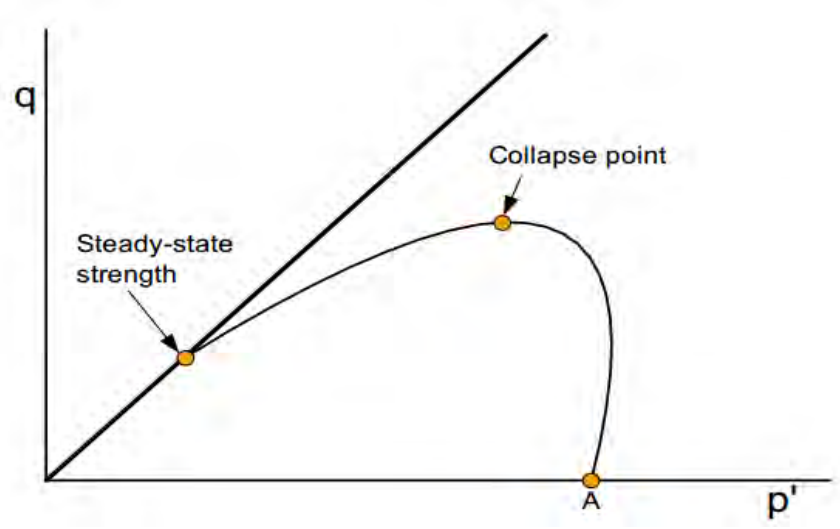

Figure 45: Effective stress path for loose sand in an un-drained tri-axial test

i. Liquefaction during MCE

In the three cases of earthquake during Maximum Credible Earthquake, the analysis shows that liquefaction will occur in all the parts of the alluvium foundation except a small region at the toe of the dam. The yellow hatched region in the below figure illustrate the area of liquefaction.

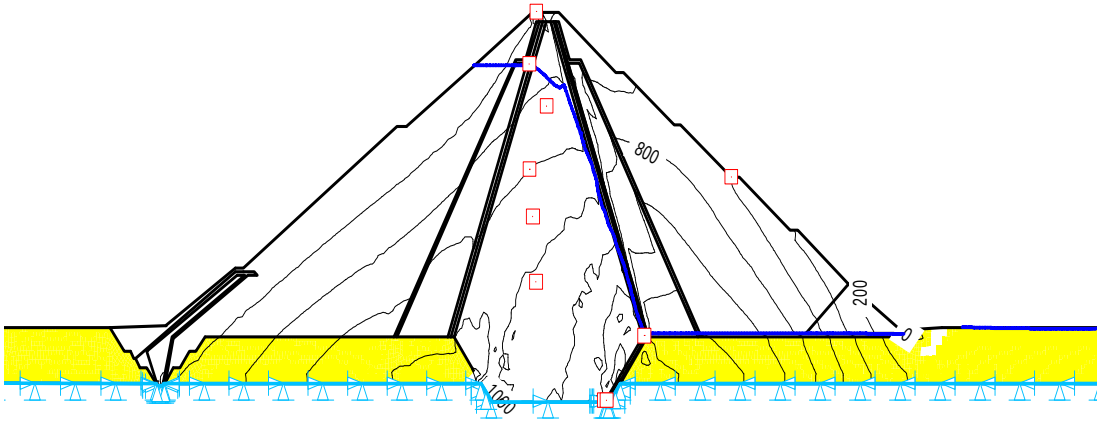

Figure 46: Region of liquefaction (Kobe earthquake)

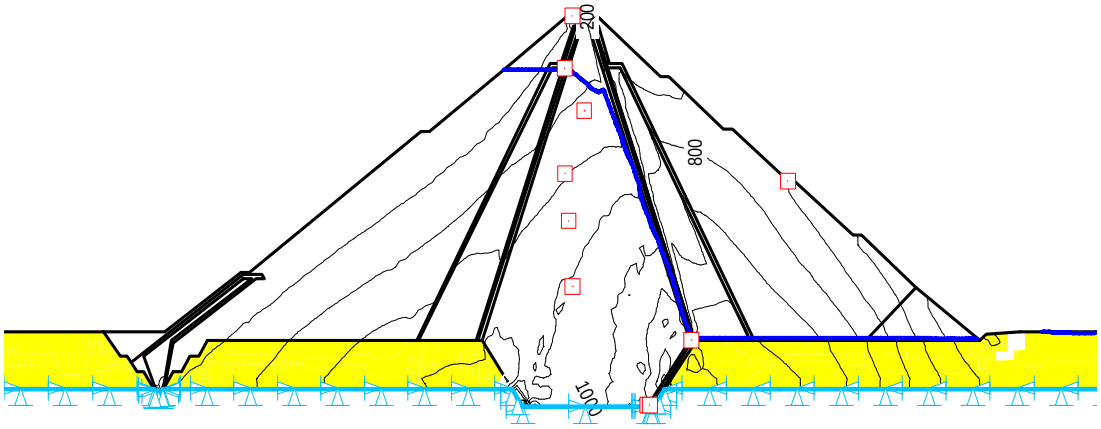

Figure 47: Region of liquefaction (Elcentro earthquake)

ii. Liquefaction during DBE

In design base earthquake, the same result with the above MCE case is determined. i.e., liquefaction will most likely occur in the all parts of the alluvium foundation except some region at the toe of the dam. See the below figure with a yellow hatched area of liquefied zone.

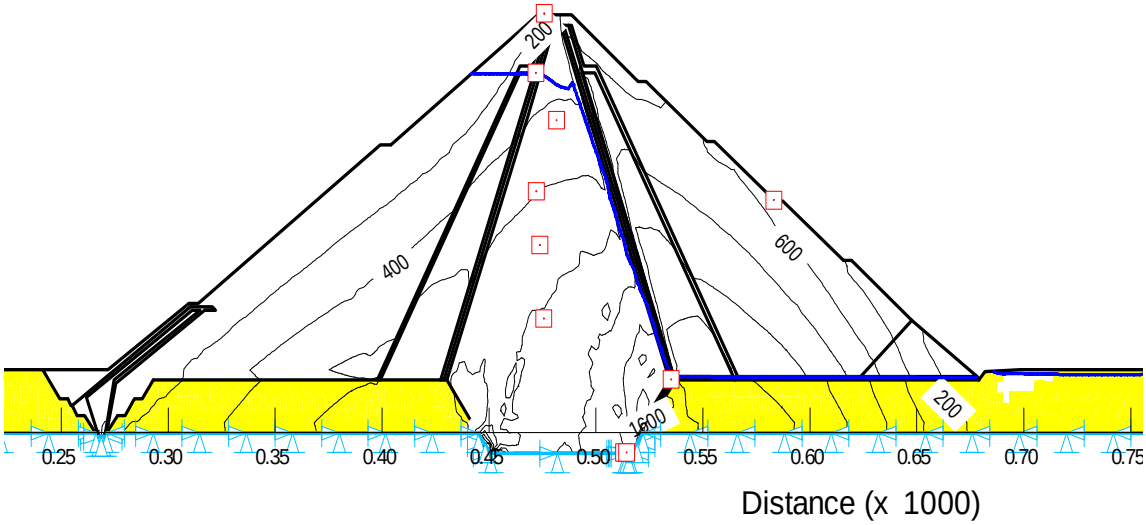

Figure 48: Liquefying zone of foundation in Elcentro earthquake

Due to the cyclic loading, which increase pore water pressure during those seconds of earthquake shaking, the effective stress on the soil gets reduced. This fact is revealed by the graph below which shows effective stress reduction at a node located in the toe of the dam during time of shaking.

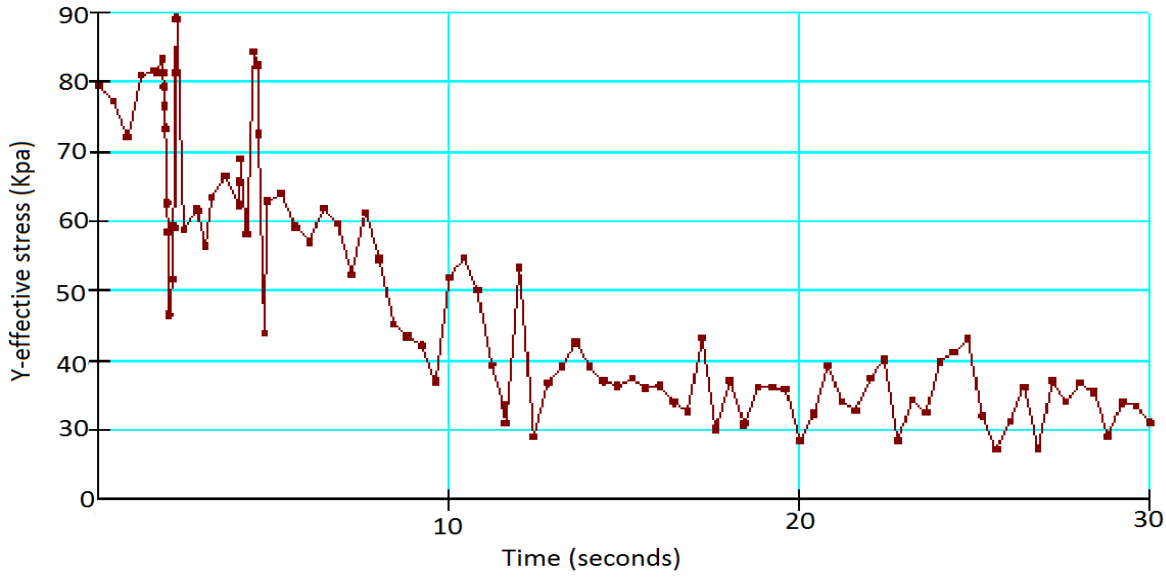

Figure 49: Effective y- stress time history (Elcentro, DBE)

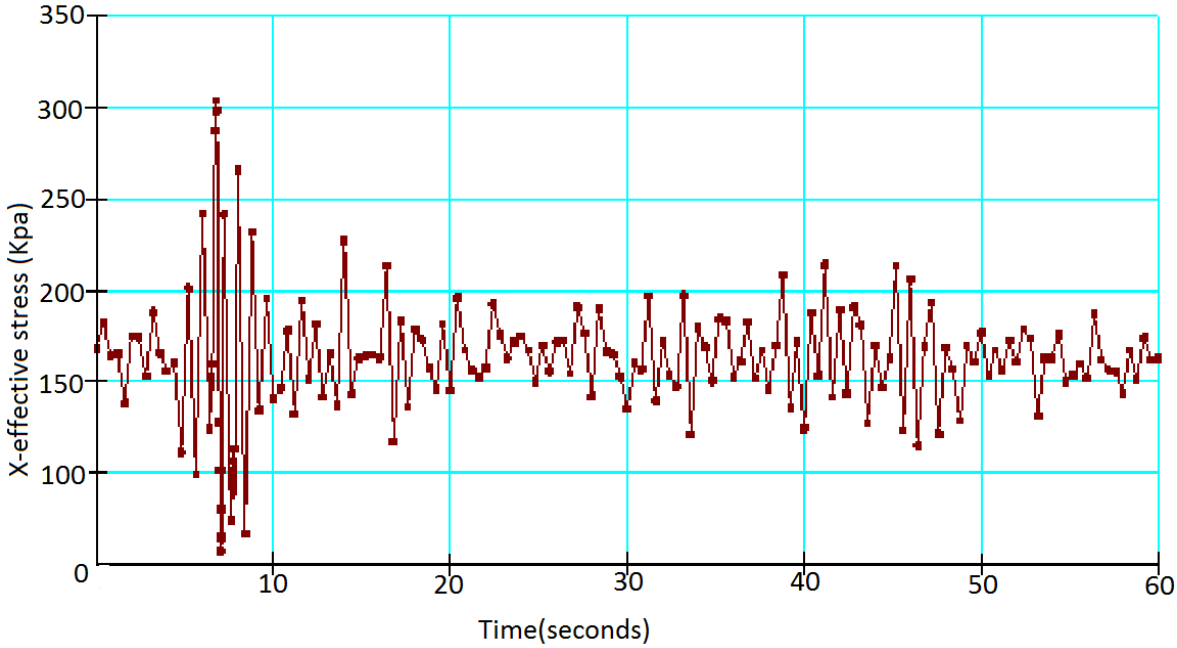

Figure 50: Effective X- stress time history (Hachinhoe, MCE)

4.11 Pseudo-static analysis

This analysis is done by the slope/w component of Geo-studio. Peak ground acceleration creates an additional inertial disturbing force on the sliding mass for all the slip surfaces and the minimum factor of safety is taken. This method is conservative and uneconomical. Results of pseudo static analysis is displayed in the below figures of 51, 52, 53 and 54 with the slip surfaces. Peak accelerations of 0.4107g and 0.212g for MCE and DBE inserted to create an inertial force.

Case I: Maximum credible earthquake (MCE)

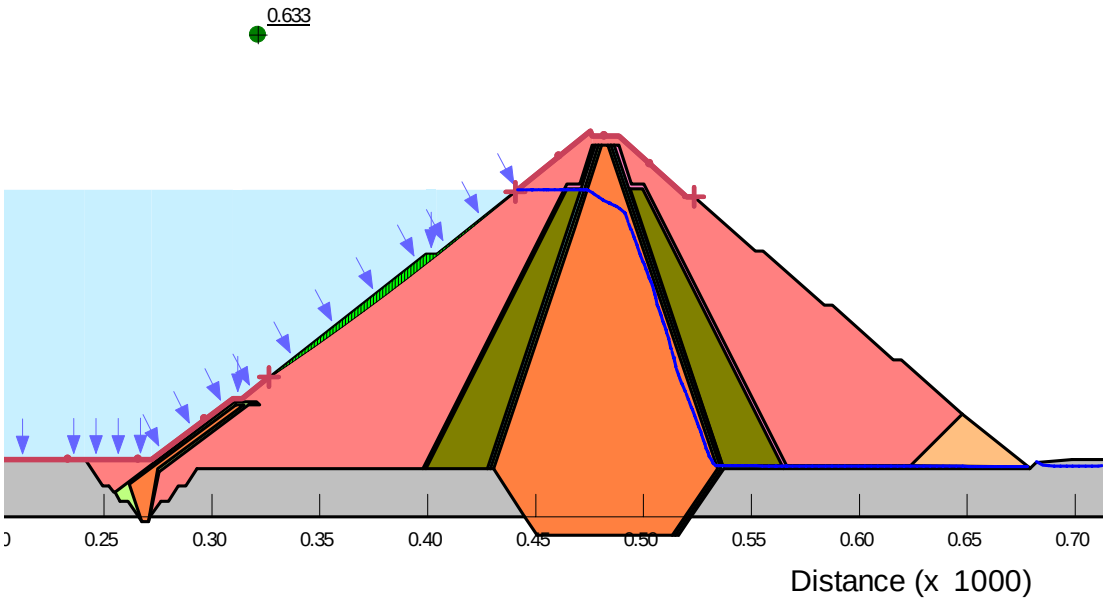

Figure 51: Upstream Pseudo-static slope stability analysis

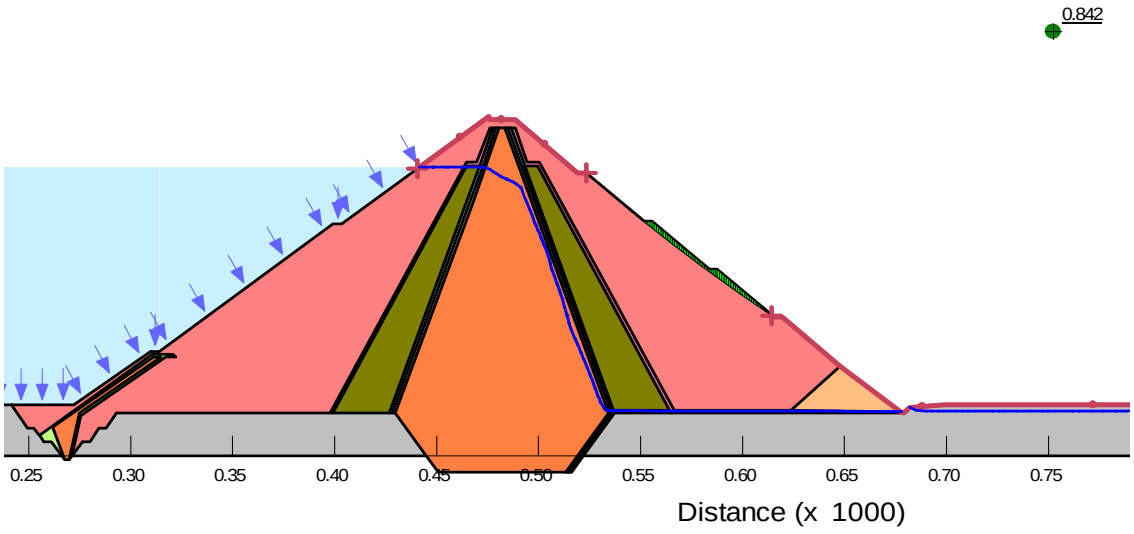

Figure 52: Downstream Pseudo-static slope stability analysis

Case II: Design base earthquake (DBE)

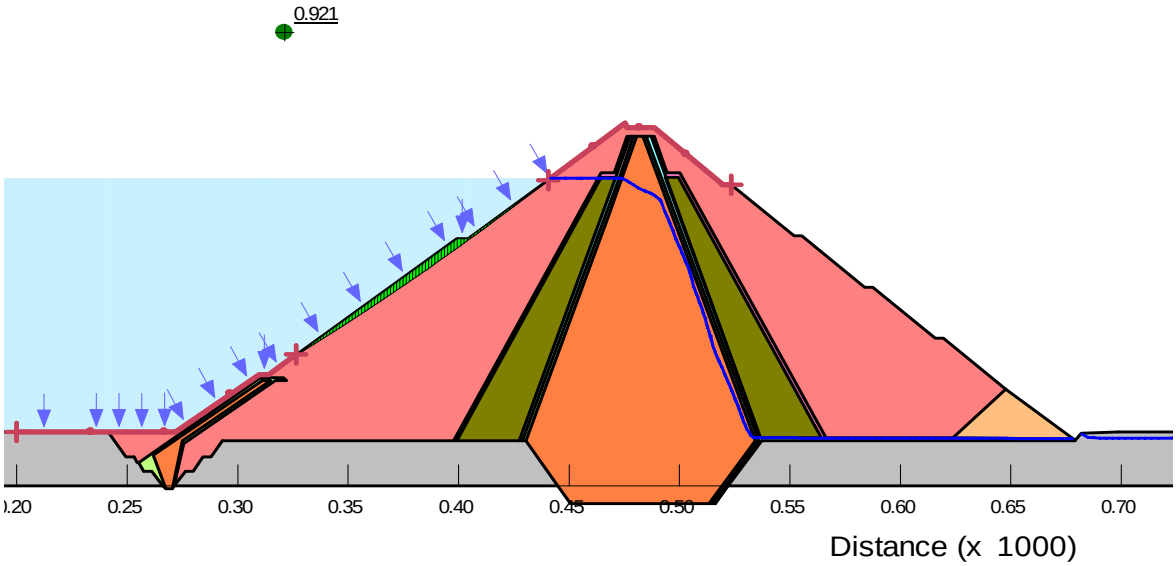

Figure 53: Upstream Pseudo-static slope stability analysis

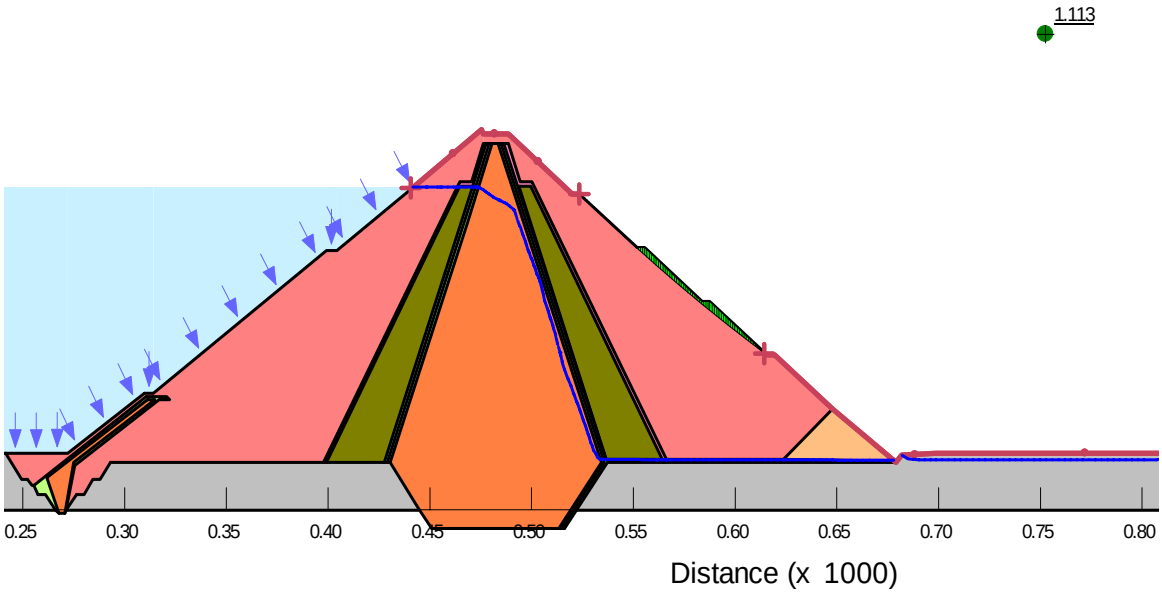

Figure 54: Downstream pseudo-static slope stability analysis

A very high conservative factor of safety is obtained in pseudo-static analysis. For a horizontal and vertical input acceleration of 0.4107g and 0.205g in MCE case, the upstream and downstream factor of safety are determined to be 0.633 and 0.842, respectively. For a horizontal and vertical input acceleration of 0.212g and 0.106g in DBE case, the upstream and downstream factor of safety are determined to be 0.921 and 1.113, respectively. The dam requires an additional 3340m^3 of rock fill per meter width of the dam, which improves the upstream slope stability factor of safety to 1.029, with a slope value flattened to 1:2.9.

4.12 Slope and section reduction options

Since the Middle Awash Multi-purpose dam slopes are safe before and after the earthquake, (LEM results) possible options of slope reduction to the economical optimized level have been considered using the LEM method. But, both the upstream and downstream faces of the dam have a static and dynamic slope stability factor of safety a little above the marginal required level. The minimum factor of safety against static slope stability analysis is 1.5, during steady state seepage. The determined static factors of safety for upstream and downstream are 1.772 and 1.66, respectively in LEM. The required factor of safety against earthquake during steady state seepage slope stability is 1. Minimum factor of safety is obtained for Hachinhoe in MCE. The LEM factors of safety against sliding for upstream and downstream are 1.273 and 1.028, in post earthquake analysis. Having these values, a slight modification of upstream slope (steepening) tried. But for downstream the post earthquake slope stability analysis result shows that it is not flexible to steepen. (1.028 is very approximate to the critical 1.0 value)

The best economical and safe slope reduction for upstream slope result shows a slope reduction of 1:1.9 to 1:1.75 doesn't minimizes the upstream slope static factor of safety to a significant level. The upstream post earthquake stability analysis for Hachinhoe in MCE determined a factor of safety result 1.342. Steepening the slope may increase the

expected permanent deformation. This is checked by Newmark method and obtained to be 1.17m, involving the crest fully. The decomposed vertical deformation becomes 0.48m. This still can be entertained by the cumber height allowed. By steepening the upstream from 1:1.9 to 1:1.75 the rockfill volume to be decreased is 220 cubic meter per meter width of the dam. The whole volume of fill to be decreased is 99,660 cubic meter. The estimated cost to be saved is 53,816,400 birr. Result of the upstream post earthquake slope stability analysis in case of LEM is displayed below for Hchinhoe in MCE case.

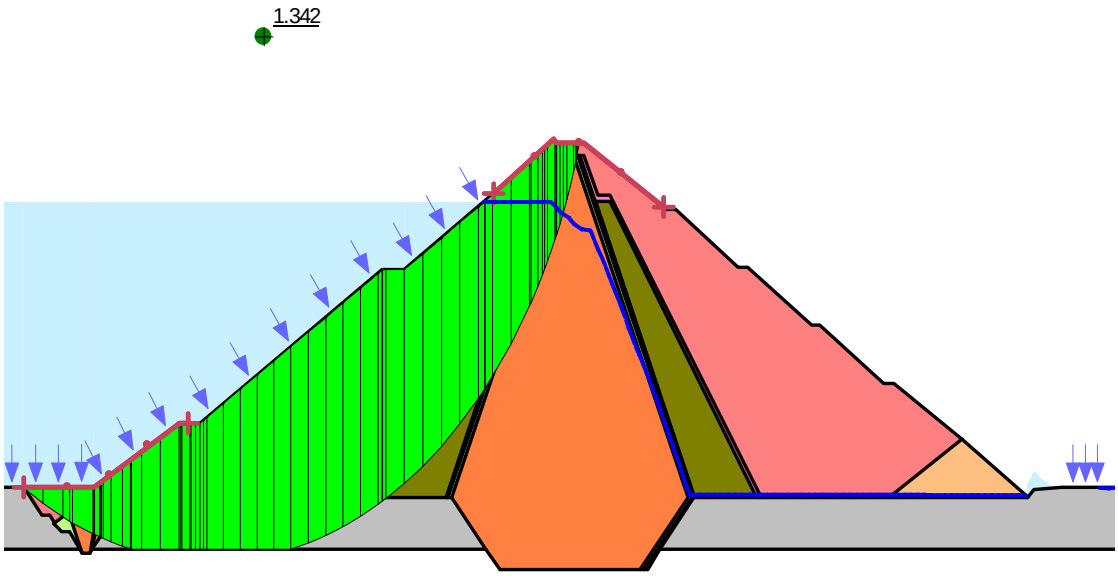

Figure 55: Upstream slope reduced factor of safety (MCE, Hachinhoe)

The slope stabilities factor of safety for upstream in static case (steady state seepage) is also in safe region. (1.812) After doing the static and dynamic stability analysis at steady state seepage, condition of rapid drawdown, a severe case for upstream stability analysis was done to check the slope reduction effect in static condition.

If the normal water level at 926 m.a.s.l is drawn to 857 m.a.s.l of minimum drawdown level within 30 days, the transient seepage analysis based slope stability assessment result a factor of safety above 1.6, for all the analyzed 100 days.(where all the water is drawn in the first 30 days) The minimum factor of safety in rapid drawdown case is 1.3. (USBR, 2001) The below picture present the water level and pheratic line in the dam body on the 100th day.

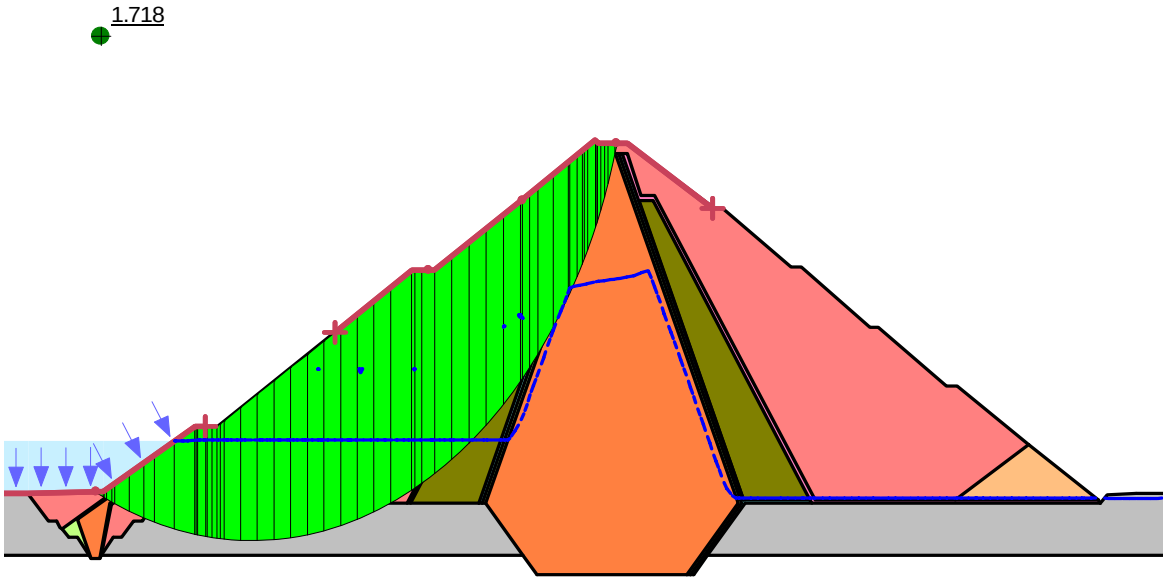

Figure 56: 100th day pheratic line and water level with the slip surface

Figure 57 shows the factor of safety for the first few days of rapid drawdown and additional dry season.

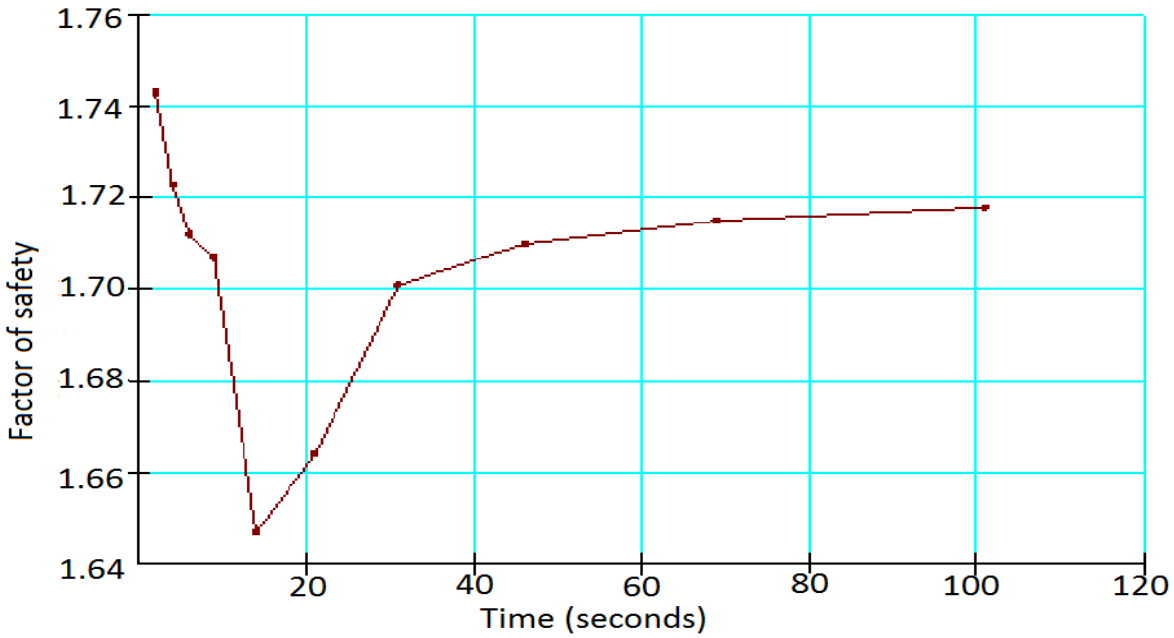

Figure 57: Rapid drawdown minimum factor of safety

5. Conclusions and Recommendations

5.1 Conclusion

After determining the seepage and contour of pore-water pressure in the dam and foundation a static slope stability analysis was done by Limit Equilibrium Method. All values of factors of safety for upstream and downstream slopes obtained to be more than the minimum critical 1.5, ensuring the safety of the dam at steady state seepage condition.

Maximum amplification of input acceleration is expected around 80% of the dam height. In both DBE (return period of 200 years) and MCE (return period of 1000 years), the input earthquake acceleration on the bed rock is amplified 1.76-3.01 times at 0.84height of the dam. Amplification is expected from 1-6 times on a dam. (Pelin Özener and Burak Kayhan Beşli, 2014) The fall of the calculated amplification in the expected range indicates the material property and the model used compatibleness and correctness.

The post earthquake slope stability analysis ensures stability of upstream and downstream after the earthquake shaking.

The post earthquake factor of safety calculated for DBE and MCE showed similarity. Minimum factor of safety is calculated for Hachinhoe type of earthquake, which have longer duration reaching peak acceleration in most of the cycles. Thus, peak ground acceleration's effect is not significant. Post earthquake slope stability is highly affected by shaking duration reaching peak acceleration in most of the cycles.

Finite Element Method provided conservative factor of safety for post earthquake analysis in which the minimum required is not satisfied for downstream slopes.

The result of vertical deformation analysis, done by Newmark method for upstream slope shows a maximum value of 19.5mm and 0.44m downward displacement of the dam during Hachinhoe earthquake for DBE and MCE cases, respectively. These permanent deformations do not require additional extension of dam height because of the allowed sufficient cumber height of 1.25m at feasibility study design. For the recommended slope reduction of upstream from 1:1.9 to 1:1.75, the vertical deformation is 0.48m, which can also be dealt by the cumber height. In creating a permanent deformation ground acceleration, shaking duration and uniformity of peak acceleration in cycles are influential factors.

The liquefaction evaluation showed that the 15m alluvium thick foundation under the dam liquefies immediately after earthquake started for all the three types of earthquake in both DBE and MCE cases. Thus, the alluvium foundation is very weak that even Kobe earthquake, which have a short duration of peak acceleration liquefies it immediately after shaking started.

Steepening upstream slope from 1:1.9 to 1:1.75 is an optimized slope considering safety and economic aspects. The modified upstream slope is checked for the severe upstream case of drawdown and ensured to be safe. Downstream slope needs no modification since it satisfies critical values at a steep slope for post earthquake analysis in Hachinhoe case.

A very high conservative factor of safety is obtained for pseudo-static analysis for comparison in both MCE and DBE cases. The dam requires an additional 3340m^3 of rock fill per meter width of the dam to improve the upstream slope stability factor of safety to 1.029, with a slope value flattened to 1:2.9. In addition to conservative results the pseudo static analysis could not capture the deformation.

LEM and FEM analysis are found to be conservative for upstream and downstream slopes in both static and dynamic stability analysis. The slopes DBE and MCE post

earthquake performance are very similar in the amount of factor of safety against sliding.

5.2 Recommendation

The alluvium foundation under both upstream and downstream slopes of the dam is determined to liquefy immediately after earthquake started. So, it is necessary to replace the alluvium foundation with a well compacted shell and gravel dominant sandy material. Especially the upstream face foundation must be replaced because of the unavailability of pore water pressure dissipating component. In the downstream face, the transition and filters could decrease the pore water pressure to be developed during earthquake. Parts of the downstream foundation which have a relative density lower than 55% should be removed and replaced by gravel dominant sandy material. This takes out the foundation material from a liquefying region.

By steepening upstream slope from 1:1.9 to 1:1.75, an economical upstream section can be adopted which satisfies minimum critical value of factor of safety.

Further increase of dam height and cumber is not required because the dam's DBE and MCE upstream deformations which includes the crest can be entertained by the allowed cumber height.

In a dam seismic stability analysis, a dynamic analysis type must be picked over pseudo-static analysis to overcome problem of conservative results which leads to uneconomical dam geometry and to capture deformation due to seismic shocks.

References

1. **DeAlba P., Seed H. B. and Chan C. K.** Sand liquefation in large scale simple shear tests [Journal] // Geotechnical engineering. - [s.l.] : ASCE, 1976. - GT9 : Vol. 102. - pp. 909 - 927.

2. **Duncan J. B.** State of the art - static stability and deformation analysis in Stability and Performance of slope and embankment [Journal] // ASCE Geotechnical Special Publication. - [s.l.] : ASCE, 1992. - 31. - pp. 222 - 266.

3. **Duncan J. M.** State of the art: limit equilibrium and finite element analysis of slopes [Journal] // Journal of Geotechnical Engineering. - [s.l.] : ASCE, 1996a. - 7 : Vol. 122. - pp. 577 - 597.

4. **Dr. Gopi Siddappa.** Effect of earthquake on embankment dams, department of civil engineering, college of Engineering, Unknown.
5. **Fantahun Getachew,** unknown. Comparison of pseudo-static and dynamic response analysis of Sibilu dam. Thesis, Addis Ababa University.
6. **FAO**, 1996. Food and Agriculture Organization of the United Nations, Production 11 yearbook (46). FAO, Rome, Italy.

7. **Fell Robin [et al.]** Geotechnical engineering of dams [Book Section]. - London : Taylor and Francis group plc, 2005.

8. **Finn, W.D.L.** Seismic safety evaluation of embankment dams, in International workshop on dam safety evaluation, Grundewald, Switzerland, 26–27 April,1993, Vol. 4, 91–135.
9. **ICOLD**, 1986. International Commission for Large Dams, Static analysis, Bulletin 53. ICOLD, Paris, France.
10. **ICOLD**, 1983. International Commission for Large Dams, Seismic and dam design, Bulletin 46. ICOLD, Paris, France.
11. **ICOLD**, 1986. International Commission for Large Dams, Earthquake analysis procedures for dams, Bulletin 52. ICOLD, Paris, France.

12. **ICOLD**, 1986. International Commission for Large Dams, Selecting seismic parameters for large dams, Bulletin 72. ICOLD, Paris, France.
13. **ICOLD**, 1999. International Commission for Large Dams, Seismic observation of dams, Bulletin 113. ICOLD, Paris, France.
14. **ICOLD**, 2001. International Commission for Large Dams, Design features of dams to resist seismic ground motion, Bulletin 120. ICOLD, Paris, France.
15. **ICOLD**, 2002. International Commission for Large Dams, Seismic design and evaluation of structures appurtenant to dams, Bulletin 123. ICOLD, Paris, France.
16. Indian Institute of Technology, 2005, IITK-GSDMA GUIDELINES for SEISMIC DESIGN of EARTH DAMS AND EMBANKMENTS.Kanpur,India.
17. **Idriss, I.M., Lysmer, J., Hwang, R. and Seed, H.B**. QUAD-4: A computer program for eval-uating the seismic response of soil structures by variable damping finite element procedures. Report No. EERC73-16, University of California, Berkeley 1973.
18. **Ishibashi I. and Zhang X.** Unified Dynamic shear moduli and damping ratios of sand and clay [Journal] // Soils and founations. - 1993. - 1 : Vol. 33. - pp. 182 - 191.
19. **J. E. Ahlberg, J. Fowler, L W. Heller.** Earthquake resistance of earth and rock fill dams U.S. Amy Engineer Waterways Experiment Station Soils and Pavements Laboratory, Vicksburg, Mississippi,1972.
20. **Kenji Ishihara.** Soil Behaviuor in Earthquake Geotechnics [Book]. - New York : Oxford University, Anthony Rowe Ltd., Eastbourne, 2003.
21. **Kramer Steven L.** Geotechnical Earthquake Engineering [Book]. - New Jersy : Prentice-Hall ,Upper Saddle River, 1996.
22. **Makdisi, F.I. and Seed, H.B.** A simplified procedure for estimating dam and earthquake induced deformations. JASCE Geotechnical Eng., 1978. Vol. 1, 105, No. GT7, 849–867.
23. **Messele Haile, Hadush Seged** Earthquake induced liquifaction analysis of Tendaho earth-fill dam[Journal] // Addis Ababa,2006.

24. **Moriwaki, Y., Beikae, M. and Idriss, I.M**. Non-linear seismic analysis of the Upper San Fernando Dam under the 1971 San Fernando earthquake. Proc. 9th World Conference on Earthquake Engng., Tokyo and Kyoto, Japan,1988, Vol. III, 237–241

25. **Newmark N. M.** Effects of earthquakes on dams and embankments, Rankine Lecture [Journal] // Geotechnique. - 1965. - 2 : Vol. 15.

26. **Pells, S. and Fell, R.** Damage and cracking of embankment dams by earthquakes, and the implications for internal erosion and piping. UNICIV Report R 406, The University of New South Wales, ISBN 85841 3752, 2002..
27. **Pan Fulan,** Analysis of Variation of Poisson's ratio with depth of soil. Proceedings 1st International conference on recent advances in geotechnical earthquake engineering and soil dynamics, Arlington. Missouri University of Science and Technology, Missouri.1981.
28. **Pelin Özener and Burak Kayhan Beşli.** Investigation of Effects on Seismic Response characterstics of earthfill and rockfill dams. Proceedings 10th conference on earthquake engineering,Alaska. Yildiz Technical University, Istanbul.2014.
29. **QUAKE/W** Dynamic modeling with QUAKE/W 2007:An engineering methodology [Book]. - [s.l.] : Geo-Slope international ltd, 2008.
30. **R.Ziaie Moayed, M.F. Ramzanpour.** Seismic behavior of zoned core embankment dam. Electronic journal of geotechnical engineering, EJGE, Vol.13, Bund A.
31. **Schnabel, P.L., Lysmer, J. and Seed, H.B.** SHAKE: A computer program for earthquake response analysis of horizontally layered sites. Report No. EERC72-12, University of California, Berkeley, 1972.
32. **Seed, H.B**. Earthquake-resistant design of earth dams. Proc., Symp. Seismic Design. Of Earth Dams and Caverns, ASCE, New York,1983, pp. 41–64
33. **Seep/W** Seepage modeling with Seep/W 2007:An engineering methodology [Book]. - [s.l.] : Geo-Slope international ltd, 2008.
34. **Sh.Salemi, M.H. Bazair, C.M. Meriifield and T. Heidari,** Investigation of dynamic behavior of Asphalt core dams. Proceedings 6th International Confress on case histories in geotechnical engineering, Arlington. Missouri University of Science and Technology, Missouri.2008.

35. **SIGMA/W** Stress-Deformation modeling with SIGMA/W 2007:An engineering methodology [Book]. - [s.l.] : Geo-Slope international ltd, 2008.
36. **SLOPE/W** Stability modeling with SLOPE/W 2007 Version:An engineering methodology [Book]. - [s.l.] : Geo-Slope international ltd, 2008.
37. **Sherard, J.L.** Earthquake considerations in earth dam design. Journal of the Soil Mechanics and Foundations Division, American Society of Civil Engineers, 1967,Vol. 93, No. SM4, 377–401.
38. **Siân Herbert**. Assessing seismic risk in Ethiopia. Government social development humanitarian conflict, 2013.
39. **USBR**, 2001. US Bureau of Reclamation, Embankment dams static stability analysis, DS-13(4)-6,2011.
40. **US Corps of Engineers. Engineering and design – stability of earth and rock fill dams, Engr. Manual** EM 1110-2-1902, Dept. of the Army, Corp of Engrs., Office of the Chief of Engineers 1970.
41. **US Corps of Engineers. Engineering and design – slope stability, Engr. Manual** EM1110-2-1902, Dept. of the Army, Corp of Engrs., Office of the Chief of Engineers 2003.
42. **US Corps of Engineers. Engineering and design – Time-History Dynamic Analysis of Concrete Hydraulic Structures, Engr. Manual** EM1110-2-6051, Dept. of the Army, Corp of Engrs., Office of the Chief of Engineers 2003.
43. **USNRC.** Liquefaction of soils during earthquakes. National Academy Press, Washington DC 1985.
44. **Wang W.** Some findings in soil liquefaction. - Beijing : Water Conservancy and Hydroelectric Power Sientific Research Institute , 1979.
45. **WWDSE**, Water Works Design and Supervision Enterprise, MIDDLE AWASH FEASIBILITY STUDY AND DETAIL DESIGN OF MULTIPURPOSE DAM PROJECT VOLUME-III, ANNEX-III SITE SPECEFIC SEISMIC HAZARD ASSESSMENT FINAL REPORT, Addis Ababa, Ethiopia, 2016.

46. **WWDSE,** Water Works Design and Supervision Enterprise, FEASIBILITY STUDY AND DETAIL DESIGN OF MIDDLE AWASH MULTI PURPOSE DAM PROJECT, Socio Economy Feasibility Study Final Report , Addis Ababa, Ethiopia, 2015.

47. **WWDSE**, Water Works Design and Supervision Enterprise, MIDDLE AWASH FEASIBILITY STUDY AND DETAIL DESIGN OF MULTIPURPOSE DAM PROJECT VOLUME-V, PART-I DAM AND APPERTENANT STRUCTURE DRAFT FEASIBILITY DESIGN REPORT, Addis Ababa, Ethiopia, 2015.

Appendix A

Liquefaction potential determination based on particle size distribution for core material

Table A-1: Grain size analysis result of Borrow Area 1 clay core material

Test Pit No	Depth(m)	Specific gravity	Grain size analysis			
			Clay %	Silt %	Sand %	Gravel
B1-TP-022	0.0-3.0m	2.6	0	89.04	10.96	~
B1-TP-1	0.0-1.1m	2.6	40.5	52.58	6.92	~
B1-TP-2	0.0-1.4m	2.65	23.5	69.64	6.84	~
B1-TP-2	0.5-2.8m					~
B1-TP-5	0.0-1.4 m	2.7	27.5	59.55	12.95	~
B1-TP-5	1.4 -2.7 m	2.77	2.65	44.87	52.48	~
B1-TP-5	0.3 -2.7 m	2.55	28.17	49.31	22.52	~
B1-TP-15	0.5 -3.0 m	2.64	12.27	72.53	12.2	~
B1-TP-16	0.1 -1.7m	2.65	14	73.16	12.84	~
B1-TP-16	1.7 -2.3 m	2.61	0	47.15	52.85	~
B1-TP-17	0.0 -0.6 m	2.6	22.4	43.79	33.81	~
B1-TP-17	1.8-2.4 m	2.75	0	35.56	64.44	~
B1-TP-20	0.25-3.0 m	2.69	17.32	57.93	24.75	~
B1-TP-21	0.0-3.0 m	2.6	10,04	52.04	23.61	~
B1-TP-23	0.0-3.0 m	2.4	16.45	78.46	5.04	~
B1-TP-31	0.0-1.0 m	2.68	7.17	82	10.83	~

TableA-2: Atterberg limits and unified soil classification groups of Borrow Area 1

Test Pit No.	Depth (m)	Site	Soil Profile Description	Soil Properties				
				Atterberg Limits (%)			USCS	PE
				LL	PL	PI		
B1-TP-022	(0.0-3.0m)	Borrow area-1		44	31	13	ML	
B1-TP-1	(0.0-1.1m)			70	18	51	CH	
B1-TP-2	(0.0-1.4m)			65	30	34	CH	
B1-TP-2	(0.5-2.8m)			39	23	16	CL	
B1-TP-5	(0.0-1.4 m)			56	29	27	CH	
B1-TP-5	(1.4 -2.7 m)			27	20	7	ML	
B1-TP-5	(0.3 -2.7 m)			56	25	32	CH	
B1-TP-15	(0.5 -3.0 m)			44	23	21	CL	
B1-TP-16	(0.1 -1.7m)			67	29	39	CH	
B1-TP-16	(1.7 -2.3 m)			35	24	11	ML	
B1-TP-17	(0.0 -0.6 m)			46	26	20	CL	
B1-TP-17	(1.8-2.4 m)			29	20	9	ML	
B1-TP-20	(0.25-3.0 m)			41	28	14	ML	
B1-TP-21	(0.0-3.0 m)			40	28	12	ML	
B1-TP-23	(0.0-3.0 m)			48	36	12	ML	
B1-TP-31	(0.0-1.0 m)			43	29	14	ML	

Table A-3: Grain size distribution of Ettissa Kurkura Area

Test Pit No	Depth(m)	Site	Specific gravity	Grain size analysis			
				Clay %	Silt %	Sand %	Gravel
E-MADCB-1	0.0 – 1.20	Ettissa site	2.48	24.0	67.99	8.01	-
E-MADCB-2	0.0 – 1.20		2.66	74.63	18.07	7.3	-
E-MADCB-3	1.0 – 1.20		2.56	3.32	2.75	1.72	92.21
E-MADCB-4	0.0 – 1.20		2.51	36.16	57.13	6.71	-
E-MADCB-5	0.0 – 1.20		2.57	80.46	14.01	5.53	-
E-MADCB-6	0.0 – 1.20						
K-CB-TP-2-1	0.2 – 2.80	Clay Borrow(Near Kurkura River)	2.63	26.0	63.16	10.84	-
K-CB-TP-3-1	0.0 – 0.80		2.58	10	73.66	16.34	-
K-CB-TP-5-1	0.0 – 0.5		2.61	10	77.96	12.04	-
K-CB-TP-6-1	0.0 – 1.0		2.60	17.84	72.57	9.52	-
K-CB-TP-6-2	1.0 – 3.0		2.63	2.14	45.04	52.82	-
K-CB-TP-9-1	0.2 – 1.0		2.57	19.08	71.70	9.22	-
K-CB-TP-9-2	1.0 – 3.0		2.67	9.39	36.17	54.44	-

TableA-4: Atterberg limits and Unified Soil Classification System groups from Ettissa Kurkura area

Test Pit No.	Depth (m)	Site	Soil Properties			
			Atterberg Limits (%)			USCS
			LL	PL	PI	
E-MADCB-1	0.0 – 1.20	Clay Borrow(Right Side)	60.45	27.36	33.09	CH
E-MADCB-2	0.0 – 1.20		68.80	26.22	42.58	CH
E-MADCB-3	1.0 – 1.20		57.45	26.85	30.60	CH
E-MADCB-4	0.0 – 1.20		70.16	31.59	38.57	CH
E-MADCB-5	0.0 – 1.20		66.60	28.84	37.76	CH
E-MADCB-6	0.0 – 1.20					
K-CB-TP-2-1	0.2 – 2.80	Clay Borrow(Near Kurkura River)	50.90	25.41	25.49	CH
K-CB-TP-3-1	0.0 – 0.80		54.30	27.83	26.47	CH
K-CB-TP-5-1	0.0 – 0.5		57.20	30.48	26.72	CH
K-CB-TP-6-1	0.0 – 1.0		41.10	25.22	15.88	CL
K-CB-TP-6-2	1.0 – 3.0		30.82	Non-PL	-	
K-CB-TP-9-1	0.2 – 1.0		61.26	29.0	32.26	CH
K-CB-TP-9-2	1.0 – 3.0		27.0	Non-PL	-	

Appendix B

Modified time history data of Kobe and Hachinhoe Earthquakes

i. The 1995 Kobe JMA Record, Japan (M=7.2, H=14.3km, R=19km)

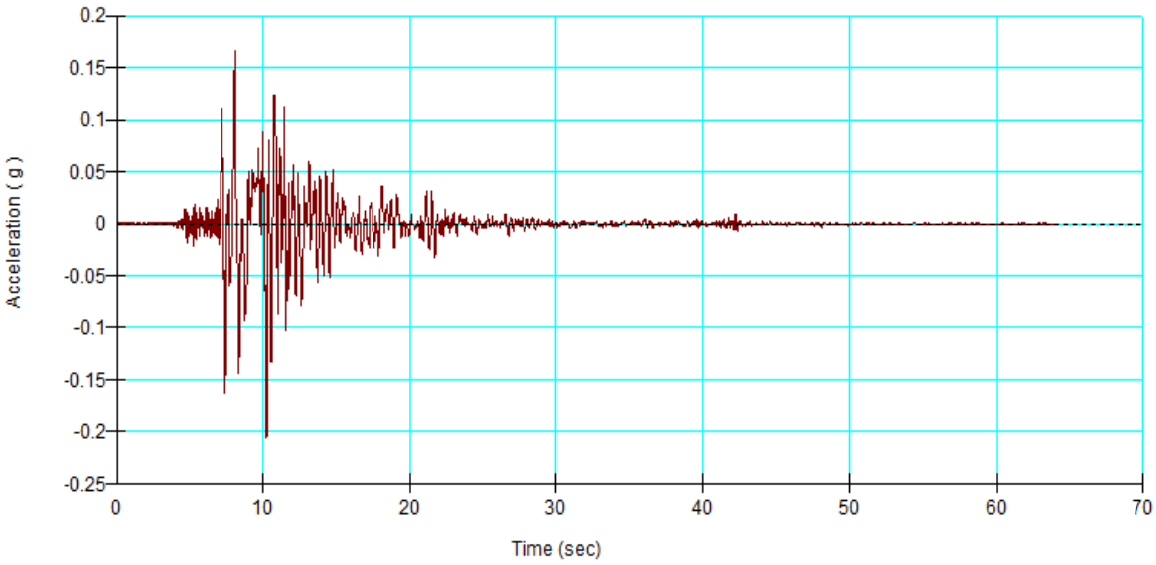

Figure B-1: Maximum Credible Earthquake: Horizontal

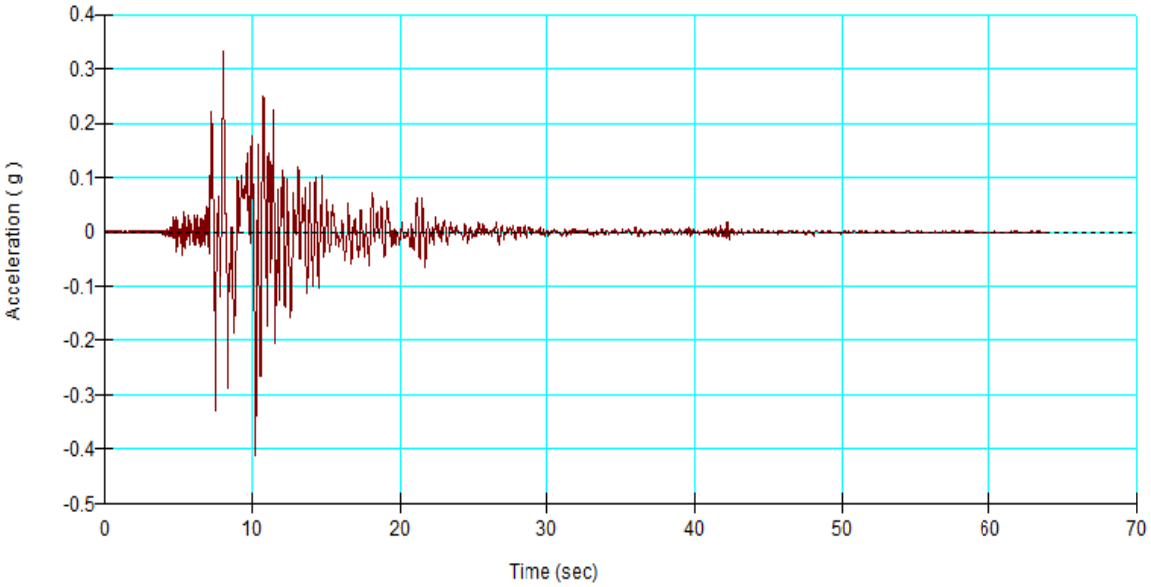

Figure B-2: Maximum Credible Earthquake: Vertical

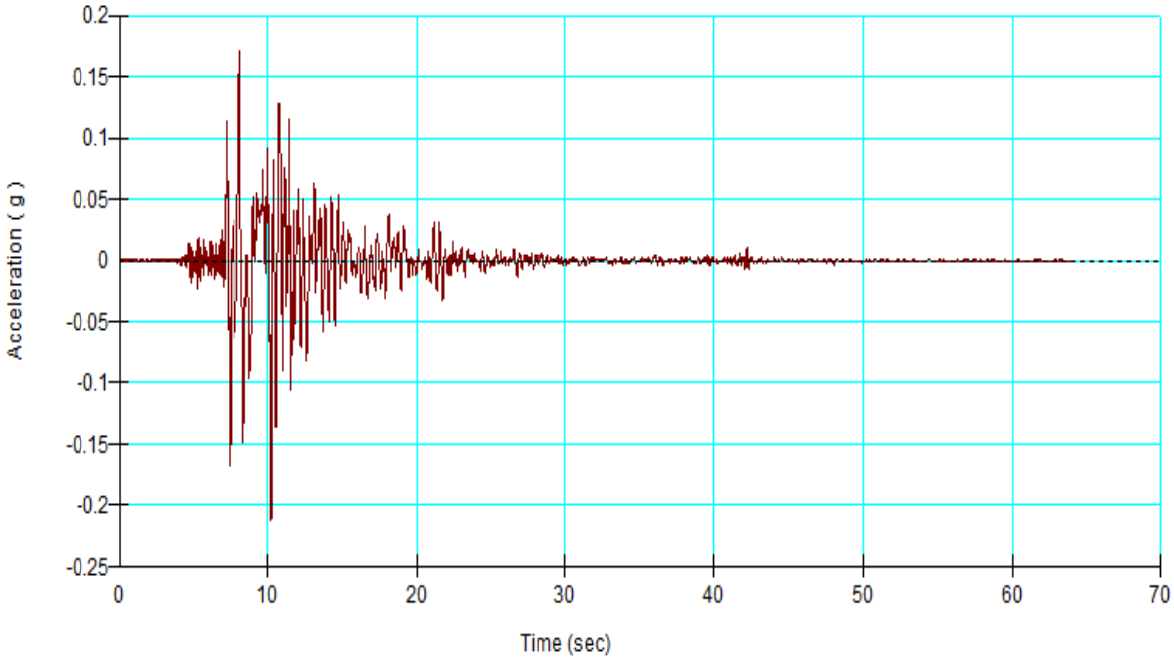

Figure B-3: Design Base Earthquake: Horizontal

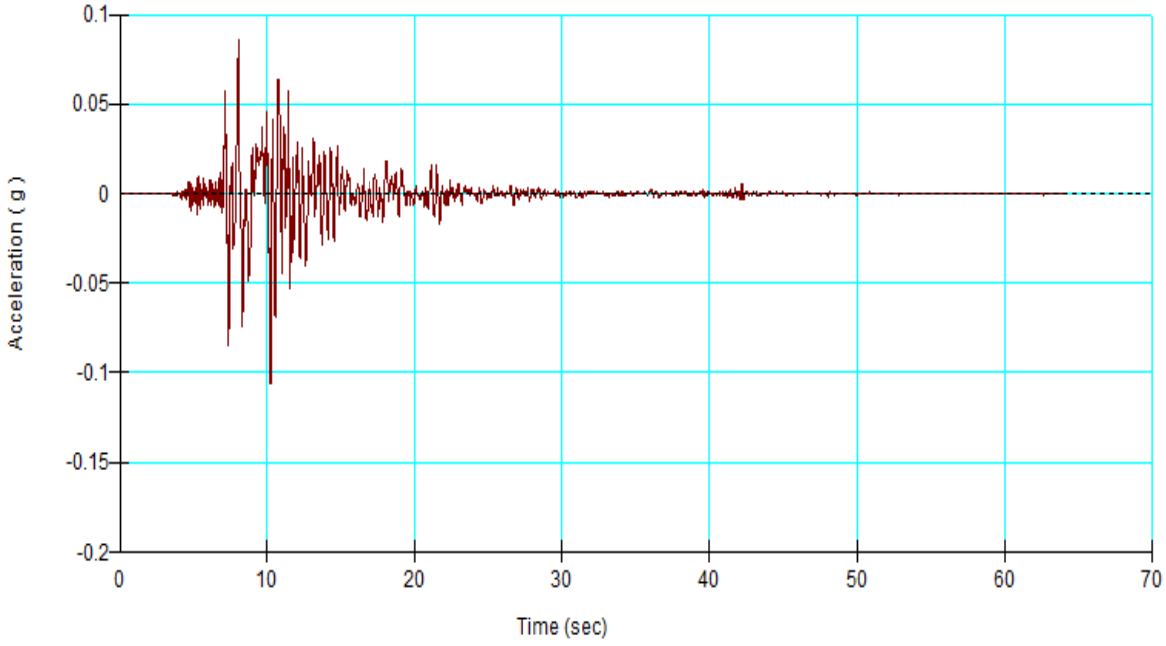

Figure B-4: Design Base Earthquake: Vertical

ii. The 1968 Hachinohe Record, Japan (M=7.9, H=0km, R=200km)

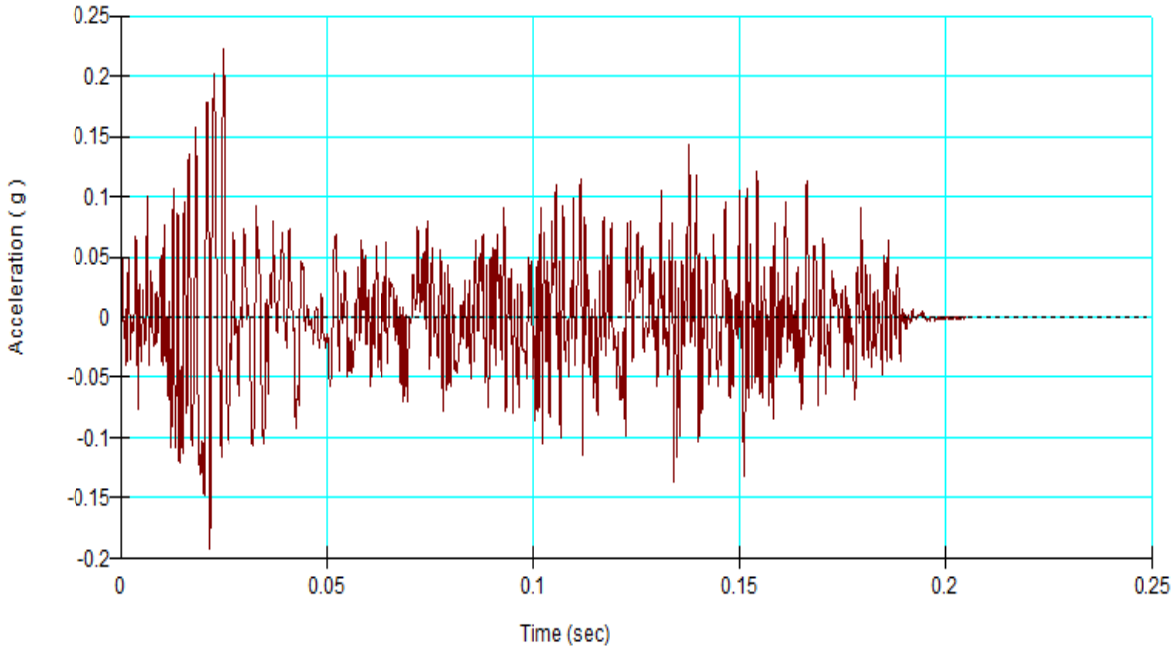

Figure B-5: Maximum Credible Earthquake: Horizontal

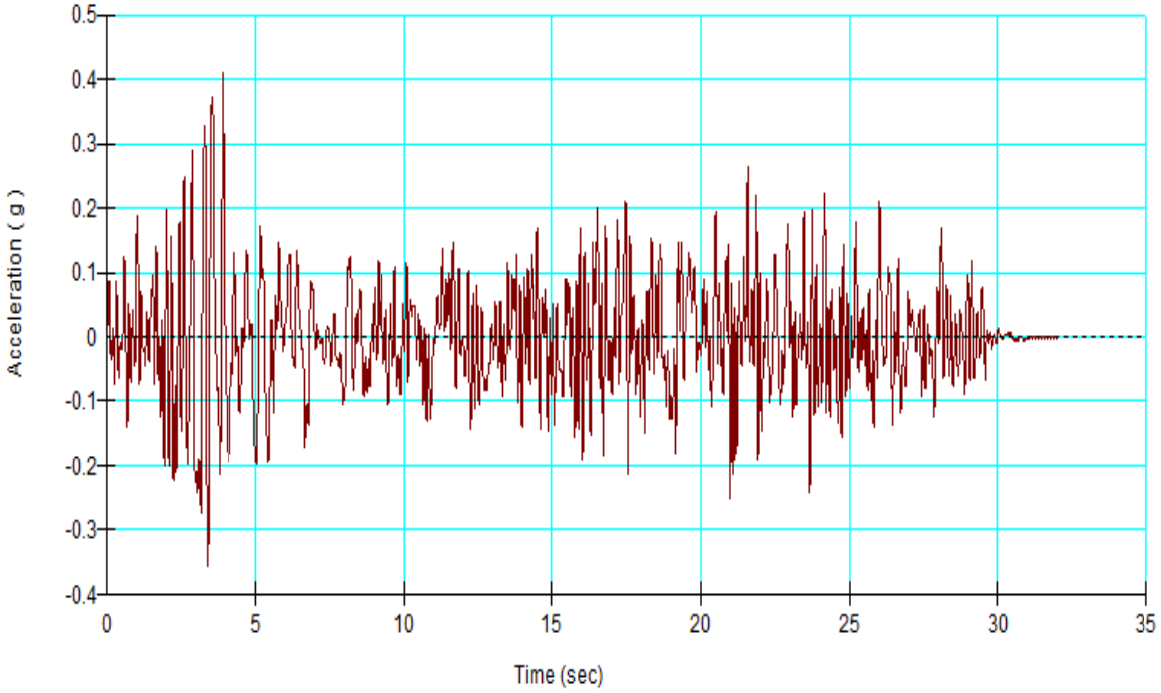

Figure B-6: Maximum Credible Earthquake: Vertical

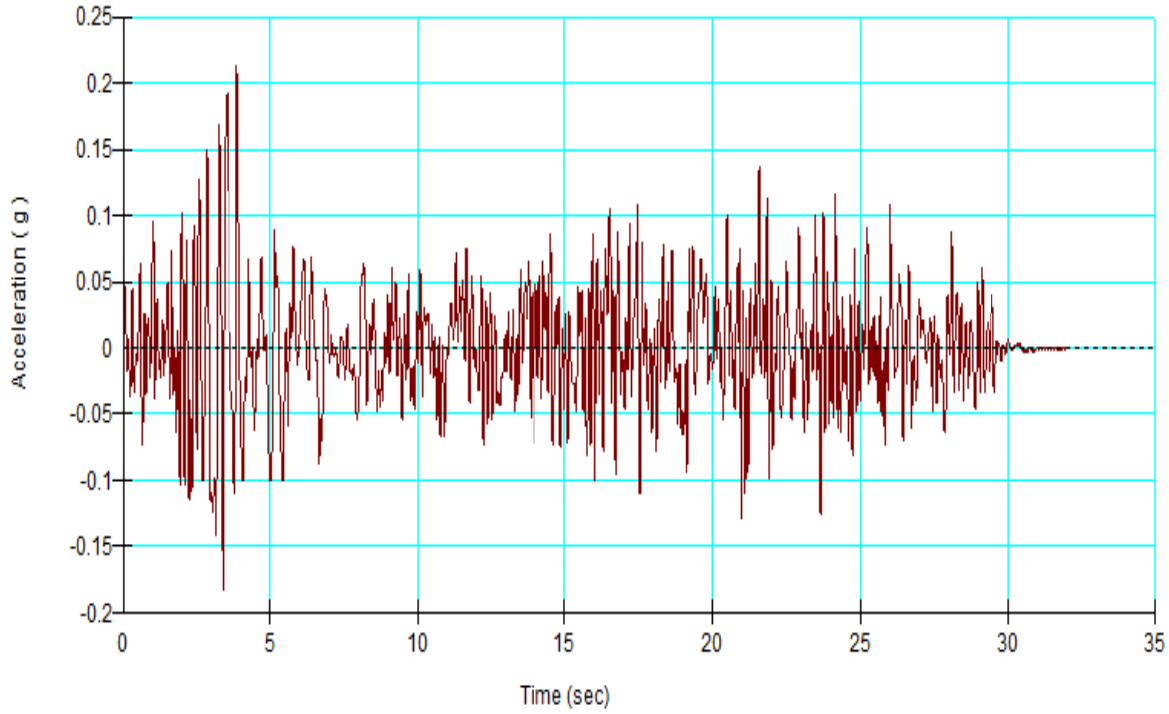

Figure B-7: Design Base Earthquake: Horizontal

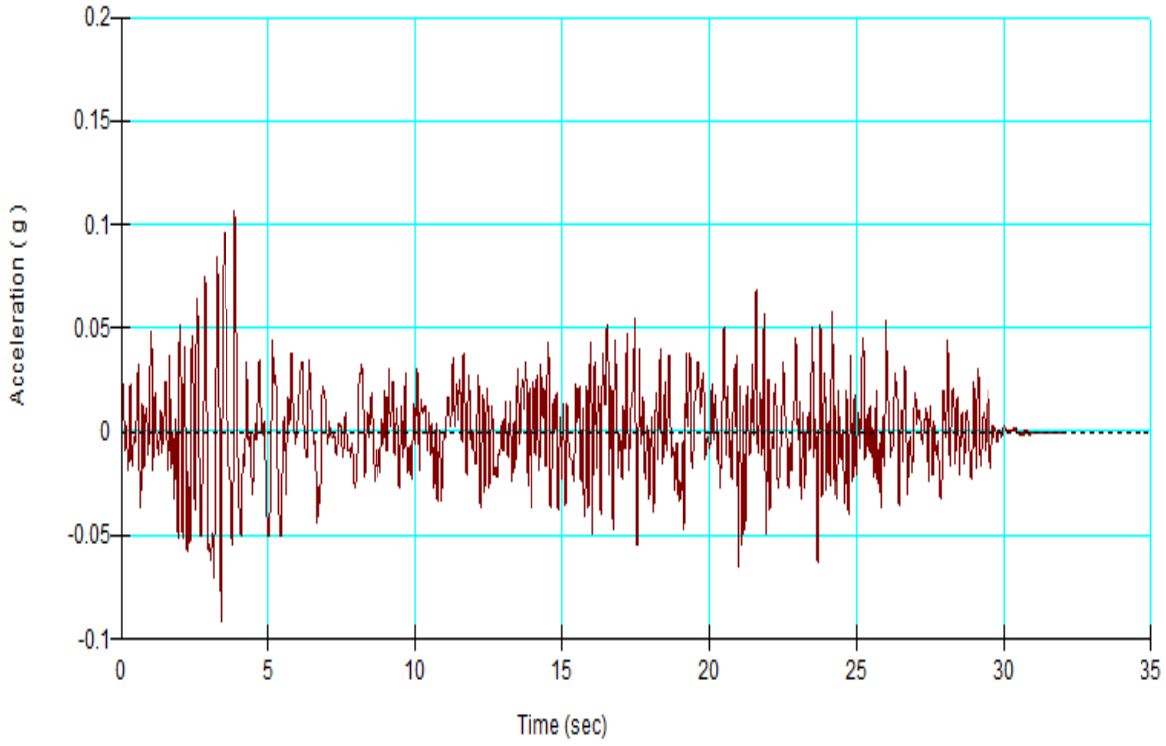

Figure B-8: Design Base Earthquake: Vertical

Appendix C

Slip surfaces and permanent deformation in design base earthquake

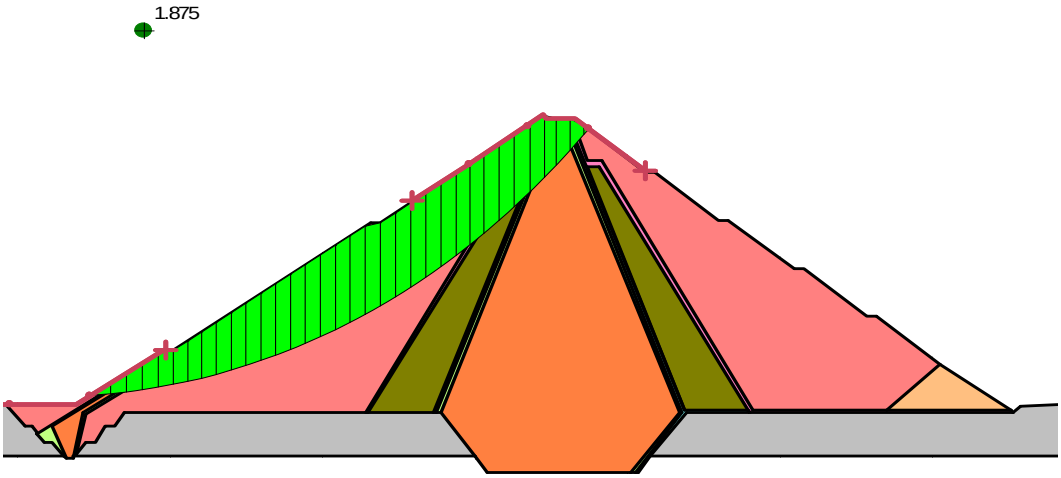

Figure C-1: Slip surface 1

Table C-1: Slip surface 1 permanent deformations

Resultant displacement	0.0079073
Slope angle of chord	23.7°
Yield acceleration	0.19029 m/s^2
Vertical displacement	0.00318m
Horizontal displacement	0.00723m

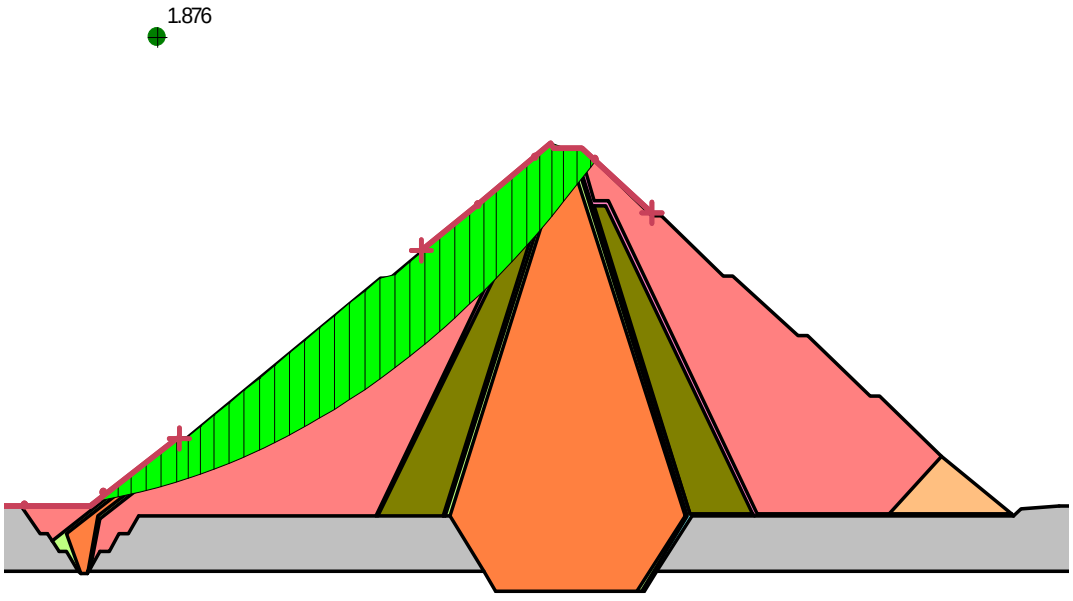

Figure C-2: Slip surface 2

Table C-2: Slip surface 2 permanent deformations

Resultant displacement	0.008472
Slope angle of chord	24°
Yield acceleration	0.19159 m/s^2
Vertical displacement	0.0032m
Horizontal displacement	0.00733m

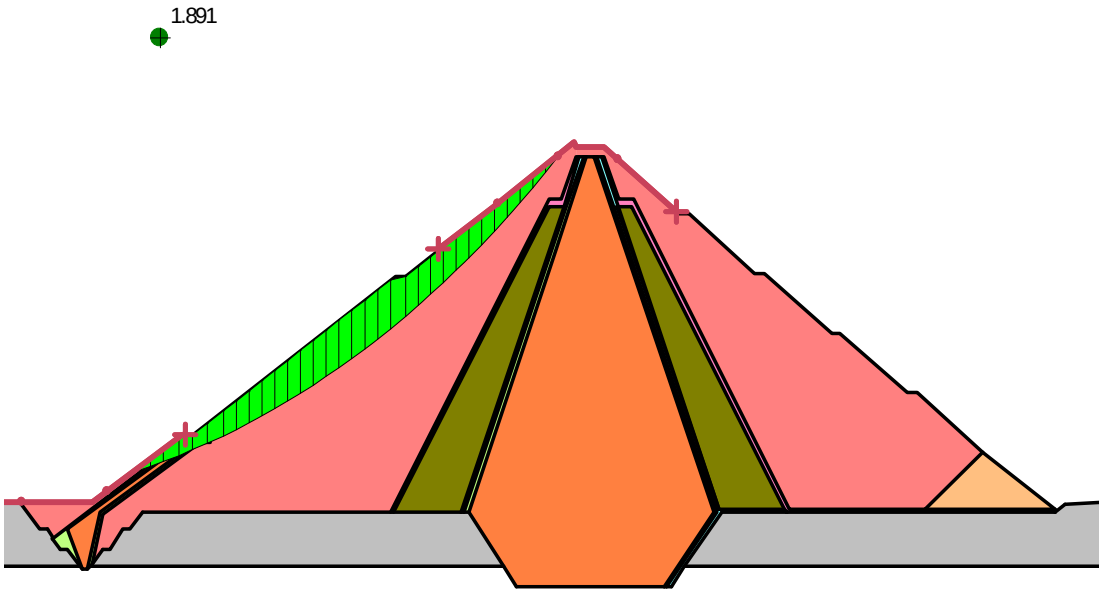

Figure C-3: Slip surface 3

Table C-3: Slip surface 3 permanent deformations

Resultant displacement	0.023237
Slope angle of chord	26.2°
Yield acceleration	0.19633 m/s^2
Vertical displacement	0.00945m
Horizontal displacement	0.02123m

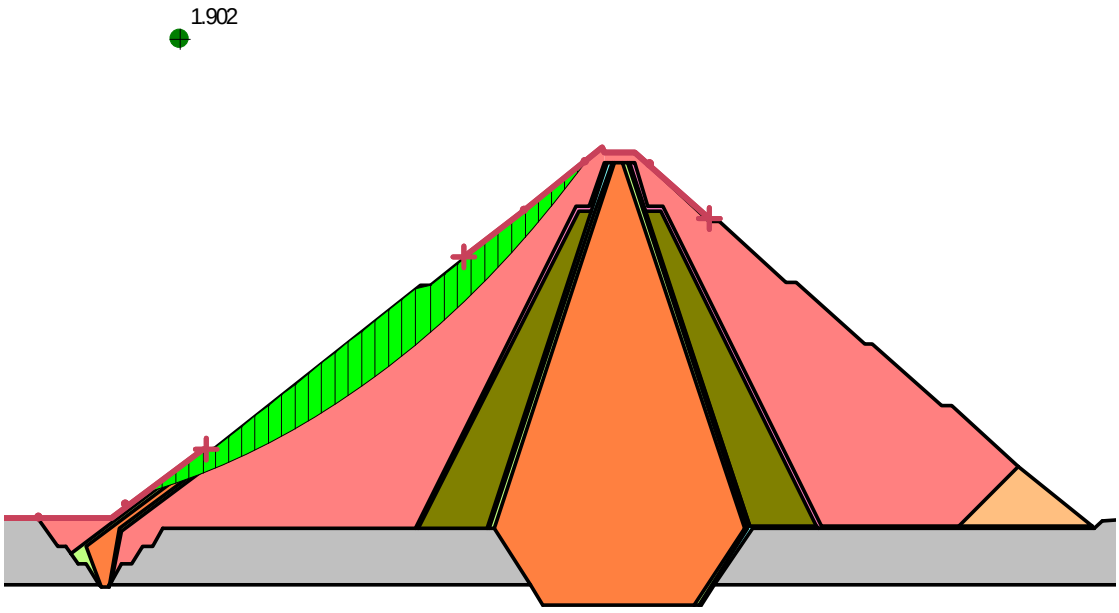

Figure C-4: Slip surface 4

Table C-4: Slip surface 4 permanent deformations

Resultant displacement	0.015436
Slope angle of chord	24°
Yield acceleration	0.19878 m/s^2
Vertical displacement	0.00618m
Horizontal displacement	0.01415m

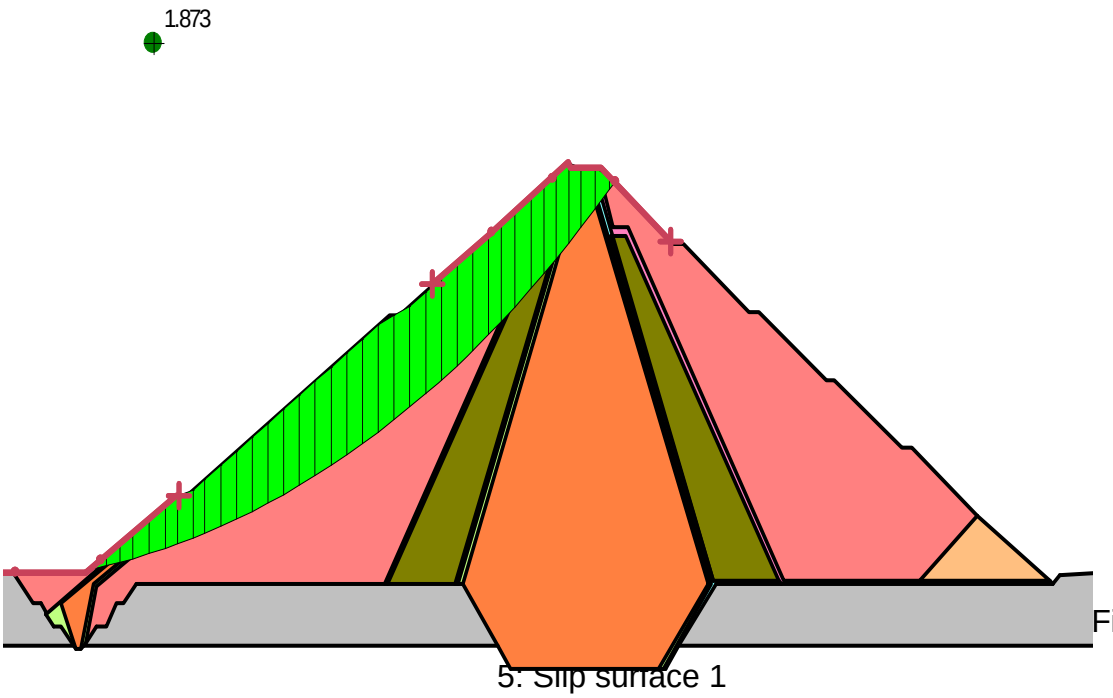

Figure C-5: Slip surface 1

Table C-5: Slip surface 1 permanent deformations

Resultant displacement	0.0090378
Slope angle of chord	23.7°
Yield acceleration	0.19144 m/s^2
Vertical displacement	0.00364m
Horizontal displacement	0.00827m